GUOZHONG XU
Aqueous Polymerization of Ethylenically Dicarboxylic Acids and Multicarboxylic Acids Studied by Mass Spectroscopy and Nuclear Magnetic Resonance
(Under the direction of Jon Amster)

Maleic acid is extremely difficult to homopolymerize due to the severe steric hindrance and polar effects of two carboxylic acid groups. For the reason, poly(maleic acid) (PMA), a versatile industrial polymer, is conventionally prepared by hydrolysis of poly(maleic anhydride). Recently, a new initiation system consisting of hypophosphite and persulfate has been found to initiate the polymerization of maleic acid quickly in water. The mechanism of the polymerization was investigated in the research.

The end-groups and molecular weight of PMA were analyzed by MALDI-TOF-MS and LC/MS. The end-groups were confirmed and the products of polymerization were quantified by $^{31}$P-NMR. A mechanism of polymerization involving the formation of hypophosphite radical and chain transfer to hypophosphite was postulated.

The new initiation system was further explored for polymerization of itaconic acid, fumaric acid, 3-butene-1,2,3-tricarboxylic acid, mesaconic acid, and trans-conic acid, the last four of which had never been reported to homopolymerize before.

INDEX WORDS: Matrix-assisted laser desorption/ionization, MALDI, Time-of-flight, TOF, LC/MS, $^{31}$P-NMR, FT-Raman, Free radical polymerization, Homopolymerization, Maleic acid, Fumaric acid, Mesaconic acid, Trans-aconictic acid, 3-Butene-1,2,3-tricarboxylic acid, Poly(maleic acid), Poly(fumaric acid), Poly(itaconic acid), Poly(mesaconic acid), Poly(trans-aconictic acid), Poly(butene-1,2,3-tricarboxylic acid), Hypophosphite.

# AQUEOUS POLYMERIZATION OF ETHYLENICALLY DICARBOXYLIC ACIDS AND MULTICARBOXYLIC ACIDS STUDIED BY MASS SPECTROSCOPY AND NUCLEAR MAGNETIC RESONANCE

by

GUOZHONG XU

B.S., Peking University, China, 1989

M.S., Beijing Institute of Chemistry, Chinese Academy of Sciences, China, 1992

A Thesis Submitted to the Graduate Faculty of The University of Georgia in Partial Fulfillment of the Requirements for the Degree

MASTER OF SCIENCE

ATHENS, GEORGIA

2001

# AQUEOUS POLYMERIZATION OF ETHYLENICALLY DICARBOXYLIC ACIDS AND MULTICARBOXYLIC ACIDS STUDIED BY MASS SPECTROSCOPY AND NUCLEAR MAGNETIC RESONANCE

by

GUOZHONG XU

Approved:

Major Professor: I. Jonathan Amster

Committee: Charles Q. Yang
Michael G. Bartlett

Electronic Version Approved:

Gordhan L. Patel
Dean of the Graduate School
The University of Georgia
December 2001

# DEDICATION

To my dear wife and friend, Ying Chen,

for her unlimited love, understanding, and supports

To my loving sons, Grant and Albert,

for the wonderful enjoyment they bring to the world

ACKNOWLEDGMENTS

I would like to express my sincere gratitude to my research advisor, Professor Jon Amster, for two years of guidance, inspiration, and support during my graduate study at the University of Georgia. He kindly accepted me for pursuing a dual degree in analytical chemistry. He opened the door of mass spectrometry for me and led me into the exciting field of research.

My special thanks go to Drs. Charles Yang and Ian Hardin of Department of Textile Science for providing research assistantship during my graduate study at The University of Georgia. My thanks also go to Drs. Dennis Phillip and Quincy Teng for their helps in mass spectroscopy and NMR experiments.

I also want to thank other group members in the both Dr. Amster's and Dr. Yang's laboratories for their friendship and help. They are Todd Mize, Keith Johnson, Kristi Taylor, Julia Johnson, Bryan Parks, Xudong Jia, and Dong Zhang.

Last, I would also like to acknowledge the members of my advisory committee, Drs. Charles Yang and Michael G. Bartlett for their helpful input to my research and constructive reviews of the dissertation.

TABLE OF CONTENTS

Page

# CHAPTER 1

# INTRODUCTION AND LITERATURE REVIEW

## HOMOPOLYMERIZATION OF ETHYLENICALLY DICARBOXYLIC ACIDS

The polymers of monoethylenically dicarboxylic acids have general industrial use as water treatment agents, detergent additives, dispersing agents, and chelating agents, corrosion inhibitors, crosslinking agents, fiber coupling agents, etc. [1, 2]. Most of these are homopolymers or copolymers of maleic acid and itaconic acid. Poly(maleic acid) has also been developed for the new generation of non-formaldehyde durable-press finish of cotton fabrics [3]. Homopolymers of maleic acid are more efficient for industrial uses than copolymers because they have more carboxylic acid groups available for reaction. However, these monoethylenically dicarboxylic acids are very difficult to homopolymerize under the conditions normally used for other vinyl monomers because of the high steric hindrance and polar effect of the two carboxylic acid groups [1].

### Maleic Acid

The homopolymerization of maleic acid is extremely difficult under conditions normally used for other vinyl monomers, such as acrylic acid. Currently, there are three possible approaches for the preparation of poly(maleic acid) (PMA).The first route to PMA is hydrolysis of poly(maleic anhydride). It is also the commercial technique for preparing PMA. Actually, maleic anhydride itself is also very difficult to polymerize. It was commonly believed that maleic anhydride would not homopolymerize [1,2], and served as a typical example for the concept that steric hindrance and polar effects impede the polymerization of 1,2-disubstituted olefins. In 1961, the long established thought was shattered by the discovery that maleic anhydride could homopolymerize by initiation with γ- [4] and UV radiation [5], radical initiators, various bases, shock waves, or by

electrochemical means. Radiation polymerization was not of any commercial interest because only a very low yield of poly(maleic anhydride) (14-28%) was achieved, even after very long reaction times (40 hours) [4]. Maleic anhydride can polymerize to form polyvinyleneketoanhydride instead of poly(maleic anhydride) by treatment with organic amines (e.g. triethylamine, pyridine etc.) and phosphines (e.g. triphenylphosphine) as initiator [6]. Maleic anhydride polymerizes in melt or organic solutions to produce the only commercial product, poly(maleic anhydride). Melt polymerization of maleic anhydride at 85-135$^{o}$C with 2-6% acetyl peroxide gives quantitative yields of poly(maleic anhydride) with evolution of copious amounts of $CO_2$ [7]. Poly(maleic anhydride) oligomers can be obtained in high yield by polymerization of maleic anhydride in benzene, toluene, o-xylene, chloroform, acetic anhydride, or chlorobenzene with 5 mol% 2, 2'-azobisisobutyronitrile (AIBN) (70$^{o}$), benzoyl peroxide (BPO) (70-110$^{o}$), lauroyl peroxide (LPO) (60-70$^{o}$), dichlorobenzoyl peroxide (70$^{o}$), or diisopropyl percarbonate (75$^{o}$) [1]. A polymerization mechanism was suggested allowing for decarboxylation and production of a polymer with cyclopentanone rings [8].

The second preparation method of PMA was disclosed in patents but not in published papers [9, 10, 11, 12]. Here, maleic acid was first transferred into mono-maleate salts by neutralizing with an alkali hydroxide or ammonia in aqueous solution, then the maleate was polymerized with peroxide initiators. A very small amount of polyvalent transition metal salts could be used to improve the conversion of monomers. The method provided efficient control of molecular weight of final products and a high yield of polymer. From an industrial and environmental standpoint, water is preferred to organic solvents for polymerization because of its simple production steps, low cost, and

absence of toxic emission and fire hazard. However, polymaleate cannot be made into all acidic polymer by removal of alkali metal without further manufacturing steps, and a significant increase in production costs. No commercial product is produced in this way.

The ideal method is to polymerize maleic acid directly in aqueous medium. To data, there has been only one report that maleic acid could homopolymerize in aqueous solution [13]. In 1979, it was found that maleic acid (MA) could form a charge-transfer polymer by initiation with potassium persulfate in water in the presence of polyvinylpyrrolidone (PVP). The formation of PVP-MA complex promoted the polymerization, resulting in a PVP-PMA complex. The complex could not be separated and decomposed at 100-130$^{o}$C. In order to separate the PMA from the polymer complex, the polymer complex was firstly methylated by diazomethane, then 50-60% of the PMA in the complex was separated as its methyl ester, which was found to be oligomers with a MW 400~500 Daltons as measured by GPC. The unseparated part of PMA seemed to be grafted onto the PVP. The method did not arouse commercial interest.

**Fumaric Acid**

There have been no patent or other published reports of the homopolymerization of fumaric acid [1, 2]. Unlike maleic acid, poly(fumaric acid) can not be prepared from poly(fumaric anhydride), because fumaric acid does not form an anhydride, and it decomposes at a temperature above 230$^{o}$C [14]. However, dialkyl fumarates, particularly with different alkyl groups, can undergo radical reaction to give homopolymers of fairly high molecular weights [1, 2]. The polyfumarates can be hydrolyzed to produce poly(fumaric acid) [15].

Both maleic and fumaric acids were reported to undergo oligomerization when subjected to high pressure and shear stress [16], to give products with molecular weights of 600-800 Daltons. Oligomerization was believed to occur by ionic addition of a carboxyl group of one monomer to the double bond of another monomer. It was also known that maleic and fumaric acids could be treated by phosgene and trialkylamines to give cis-and trans-poly(vinyleneketoanhydrides) [17], which exhibited the characteristic properties of conjugated polymers: dark color, electron paramagnetic resonance signal, and solubility only in strongly polar solvents.

**Itaconic Acid**

Itaconic acid appears easier to homopolymerize than maleic acid and fumaric acid because of its 1, 1-disubstituted structure rather than 1,2-disubstituted one for maleic and fumaric acids. The homopolymerization of itaconic acid was first described by Marvel and Shepherd in 1959 [18]. Itaconic acid underwent aqueous polymerization in the presence of 0.5 N hydrochloric acid using potassium persulfate as initiator. The polymerization preceded for 60 hours with a low polymer conversion around 35%. According to a paper of B. E. Tate [19, 20], the conversation of itaconic acid could reach 93%, but this claim was not demonstrated in any paper or patent. For poly(itaconic acid) (PIA) or poly(itaconic anhydride) prepared from both aqueous or organic solutions, the carboxylic content of PIA accounted to only 45-50% of the expected value [21]. The inconsistent composition suggested that decarboxylation accompanied the polymerization process of itaconic acid and itaconic anhydride [22]. Serious decarboxylation, leading to

complex structure of polymers, was the reason why characteristics of PIA in solution have so far been inadequately described in literatures.

PIA could be prepared by polymerizing IA at 30$^{o}$C in an acidified aqueous solution with $K_2S_2O_8/K_2S_2O_6$ initiator/activator for several days [23] or in methanol with AIBN as initiator for 30 days [21]. The polymer yields were close to 70%.

PIA could be prepared at high conversion up to 99% by aqueous polymerization of partially neutralized monomer (<2 moles base for every mole of IA) solution with polyvalent metal ion and peroxide as initiator for a period of 3 to 4 hours [24]

**Substituted Dicarboxylic Acids and Tricarboxylic acids**

The substituted maleic acid, fumaric, and tricarboxylic acids are even more difficult to homopolymerize than maleic acid and fumaric acid. These acids include mesaconic acid, cis-aconictic acid, trans-aconictic acid, citraconic acid, and 3-butene-1, 2, 3-tricarboxylic acid, etc. Their structures are shown in Scheme 1.1. There have been no reports of homopolymerization and copolymerization for these vinyl multicarboxylic acids.

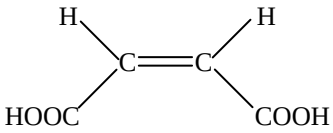


Maleic Acid (MA)
MW=116.01

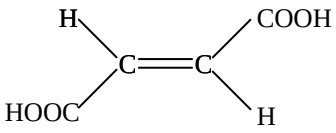


Fumaric Acid (FA)
MW=116.01

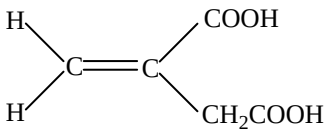


Itaconic Acid (IA)
MW=130.1

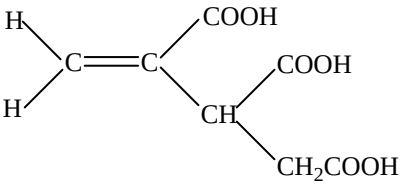


3-Butene-1,2,3-tricarboxylic Acid (BTA)
MW=188.1

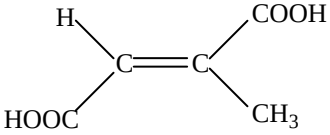


Mesaconic Acid (MSA)
MW=130.1

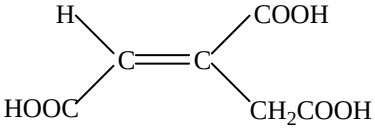


Trans-aconictic Acid (TAA)
MW=174.1

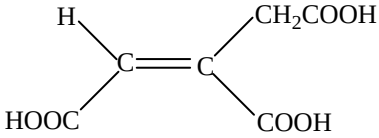


Cis-aconictic Acid
MW=130.1

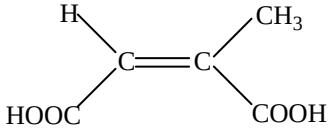


Citraconic Acid
MW=130.1

Scheme 1.1. Structures of the ethylenically dicarboxylic acids and multicarboxylic acids:

# MASS SPECTROSCOPIC ANALYSIS OF SYNTHETIC POLYMERS

## MALDI and ESI

Matrix-assisted laser desorption/ionization (MALDI) was introduced by Karas and Hillenkamp in 1988 [25, 26]. The principle of desorption and ionization is schematically shown in Figure 1.1. The desorption of matrix under laser irradiation produces an ion plume and facilitates the desorption and ionization of macromolecules as intact macro-ions. Because the soft ionization technique produced singly charged ions of very high mass with minimum fragmentation, it was soon established for determination of high molecular weight (MW) biological macromolecules in a mass range even above 100,000 Da [27]. High MW narrow polydisperse polystyrene up to 1.5 million Daltons was also detected by MALDI. [28].

MALDI has found increasing uses for characterization and analysis of synthetic polymers [29, 30]. Much work has been done on the fundamentals desorption for synthetic polymers, including instrumental settings, polydispersity of polymers, analysis of complex polymeric structures, sample preparation conditions, and coupling with separation techniques, etc [29]. MALDI-MS provides the average molecular weight, molecular weight distribution, composition of end-groups and repeating units, composition distribution in copolymers, and even additives or impurities for a wide variety of polymers [29, 30]. It has been also used to monitor polymerization and analyze the free radical propagation rate coefficient [31], chain transfer coefficient [32], and mode of chain termination [33].

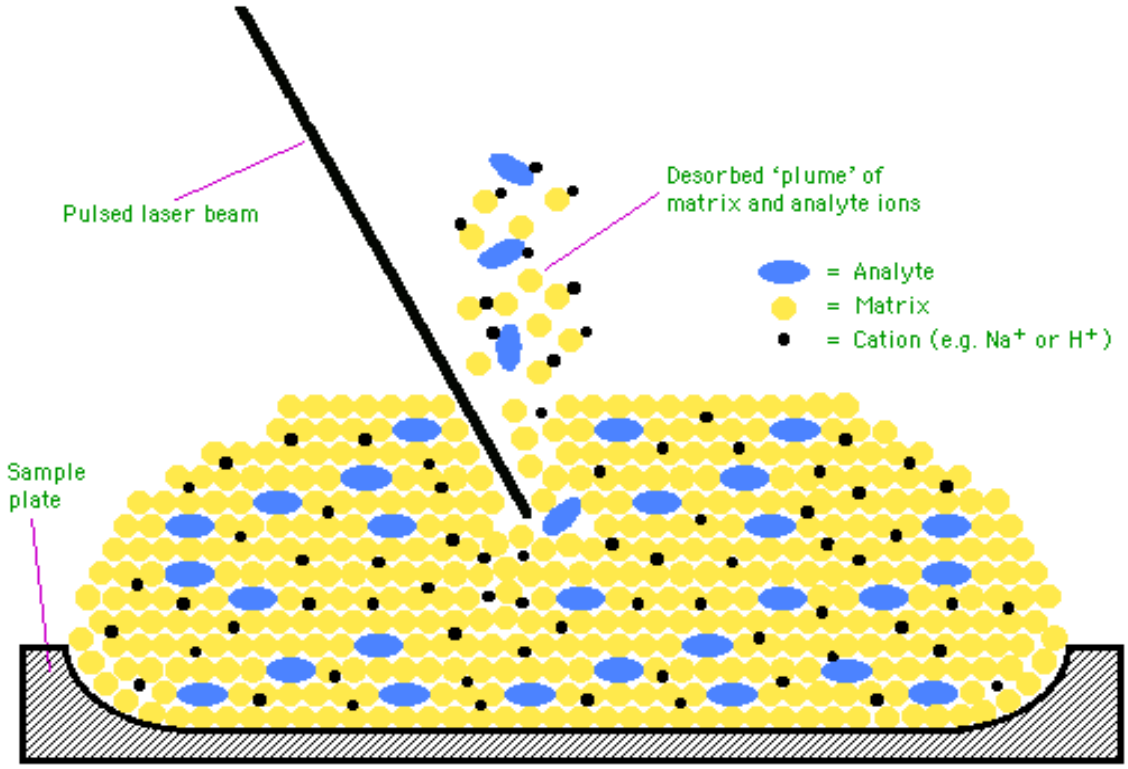


Figure 1.1 Schematic representation of matrix assisted laser desorption/ionization of macromolecules

Electrospray (ESI) [34] is another soft ionization technique that is useful for synthetic polymers [29]. The principle [35] of ESI is presented in Figure 1.2. A solution of analyte is passed through a capillary which is held at high electric potential of 1 to 5 thousand volts. The solution emerges out the capillary as a mist of highly charged droplets under the influence of the high electric field. The nebulization of solution can be facilitated by using a sheath flow of gas. As they pass through a potential and pressure gradient to the mass analyzer, the droplets reduce in size and increase in charge density as a result of solvent evaporation. They split into smaller droplets as the increasing charge repulsion overcomes the surface tension. Continuous desolvation and depletion of droplets finally results in the formation of droplets containing a single ion. ESI possesses high ionization efficiency, usually generates multiple charged ions for large biomolecules, and allows the analysis of higher mass species in mass spectrometers with a limited mass-to-charge range. However, the propensity for multi-charging increases the spectral complexity of disperse synthetic polymers [29]. Even though the complex spectra can be deconvoluted in high resolution mass spectra such as those obtained from FT-ICR [36], ESI is generally more useful for low MW oligomers [37].

MALDI has the advantage of spectral simplicity due to the production of mostly singly charged molecular ions (vs multiply charged ions for ESI) and high tolerance to contamination and non-volatile buffers (volatile buffers should be used for ESI). On the other hand, ESI possesses advantages over MALDI in its versatility, and high ionization efficiency for low MW oligomers, and compatibility for on-line coupling with liquid separation.

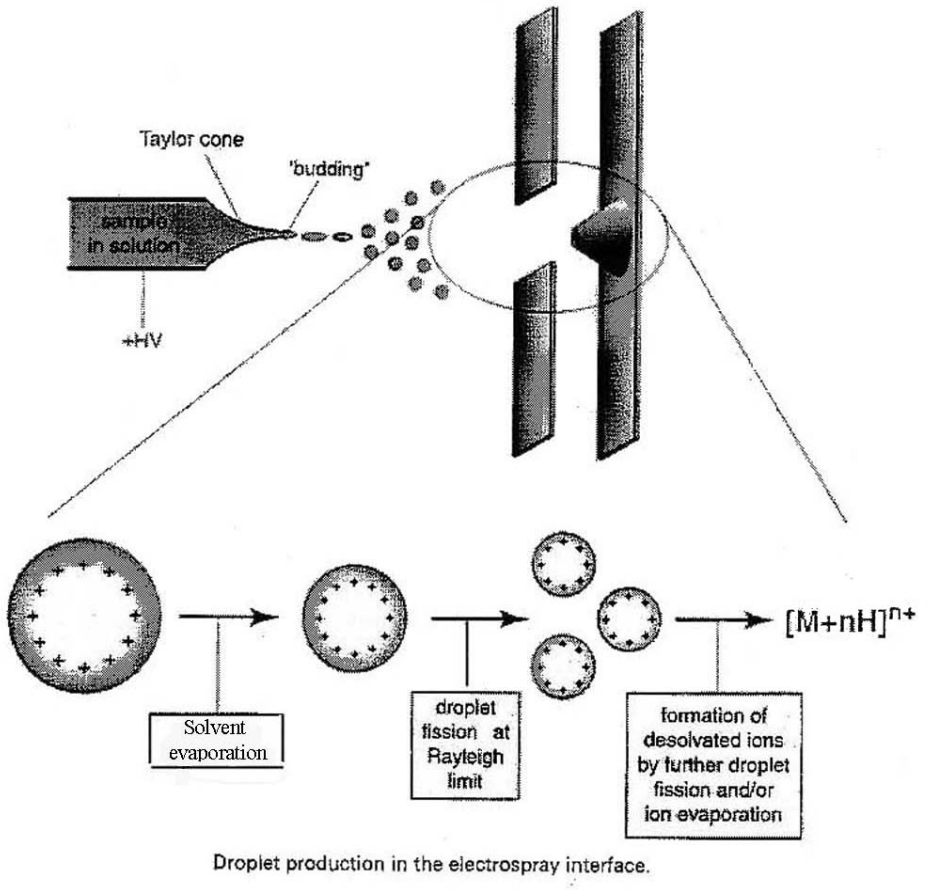


Figure 1.2 Droplet production in ESI interface, the most acceptable ionization mechanism [35]

MALDI analysis of synthetic polymers is more complex and difficult than for biopolymers in two aspects [38]. Synthetic polymers are heterogeneous in compositions and molecular mass and require more demanding sample preparation methods than biopolymers, which ideally consist of only one sort of molecule with a single molecular weight. The sample preparation methods for peptides and proteins have been well developed, are easy to implement, and homogeneous samples are easily obtained. For synthetic polymers, samples are typically inhomogeneous, requiring one to search the sample for a crystal that provides good resolution and signal intensity. Moreover, the polydispersity of synthetic polymers causes reduced signal/noise ratio, mass discrimination, and lower signal reproducibility. The sample preparation and mass discrimination of synthetic polymers are discussed in detail below.

## MALDI Sample Preparation

### Selection of Matrix

MALDI matrices are nonvolatile solid materials that strongly absorb the laser radiation and produce an ion plume. The matrix facilitates the desorption and ionization of macromolecules embedded in the matrix without damage from laser radiation [39]. The matrix also serves to dilute the analyte and prevent sample molecules from aggregating through strong intermolecular interaction [40].

The matrix needs to meet several requirements [38]: (1) high electronic absorption at the employed laser wavelength (typically 337 nm or 355 nm), (2) good vacuum stability, (3) good solubility in the solvent that also dissolves the analyte, and (4) good miscibility with the analyte in the solid state. In the analysis of biological samples, where

the ionization is generally achieved via proton transfer, the matrix also serves as the proton source. In the situation of synthetic polymers, however, ionization usually takes place by cation attachment, which is a matrix independent process. For water-soluble polymers such as polyethylene glycol, the same matrices used for peptides can be applied. For other polymers, some general guidelines can be extracted from polymer and matrix solubility data [41]. It is recommended to match the matrix polarity with the polymer under investigation. However, the selection of ideal matrix for a given polymer is still a trial and error process. An overview of matrices and solvents for UV- and IR-MALDI of synthetic polymers has been given by Nielsen [42]. Some widely used matrices include 2, 5-dihydoxybenzoic acid (DHB), α-cyano-hydroxycinnamic acid (α-CHHA), ferulic acid (FA), sinapinic acid (SA), indoleacrylic acid (IAA), dithranol [42].

Selection of Cationizing Salt

A metal ion is often required to enhance cationization of synthetic polymers. Unlike biomacromolecules, where the ionization is generally achieved via proton transfer, synthetic polymers are ionized usually by cation attachment. Polar polymers with high cation affinity can form sodium/potassium adduct ions with the trace amount of sodium/potassium ions which are present as impurity in glassware, solvents, reagents, etc [43]. Most polymers with heteroatoms can be successfully cationized after addition of sodium or potassium salts. Non-polar polymers without heteroatoms but with unsaturated double bonds (e.g. polystyrene) can be ionized by adding silver or copper salts, which interact with double bonds of the polymers. A suitable solvent should be selected for dissolution of sample, matrix, and cationizing salt. Polymers without heteroatoms and

without any double bonds such as polyethylene and polypropylene are still not amenable to MALDI analysis because of the extremely low binding energy of the cation-polymer complexes [44].

Selection of Solvent

The solvent(s) must be selected for its compatibility with the matrix, sample, and cationization salts [42]. The best solvent system allows matrix to crystallize simultaneously with polymer. Appropriate amounts of matrix and polymer dissolved in compatible, preferentially identical solvents are mixed to yield a molar ratio of about 1000:1 (matrix:polymer). In the high mass range, multimer formation can occur which contributes an error to measurement of the molecular weight distribution (MWD) of the polymer. Increasing the matrix to polymer ratio reduces multimer formation [43]. Ideally only one solvent is present in the final mixture which reduces the risk of segregation during crystallization on the MALDI target. Because salts are generally difficult to dissolve in organic solvent used in non-polar polymers, they are prepared as a stock solution in an intermediate solvent such as propanol. When mixed solvents are used for sample preparation, the solvent composition will change during the evaporation process and result in a change of polymer solubility. If some less volatile solvent of low dissolving power is present in the final mixture, the polymer may precipitate before matrix crystallization.

Sample Preparation Techniques

The final goal of sample preparation is to transfer the mixture of matrix, sample, solvent, and salt onto the MALDI target as a thin layer of fine and homogeneous cocrystallization of polymer and matrix molecules. Several sample preparation techniques are available for selection [42].

The s*low-crystallization* procedure, which is also called the dried-droplet (one-layer) method, is the original technique introduced by Karas and Hillenkamp in 1988 [23]. In this method, appropriately 0.5-1.0 μL of mixed solution of matrix, sample and salt is applied to the MALDI target and air-dried at room temperature. The slow crystallization process suffers from poor homogeneity and segregation between sample, matrix, and cationization salt, or segregation of one of the distributions of the polymers [47].

*Fast-crystallization* methods were introduced more recently to improve the homogeneity of the crystals [48]. The target with sample is put in a vacuum chamber in order to promote rapid crystallization, typically within a few seconds. The fast crystallization results in smaller crystals with less segregation, and improves shot-to-shot reproducibility, signal intensity, and resolution. Accelerated drying using a stream of dry air or $N_2$ gas is another procedure for achieving the same goal [49, 50]. A spin-coating (two-layer) technique [51] was also used to improve homogeneity and sensitivity. In the two-layer method, a thin layer of matrix is allowed to crystallize and then the sample is added and dried.

*Electrospray deposition* is the most promising sample preparation technique for synthetic polymers [52, 53]. The mechanism is similar to those described for the ESI

ionization of mass spectrometry [54]. In the method, the solution is sprayed out at a flow rate of 1-10 μL/min as fine liquid droplets from a micro-needle with potential of 8 kv onto a target located about 2-4 cm below the needle to create a circular spot about 1 cm in diameter. Electrospray deposition with either an one-layer or two layer approach yields much higher signal intensity and shot-to-shot and spot-to-spot reproducibility, slightly favoring the one-layer electrospray approach. The improved results of electrospray deposition was considered to be a direct result of formation of small and evenly-size cocrystals [53, 55].

**MALDI Mass Discrimination of Synthetic Polymers**

MALDI-MS is an absolute method for the analysis of molecular weight and molecular weight distributions of monodisperse (polydispersity<1.1) polymers [56, 57]. Investigations have shown a dependence of the measured average molecular weight on adduct-forming cation type [58, 59], sample preparation methods [60, 61], laser irradiance [62], and even the types of mass analyzer [43]. MALDI fails to give reliable results for polymers with polydispersity indices greater than 1.1 [63, 64]. Because a synthetic polymer is generally a mixture of polymer chains of different MW, end groups, branching, etc., the accurate analysis of MW requires the sample preparation, ionization, ion transmission, and ion detection to be independent of mass and oligomer structure over a wide mass range.

One source of the apparent discrepancy between MALDI-MS and SEC-light scattering (LC) results for polymers of broad mass distribution is the different data displays of MALDI-MS and SEC [65]. MALDI-MS is a number counting technique and

uses a number-fraction abundance axis and a linear mass scale, whereas SEC-LS is molecular size measuring technique and the data are displayed as weight-fraction intensity vs a log mass scale. A few high molecular weight molecules represent only a few ions in MS but still show a significant effect on the bulk property as detected by refractive-index in SEC-LS. Therefore, the high molecular weight end will disappear much earlier into the baseline noise in a mass spectrum than in a SEC distribution, and the mass spectrum shows a skew or decaying shape rather than the Gaussian distribution pattern of a SEC chromatogram.

The sample preparation procedure may contribute significantly to the error of measurement of the average molecular weight of polymers [45]. Significant influence may arise from the formation of multimers. Due to the high analyte concentration typically used in the MALDI experiment of polymer, the multimers are almost always of high intensity in the analysis of mid-to high-mass polymers (e.g., above 15,000 u for polystyrene). The multimer formation may not be eliminated by simply minimizing the polymer concentration on the probe tip. The efficiency of desorption and ionization is also dependent on the mass of polymers. The dispersion and crystallization of matrix and polymer molecules have significant implication for the efficiency of desorption/ionization and the damage of polymer from laser irradiation. Therefore, appropriate selection of matrix, solvent, cationizing agent, mixing ratio, and application of best preparation technique (i.e. electrospray) are all critical for the MALDI analysis of polymer.

Various ionization efficiencies of different mass polymer molecules contribute to one of the major sources of mass discrimination in the MALDI analysis of polydisperse

polymers. Compared to SEC-LS, MALDI-TOF often yields relatively lower average molecular weight and narrower molecular weight distributions (MWD) for polydisperse polymers. The laser power should be optimized to minimize the ionization discrimination and fragmentation of polymer molecules. Higher thresholds of laser power are needed for desorption and ionization of higher molecular weight polymers [66]. An increase in laser power brings about increased intensity of high molecular weight species, accompanied by an increase in matrix peak intensity. High laser power can also induce dimerization by gas-phase clustering, yielding an MWD shift towards higher mass [67]. Moreover, high laser power can initiate unintended scissions in the polymer structure [68]. The mass discrimination may also occur on the low molecular weight end and yield incorrectly higher MWD [69]. The phenomenon may result from the fact that shorter oligomers have fewer binding sites for cation attachment, and corresponding lower ionization efficiency. The low molecular weight components may also be lost by evaporation.

The ion transmission in MALDI-TOF-MS has also been reported to contribute to mass discrimination, particularly when a polydisperse polymer is analyzed by an instrument with a long flight tube and a detector of small detection area [70]. In the delayed-extraction instrument, the lensing properties of the source electrode can be adjusted by the amplitude of the pulse voltage and time delayed applied. Depending on the pulse voltage and time delay, only a narrow mass range will be focused, thus only a part of the molecular weight distribution has a better resolution, and a different average mass is obtained depending on the calculation methods [71].

Ion detection may make another contribution to mass discrimination. Channel plate detectors have a limited dynamic range and can get saturated easily by low MW

components such as matrix ions and/or oligomers, particularly in the situation of polydisperse polymers where the majority of ions is of low MW [64, 72, 46, 71]. The sensitivity at the high mass end of the MWD will be insufficient due to the lower impact velocity of a high mass ions compared with low mass ions, and generally causes a lower number of secondary electrons [67]. Different techniques have been sought to deal with this problem but usually compromise the resolving power of the detection system.

Functionality distribution of oligomers may make another contribution to mass discrimination [30, 73, 74]. Oligomers with different end groups and architectures may exhibit different crystallization behaviors during sample preparation and different ionization efficiencies. The impact of end groups and cationizing efficiencies is expected to be more pronounced for lower molecular weight oligomers. Until now, very little has been reported on this latter effect topic.

**MALDI─SEC Coupling**

The mass discrimination of polydisperse polymers can be circumvented by pre-fractionation of polymer samples into several fractions of narrow MWD (polydispersity<1.2) by SEC [75, 76]. SEC-MALDI coupling is an ideal marriage for overcoming the drawbacks of both techniques: SEC is limited by the availability of well-characterized calibration standards, while MALDI-MS of polymers of broad distribution suffers from mass discrimination. The polydisperse synthetic polymers can be analyzed using an absolute calibration method based on the investigated polymer itself. SEC can be used with MALDI-MS in either off-line or on-line modes.

Off-line SEC-MALDI Coupling

In the off-line SEC-MALDI-MS, the polymer fractions from SEC column are collected and analyzed by MALDI-MS in turn after the entire separation procedure has been completed [75, 76, 77]. The mass measured fractions can be used as absolute calibration points for SEC. Meanwhile, the mass spectra of low mass fractions provide structural information such as repeating mass increment and end-groups. The main instrumental issues are maintaining the separation efficiency and, in the case of small-scale separation, avoiding an excessive dilution of analyte by matrix. Fractions can be collected into individual vials, or the separation effluent can be directly deposited onto a target. An on-line UV or RI detector can be used to aid the fraction identification. A pneumatic nebulizer was used to spray SEC effluent onto a slowly rotating matrix-coated target [78] and the resulting 3mm wide and 7cm long semicircular track was subjected to MALDI analysis. The sample preparation technique is easily automated. One problem is the variation of matrix/analyte molar ratio throughout the separation, and the accuracy of the MW may be somewhat compromised. Meanwhile, for small-scale separation, sample dilution may cause the loss of sensitivity.

Off-line SEC-MALDI detection allows the separation and MALDI analysis to function independently and to be optimized individually. It provides the general advantages of fast analysis and high contamination tolerance. Although the off-line approach simplifies the coupling, it only provides the mass spectral data for limited number of discrete peaks or bands which limits the method flexibility and applicability for a comprehensive chemical analysis.

On-line SEC-MALDI Coupling

For continuous monitoring of the entire separation, MALDI can be coupled on-line (real-time detection) with SEC. Here, the separation effluent is delivered directly to the mass spectrometer. The major challenge is to preserve the quality of mass spectra (resolution, accuracy, and sensitivity) without compromising the efficiency of separation. The on-line nature requires continuous solvent evaporation, real-time interface regeneration (or cleaning) without compromising mass spectral quality, chromatographic resolution, and memory effect. Most approaches for on-line MALDI coupling are similar to those previously applied to different ionization methods. There have been three methods for direct liquid introduction: continuous flow, aerosol introduction, and rotating ball or wheel MALDI interface [75, 76]

In the *continuous flow* (CF) mode, the matrix solution and column effluent are introduced into sample probe through a capillary at a rate of 1-10 μL/min [79], similar to that for continuous flow FAB. CF-MALDI has been coupled to conventional LC with a flow splitter located between column and mixing tee, and directly coupled to microbore LC [80]. An improved mass resolution for CF-MALDI has been achieved with a hybrid ion trap/reflection time-of-flight mass spectrometer [81]. One problem of the flow injection is the strong memory effect due to the buildup of sample on the probe tip. A new method employing IR MALDI and 0.1% glycerol in ethanol as matrix has been reported for CF MALDI [82]. Strong material ablation associated with IR MALDI should reduce the memory effect.

MALDI *aerosol liquid introduction* developed by Murray and Russell [83, 84] is similar to thermospray ionization and the particle beam interface for electron impact and

chemical ionization, which rely on fast pumping to remove solvent that evaporated from the particles. Column effluent was mixed with matrix solution prior to pneumatic nebulization and sprayed directly into the mass spectrometer. The particles are dried in a heated tube, and ions are formed when the aerosol particles are irradiated with a pulsed UV laser. The liquid flow rate of 0.5-1.0 mL/min is compatible with conventional SEC. The problem of high sample consumption is less a problem for relative inexpensive synthetic polymers. SEC-MALDI coupling has a significant advantage over SEC-ESI coupling, since the multiple charge distribution in ESI leads to overlapping peaks for disperse synthetic polymers.

*Rotating Ball inlet (ROBIN) and continuous vacuum desorption interface* translate a separation in-time (on-column) into a separation in-space (on-surface) by continuous eluent deposition onto a rotating wheel or ball [85, 86]. They involve continuous deposition/crystallization of analyte and solid matrix dissolved in appropriate solvent on the rotating surface followed by direct analysis by UV MALDI.

## OBJECTIVE OF THE RESEARCH IN THIS THESIS

Currently, the major commercial polymer of dicarboxylic acid, poly(maleic acid), is prepared by the two steps technique, i.e., polymerizing maleic anhydride in organic solvents then hydrolyzing the poly(maleic anhydride) in water. It is economically and environmentally preferred to prepare the polymer directly in water rather than in organic solvents.

Recently, a new free radical initiation system consisting of hypophosphite and persulfate was found to be able to initiate the homopolymerization of maleic and itaconic

acids in aqueous solution. During the investigation of polycarboxylic acid for crosslinking of cotton cellulose [87], it was found that maleic acid was able to polymerize in situ and crosslink cotton cellulose in the presence of $K_2S_2O_8$ and $NaH_2PO_2$, which was also the catalyst for esterification of cellulose with polycarboxylic acid. When a solution of 40% maleic acid, 20% $NaH_2PO_2$, and 4% $K_2S_2O_8$ was heated to 90$^oC$ for several hours, it was found by FT-Raman spectroscopy that the C=C bond of maleic acid disappeared [88]. The same phenomenon was also found for itaconic acid. The disappearance of C=C suggested the polymerization of maleic acid and itaconic acid.

Size exclusion chromatography (SEC) coupling to light scattering was found to fail in the characterization of product PMA in the study. For low MW polyelectrolytes such as PMA, SEC separation is inversely affected by the ionic interactions between oligomers and column packing and among analyte molecules themselves. The low MW polyelectrolyte may elute out of the column at its high mass limit even though an electrolyte buffer was used to reduce the ionic interaction. Meanwhile, light scattering (LS) is not suitable for polyelectrolytes of molecular weight below several thousand Dalton. It was reported in the literature that PMA with a cryoscopic molecular weight of 300-1000 was equivalent to light scattering molecular weights of 50,000 [1, 7]. In this study, the low MW PMA was prepared in the presence of large amount of hypophosphite and persulfate. It is very difficult to desalt the sample without loss of some components of the product oligomers. Therefore, SEC-LS is of little use for characterization of PMA.

So far no characterization of the polymerization products was performed and the mechanism of polymerization is unknown. Understanding the mechanism of polymerization is very important for control of the reaction and optimization of the

products for different purposes. It is also interesting to know how a monomer with such high steric crowding and polar hindrance is able to homopolymerize.

The purpose of the study is to characterize the polymerization product, poly(maleic acid), and elucidate the mechanism of polymerization. MALDI-TOF-MS, LC/ESI/MS, and $^{31}$P-NMR will be employed for the study. Another purpose of the research is to further explore the potential of the new initiation system for other monoethylenically dicarboxylic acids and multicarboxylic acids, such as fumaric acid, 3-butene-1,2,3-tricarboxylic acid, mesaconic acid, trans-aconictic acid, et al.. These unsaturateddicarboxylic acids and multicarboxylic acids have never been reported to homopolymerize, and their polymers have great commercial potential for many industrial uses such as water treatment.

## REFERENCES


1. Trivedi, B. C., Culbertson, B.M., "*Maleic anhydride*", Plenum Press, New York and London, 1982
2. Culbertson, B..M., "Maleic and fumaric polymers", in "*Encyclopedia of polymer science and technology*", 3rd Ed.,Vol. 9, H. M. Mark and N.M. Bikales N.M. Ed., Intersciences Publishers, New York, 1987
3. Yang, C.Q., *U.S. Patent* 6,165,919 (2000), Assigned to Research Foundation of The University of Georgia
4. Lang, J. L., Pavelich, W. A., Clarey, H. D., *J. Polym. Sci. Part A-1* 1:1123 (1963)
5. Nagahiro, I., Nishihara, K., Sakota, N., *J. Polym. Sci.*12(1): 785 (1974)
6. Schopov, V. I., *Makromol. Chem.* 137: 285-292; 293-301(1970)

7. Procter & Gamble Co., *Brit Pat*. 1,073,323 (1967)
8. Braun, D., Aziz, E.l., Sayed, I. A., Pomakis, J., *Makromol. Chem*. 124:249 (1969)
9. Fukumoto, Y., Moriyama, N., *US Pat. 4,668,735; 4,709,091 (1987),* Assigned to Kao Corp., Tokyo, Japan.
10. Yamaguchi, S., Shioji, Y.I., *US Pat. 5,135,677* (1992), Assigned to Nippon Shokubai Co., Ltd., Osaka, Japan.
11. Yamaguchi, S., Yokoi, T., Shioji, S., Irie, Y., *US Pat. 5,064,563 (1991),* Assigned to Nippon Shokubai Co., Ltd., Osaka, Japan.
12. Fiarman, I.S., McCallum, T.F. *US Pat. 5,451,644(1995),* Assigned to Rohm & Haas Company, Philadelaphia, PA, USA
13. Sato, T., Nemoto, K., Mori, S., Otsu, T., *J. Macromol. Sci.-Chem. A*13(6):751-766 (1979)
14. Gerhartz, W., Ed., *Ullmann's Encyclopedia of Industrial Chemistry*, 4th ed., Vol. 8, VCH Publisher, New York, 1987
15. Kitano, T., Ishigaki, A., Uematsu, G., Kawaguchi, S., Ito, K., *J. Polym. Sci. Part A. Chem*. 25:979-986(1987)
16. Soloveva, A. B., Zhorin, V.A., Enikolopyan, N.S., *Chem. Abstr*. 89, 42379y (1978)
17. Schopov, V.I., *Makromol. Chem*. 137: 285-292; 293-301 (1970)
18. Marvel, C.S., Shepherd, T.H., *J. Org. Chem*. 24: 599-605 (1959)
19. Tate, B.E., *Adv. Polym. Sci*. 5: 214-232 (1967)
20. Tate, B.E., *Makromol. Chem*.109:176-193 (1967)
21. Veliĉkovi̇ć, J., Filipovi̇ć, J., Djakov, D.P., *Polym. Bull*. 32:169-172 (1994)
22. Susumu, N., Fujiwara, F., *Polym. Lett*. 7: 177-180 (1969)

23. Grespos, E., Hill, D.J., O'Donnel, J.H., O' Sullivan, P.D., Young, C.L., *Makromol. Chem. Rapid Commun*. 5:589 (1984)

24. Swift, G., Yocom, K.M., *US 5,336, 744* 91994), Assigned to Rohm and Haas Co, Philadelphia, PA.

25. Karas, M., Hillenkamp, F., *Anal. Chem*., 60: 2299-2301 (1988)

26. Karas, M., Bachmann. D., Bahr, U., Hillenkamp, F., *Int. J. mass. Spectrom. Ion Processes*, 78: 53 (1987)

27. Hillenkamp, F., Karas, M., Beavis, R.C., Chait, B.T., *Anal. Chem*., 63: 1193 (1991)

28. Schriemer, D.C., Li, L., *Anal. Chem*. 68(17): 2721-2725(1996)

29. Hanton, S. D., *Chem. Rev*. 101(2):527-569 (2001)

30. Nielen, M.W.F., *Mass Spectr. Rev*. 18:309-344 (1999)

31. Schweer, J., Sarnecki, J., *Macromolecules* 29(13):4536-4543(1996)

33. Kapfenstein, H.M, Davis, T.P., *Macrom. Chem. Phys*. 199(11):2403-2408(1998)

34. Zammit, M. D., Davis, T. P., Haddleton, D. M., Suddaby, K. G., *Macromolecules* 30(7):1915-1920 (1997)

35. Cole, R.B., "*Electrospray ionization mass spectrometry: fundamentals, instrumentation, and applications*", John Wiley & Sons, 1997.

36. Gaskell, S. J., *J. Mass Spectrom.* 32:677-688 (1997)

37. Lorenz, S.A., Maziarz III, E.P., Wood, T.D., *Applied Spectrometry* 53(1):18A-36A (1999)

38. Vonk, E.C, Langeveld-Voss, B.M.W., van Dongen, J.L.J., Janssen, R.A.C., Cramers, C.A., *J. Chromatography A* 911:13-26(2001)

39. Räder, H.J., Schrepp, W., *Acta Polymer* 49:272-293 (1998)

40. Siuzdak G., *"Mass spectrometry for biotechnology"*, Academic Press, New York, 1998, p.13

41. Karas, M., Bahr, U., "Matrix-assistant laser desorption-ionization mass spectrometry: principle and application", in *"Selected topics and mass spectrometry in biomolecular science"*, C. R. Caprioli et al. Eds. 1997

42. Hanton, S. D., Owens, K. G., *Proc 46th ASMS Conf Mass Spectrom Allied Topics*, Orlando, FL, 1998, p 1185

43. Nielen, M.W.F., *Mass Spectrom. Rev.* 18: 309-344 (1999)

44. Danis, P.O., Karr, D.E., Mayer, F., Holle, A., Watson, C.H., *Org. Mass Spectrom*. 27:843 (1993)

45. Reinhold, M., Meier, R.J., de Koster, C.G., *Rapid Comm. Mass Spectrom*. 12: 1962 (1998)

46. Schriemer, D.C, Li, L., *Anal. Chem*. 69:4169-4175(1997)

47. Schriemer, D.C., Li, L., *Anal. Chem*. 69:4176-4183 (1997)

48. Allwood, D.A., Perera, I.K., Perkins, J., Dyer, P.E., Oldershaw, G.A., *Appl. Surf. Sci.*103(3) (1996)

49. Weinberger, S.R., Boernsen, K.O., Finchy, J.W., Robertson, V., Musselman, B.D., *Proc. 41st ASMS Conf Mass Spectrom Allied Topics*, San Francisco, CA. p.775(1993)

50. Castoro, J.A., Koster, C., Wilkins, C.L., *Rapid Comm. Mass Spectrom*. 6:239(1992)

51. Gusev, A.I., Wikinson, W.R., Proctor. A., Hercules, D.M., *Anal. Chem*. 67:1805(1995)

52. Perera, I.K., Perkins, J., Kantartzoglou, S., R*apid Comm. Mass Spectrom*. 9: 180 (1995)

53. Hensel, R. R., King, R., Owens, K.G., *Proc. 43rd Annual Conf. on Mass Spectrom. and Allied Topics*, 31 May-4 June, San Francisco, CA, p.947(1993)

54. Axelsson, J., Hoberg, A.M., Waterson, C., Myatt, P., Shield, G.L., Varney, J., Haddleton, D.M., Derrick, P.J., *Rapid Comm. Mass Spectrom.* 11: 209(1997)

55. Gaskell, S., *J. Mass Spectrom*. 32: 677-688. (1997)

56. Sadeghi, M., Vertes, A., *Appl. Surf. Sci*. 127:226 (1998)

57. Räder, H.J., Spickermann, J., Muller, K., *Macromol. Chem. Phys*. 196:396791995)

58. Schweer, J., Mayer-Posner, F., Mullen, K., Räder, H.J., *Macromol*. 29: 4536 (1996)

59. Dogruel, D., Nelson, R.W., Williams, P., *Rapid Comm. Mass Spectrom*. 10:801-804 (1996)

60. Yates, H.T., Scrivens, J., Jackson, T., Deery, M., *Proc. 44th ASMS Conf. Mass Spectrom. & Allied Topics*, May 12-16, Portland, OR, p.903 (1996)

61. Cottrell, J.S., Dwyer, J.L., *Proc. 44th ASMS Conf. Mass Spectrom. & Allied Topics*, May 12-16, Portland, OR, p.900 (1996)

62. Kassis, C.M., Belu, A.M., DeSimone, J.M., Linton, R.W., Lange, G.W., Friedman, R.M., *Proc. 44th ASMS Conf. Mass Spectrom. & Allied Topics*, May 12-16, Portland, OR, p.1096 (1996)

63. Mowat, I.A., Donovan, R.J., Monaghan., J., *Proc. 44th ASMS Conf. Mass Spectrom. & Allied Topics*, May 12-16, Portland, OR, p.897 (1996)

64. Montaudo, G., Garozzo, D., Monyaudo, M.S., Puglisi, C., Samperi, F., *Macromolecules*. 28: 7983 (1995)

65. McEwen, C., Jackson, C., Larson, B., *Polym. Prepr*. 37(1):314. (1996)

66. Jackson, C., Larsen, B., McEwen, C., *Anal. Chem*. 68(8): 1303-1308 (1996)

67. Lloyd, P. M., Suddaby, KS, Barney, J.E., Scrivener, E., Derrick, P.J., Haddleton, D., *Euro. Mass Spectrom*. 1:293 (1995)

68. Axles, J., Scrivener, E., Haddleton, D.M., Derrick, P.J., *Macromolecules* 29:8875 (1996)

69. Lehrle, R,S., Sarson, D.S., *Polym. Degradation & Stability* 51: 197 (1996)

70. Barry, J.P., Carton, W.J., Pesci, K.M., Anselmo, R.T., Radtke, D.R., Evans, J.V., *Rapid Comm. Mass Spectrom*. 11:437 (1997)

71. Guo, B., Rashidzadeh, H., Chen, H., *Proc. 45th ASMS Conf. Mass Spectrom. Allied Topics*, Palm Springs, CA, p.1278 (1997)

72. Zhu, H., Li, L., *Proc. 45th ASMS Conf. Mass Spectrom. Allied Topics*, Orlando, FL, p.1054 (1998)

73. McEwen, C.N., Jackson, C., Larsen, B.S., *Int. Mass Spectrom. Ion Proc*. 160:387 (1997)

74. Belu, A,M., DeSimone, J.M., Lintmon, R.W., Lange, G.W., Friedman, R.M., *J. Am. Soc. Mass Spectrom*. 7:11 (1996)

75. Nielen, M.W.F., Buijtenhuijs, F.A., *Anal. Chem*. 7: 1806 (1999)

75. Gusev, A.I., Fresentius *J. Anal. Chem.* 366:691-700 (2000)

76. Murray, K.K, *Mass Spectrom. Rev*. 16: 283-299 (1997)

77. Lou, X., Joost, Van Dongen, J.L.J., Meijer, E.W., *J. Chromatogr. A* 896:19-30 (2000)

78. Kassis, C.E., DeSimone, J.M., Linton, R.W., Remsen, E.E., Lange, G.W., Friedman, R.M., *Rapid Commun.Mass. Spectrm.* 11:1134-1138 (1997)

79. Li, L., Wang, A.P.L., Coulson, L.D., *Anal. Chem*. 65:493-495(1993)

80. Nagra, D., Li, L., *J. Chrom. A.* 711:235-245 (1995)

81. He, L., Liang, L., Lubman, D.M., *Anal. Chem*. 67:4127-4132 (1995)

82. Lawson, S.J., Murray, K.K., *47th ASMS Conference on Mass Spectrometry and Allied Topics*, Dallas, TX, 1999.

83. Murray, K.K., Russell, D.H., *Anal. Chem*. 65:2534 (1993)

84. Murray, K.K., Russell, D.H., *J. Am. Soc. Mass Spectrom*. 5:1-9 (1994)

85. Preisler, J., Foret, F., Karger, B.L., *Anal. Chem*. 70:5278-5287 (1998)

86. Ørsnes, H., Graf, T., Degn, H., Murray, K.K., *Anal. Chem*. 72(1): 251-254 (2000)

87. Yang, C.Q., Wang, X., Lu, Y., *J. Appl. Polym. Sci*. 75(2):327-336 (2000)

88. Yang, C.Q., Gu, X., *J. Appl. Polym. Sci*. 81(1):223-228 (2001).

# CHAPTER 2

# EXPERIMENTAL

# POLYMERIZATION

## Materials

Maleic acid (MA), fumaric acid (FA), itaconic acid (IA), mesaconic acid (MSA), trans-aconictic acid (TAA), sodium hypophosphate, potassium persulfate, 2,5-dihydroxy benzoic acid (DHB), 1-hydroxy isoquinoline (HIQ), and ammonium hypophosphite (AHP) were purchased from Aldrich Chemical Inc. (Milwaukee, WI). 3-butene-1,2,3-tricarboxylic acid (BTA) was supplied from Lancaster Synthesis Inc. (Windlam, NH). Ammonium persulfate (APS) and HPLC-grade acetonitrile (ACN) came from J. T. Baker Inc. (Phillipsburg, NJ). All chemicals except acetonitrile were reagent grade and used without further purification.

## Polymerization of Maleic Acid

Maleic acid was polymerized by following two methods.

(1) In a three-neck flask equipped a condenser, a magnetic stirrer, a $N_2$ inlet, 25.0g maleic acid, 11.4g $NaH_2PO_2$, and 61.1g deionized water were added. The system was purged with $N_2$. When the reaction mixture became a clear solution upon heating to 65$^oC$, 2.46g $K_2S_2O_8$ was added in several portions during polymerization. The reaction was maintained at 65$^oC$ for 7 hours and monitored by FT-Raman spectroscopy until the characteristic C=C stretch at 1650 $cm^{-1}$ and =C-H stretch at 3050 $cm^{-1}$ of maleic acid disappeared.

(2) To simplify the sample treatment (desalting) for mass spectroscopic analysis, maleic acid was polymerized using $NH_4H_2PO_2$ and $(NH_4)_2S_2O_8$ instead of $NaH_2PO_2$ and $K_2S_2O_8$. In the 10ml reaction vials with a small magnetic stirrer, maleic acid, $NH_4H_2PO_2$,

$(NH_4)_2S_2O_8$, and deionized water were added. The vials were purged by $N_2$ through a syringe needle. The vials were loaded in a Pierce Reacti-Therm Heating Stirring Module kept at 55°C. The reaction is monitored by FT-Raman spectroscopy until all maleic acid was consumed in around 7 hours. The additional amounts of reactants and mole ratios were shown in Table 2.1.

Table 2.1. The amounts and mole ratios of reactants for preparation of three PMA oligomers

| PMA | $MA/H_2PO_2^-$ | $MA/S_2O_8^{2-}$ | MA (g) | $NaH_2PO_2$ (g) | $NH_4H_2PO_2$ (g) | $K_2S_2O_8$ (g) | $(NH_4)_2S_2O_8$ (g) | Total solution (g) |
|---|---|---|---|---|---|---|---|---|
| 1 | 2:1 | 23:1 | 25.0 | 11.40 | N/A | 2.50 | N/A | 100 |
| 2 | 2.5:1 | 20:1 | 2.00 | N/A | 0.5724 | N/A | 0.1967 | 5.0 |
| 3 | 2:1 | 30:1 | 2.00 | N/A | 0.7155 | N/A | 0.1311 | 5.0 |

**Polymerization of Other Dicarboxylic Acids and Tricarboxylic Acids**

The polymerization of fumaric acid (FA), itaconic acid (IA), 3-butene-1,2,3-tricarboxylic acid (BTA), mesaconic acid (MSA), and trans-aconictic acid (TAA) was carried out in a 10 ml reaction vial with a small magnetic stirrer. The unsaturated monomer (FA, IA, BTA, MSA, or TAA), $NH_4H_2PO_2$, $(NH_4)_2S_2O_8$, and deionized water were added to the vial in the ratio listed in Table 2.2. The vials were purged by $N_2$ through a syringe needle and loaded in a Pierce Reacti-Therm Heating Stirring Module kept at specific temperatures. For FA and IA, all $(NH_4)_2S_2O_8$ was added at the beginning of reaction. In the case of BTA, MSA, and TAA, the polymerization was slow, and $(NH_4)_2S_2O_8$ was added as two or three portions at the beginning and in the course of

reaction. The polymerization is monitored by FT-Raman spectroscopy until all monomers disappeared. The temperature and reaction time were also shown in Table 2.2.

Table 2.2. The weight and molar ratios of reactants for polymerization of different monomers

| | Monomer (g) | $NH_4H_2PO_2$ (g) (Acid/AHP) | $(NH_4)_2S_2O_8$ (g) (Acid/APS) | Water (g) | Temperature ($^oC$) | Time (hours) |
|---|---|---|---|---|---|---|
| PMA | 2.000 | 0.7155 (2:1) | 0.1311 (30:1) | 2.8467 | 55 | 7 |
| PFA | 2.000 | 0.7151 (2:1) | 0.3932 (10:1) | 1.8917 | 95 | 0.4 |
| PBTA | 1.4617 | 0.3224 (2:1) | 0.5319 (10:3) | 3.3803 | 75 | 30 |
| PIA-1 | 2.400 | 0.7658 (2:1) | 0.4210 (10:1) | 2.4132 | 90 | 0.5 |
| PIA-2 | 3.000 | 0.1914 (10:1) | 0.2631 (20:1) | 4.0455 | 75 | 2 |
| PMSA | 1.200 | 0.3828 (2:1) | 0.6315 (10:3) | 3.6050 | 75 | 33 |
| PTAA | 2.000 | 0.4769 (2:1) | 0.4631 (10:1.8) | 2.2610 | 55 | 28 |

**Further Oxidation of Poly(maleic acid)**

For investigation of end-groups and structure of the PMA oligomers, the PMA sample prepared with a MA/AHP/APS molar ratio 30:15:1 was further oxidized with $(NH_4)_2S_2O_8$. In a 10 mL reaction vial with a small magnetic stirrer, 1.0 g PMA solution (40%), and 0.1815 g $(NH_4)_2S_2O_8$ were added. The mole ratio between maleic acid unit and the added $(NH_4)_2S_2O_8$ was 4:1. The vial was loaded in a Pierce Reacti-Therm Heating Stirring Module kept at 70$^o$C and reacted for 7 hours.

## INSTRUMENTAL ANALYSIS

**FT-Raman**

The polymerization was monitored by FT-Raman spectroscopy. Raman spectra were acquired in a Nicolet 950 FT-Raman spectrometer with a liquid sample accessory and a Ge detector cooled with liquid $N_2$. The resolution was set at 8cm$^{-1}$, and 128 scans

were cumulated to improve the signal. During polymerization, about 0.15 mL of solution was transferred to Raman sample tube for measurement.

**Sample Treatment for Mass Spectroscopic Analysis**

All samples prepared with $NH_4H_2PO_2$ and $(NH_4)_2S_2O_8$ were analyzed by mass spectroscopy without further purification.

The PMA sample, which was synthetic with $NaH_2PO_2$ and $K_2S_2O_8$, was desalted by ion exchange. The ion exchange column was made of a PTFE tube of 50 cm length and 2.0 mm internal diameter. The tube was packed with $HNO_3$-treated DOWEX 50WX4-200 acidic exchange resin (100-200 mesh, Aldrich) and rinsed with deionized water until pH 7.0. The tube was connected with a 0.25 μm Nylon syringe filter (Whatman) and a syringe. 15 μL PMA solution was dropped into PTFE tube and then 3.0 mL water was injected slowly into the tube to rinse out the sample. By testing with pH paper, the first and last portions of elution with neutral pH were discarded. About 1.5 mL medium part of elution with acidic pH was collected and analyzed by MALDI-TOF-MS.

**MALDI-TOF-MS**

The matrix solution was prepared by dissolving 15.4mg DHB and 4.35 mg HIQ in 1.0 mL ACN/$H_2O$ (1:1, v/v). The mixed matrix was originally used for analysis of carbohydrates [1], and was found to give excellent signals for low molecular weight polycarboxylic acids [2]. The structures of matrices are shown as Scheme 2.1. All polymer samples were diluted to concentration of 5.0 mg/mL with ACN/$H_2O$ (1:1 v/v). 10 μL sample solution and 10 μL matrix solution were premixed in a 0.25 mL tube, and

1.0 μL mixed solution was dropped on the MALDI sample probe and dried under dry air stream.

MALDI-TOF mass spectra were obtained on a Bruker Reflex time-of-flight (TOF) mass spectrometer equipped with a delayed extraction optics and a pulsed $N_2$ laser emitting at 337 nm. Figure 2.1 shows a simplified layout of the instrumentation [9]. The laser attenuation was adjusted to slightly above the threshold value. The positive signal was accumulated for about 150 shots until an acceptable signal/noise ratio was obtained. Polyethylene glycol was used for external calibration.

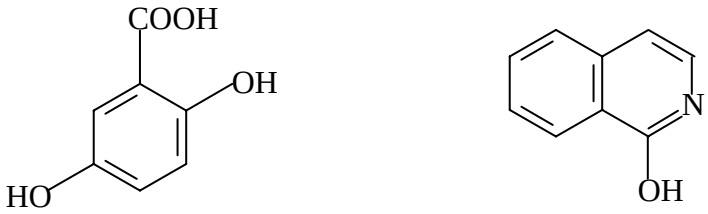


2, 5-dihydroxybenzoic acid (DHB) 1-hydroxyisoquinoline(HIQ)

Scheme 2.1 Chemical structures of matrices

**LC/MS**

Poly(maleic acid) samples prepared from ammonium salts were also analyzed by LC/ESI/MS. The experiment was accomplished using a Perkin Elmer Sciex API I Plus liquid chromatography-quadruple mass spectrometer. Figure 2.2 shows a simplified layout of the electrospray ionization interface to the quadrupole mass analyzer. Separation was performed at room temperature using a Kromasil $C_{18}$ column (Keystone, 250x1 mm, dp 5.0 μm, pore size 10 nm) with a flow rate of 30 μL/min, of which 20 μL

of column eluent was split and delivered to the mass spectrometer. The samples were prepared in water with a concentration about 0.4% (*w/w*). 20 μL solution was injected to LC column and eluted out in 0.1% TFA aqueous mobile phase. Mass spectral signals were obtained in a mass range of m/z 100-1500 with 4.0 kV spray potential. Positive mass spectral signals were obtained for all samples because it was found the samples gave better signals in positive mode than in negative mode. UV signals were recorded at 220 nm.

**NMR**

All polymerization products were analyzed by NMR without any purification. The polymer samples were made as concentrated as possible (~15-20% *w/w*) in water, and pH was adjusted to near 9.0 with NaOH in order to optimize the signal separation and the longitudinal relaxation times [3, 4]. All NMR measurements were made using a 5.0 mm sample tube with a coaxial capillary tube containing $D_2O$ as lock solvent. The arrangement avoided spectral complexity caused by H-D exchange.

$^{1}H$, $^{31}P$, and 2D-$^{31}P$ NMR spectra were acquired at room temperature on a Bruker AMX400 multi-nuclear spectrometer operating at 400.13 MHz for proton and 161.98 MHz for phosphorus. Water signal was suppressed in $^{1}H$ experiments by presaturation. The $^{31}P$ was decoupled during $^{1}H$ acquisition by GARP[5] sequence with a 90 degree decoupling pulse of 70 μs, while $^{1}H$ was decoupled in $^{31}P$ experiments using Waltz [6] sequence with 90 degree pulse of 110 μs. 2D-HMQC (heteronuclear multi-quantum coherence) [20] was collected using $^{1}H$-$^{31}P$ J coupling of 490 Hz measured in $^{31}P$ spectra. Long range $^{1}H$-$^{31}P$ coupling of 10 Hz was used in 2D-HMBC (heteronuclear multi-

bond correlation) [7] experiment. The chemical shift of $^{31}P$ spectra was referenced externally to 85% phosphoric acid.

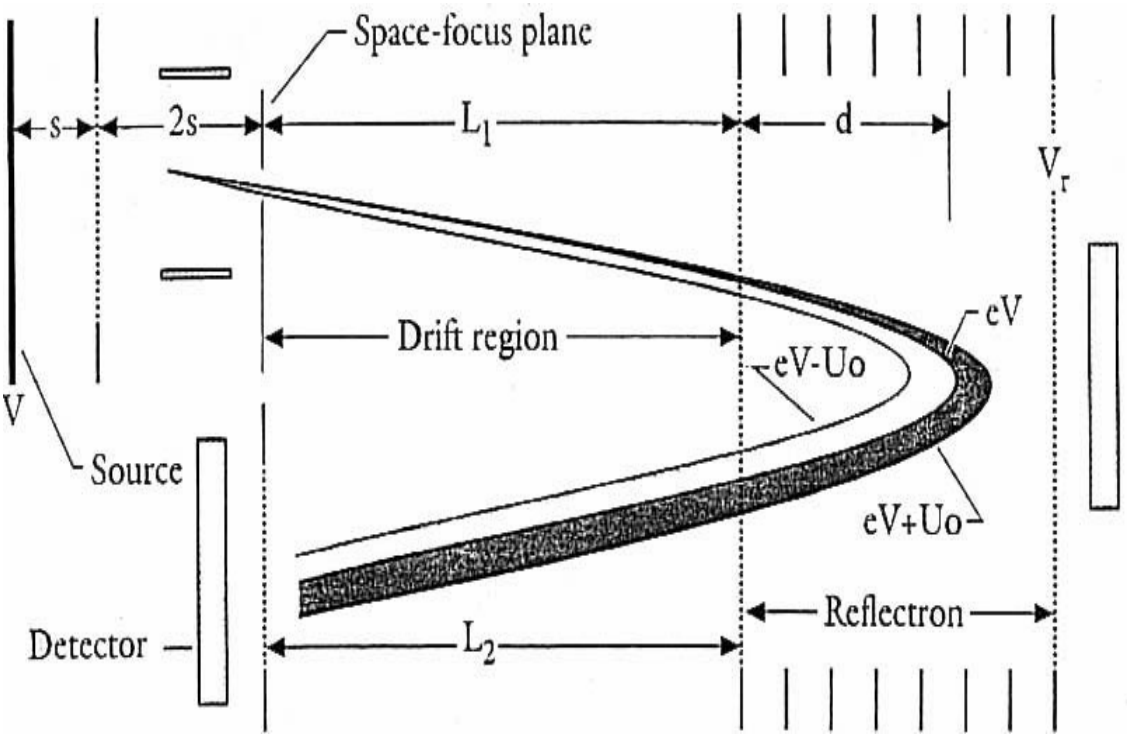


Figure 2.1 Scheme of a configuration for a single-stage ion extraction and single-stage ion reflection time-of-flight mass spectrometer [9]

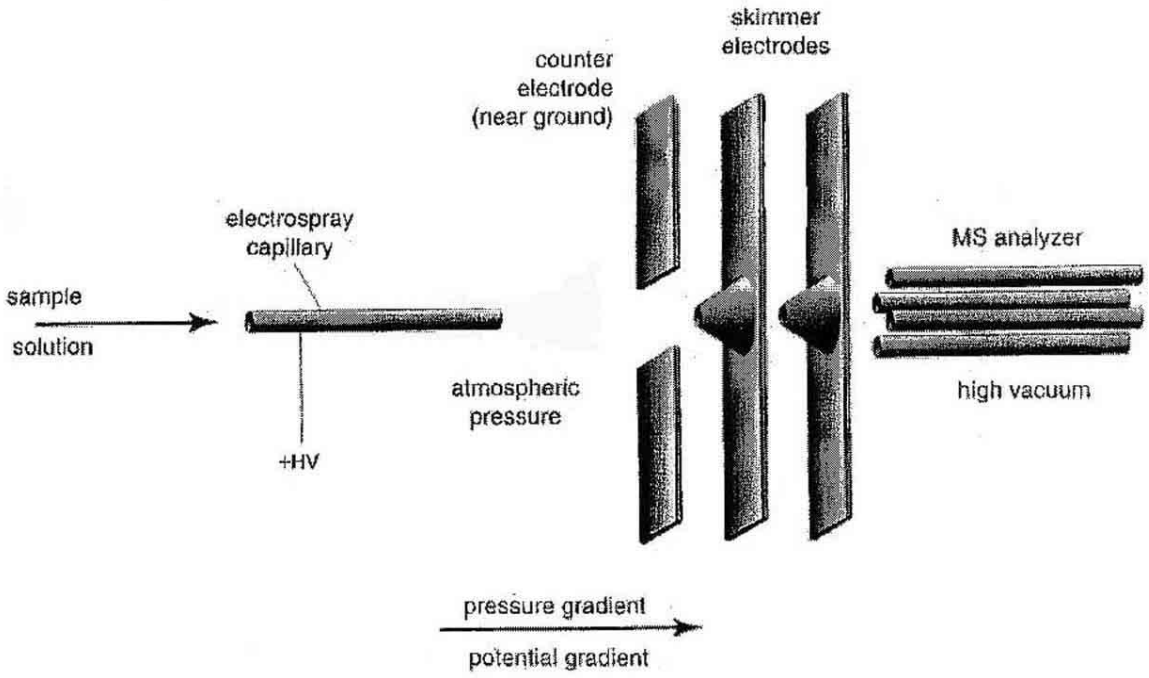


Figure 2.2 Scheme for electrospray coupling to Quadrupole mass analyzer [10]

## REFERENCES


1. Mohr, M.D, Börnsen, K.O, Widmer, H. M., *Rap. Comm. Mass Spectrom*. 9:809-814 (1995)
2. Xu, G., Mize, T.,Yang, C. Q., Amster, I. J., *Proc. 49th ASMS Conf Mass Spectrom Allied Topics*, Chicago, IL (2001)
3. Ruben, I.B., *Anal. Lett*. 17:1259 (1984)
4. Glonek, T., Wang, P. J., Van Wazer, J. R., *J. Am. Chem. Soc*. 98:7968 (1976)
5. Shaka, A. J., Barker, P. B., and Freeman, R., *J. Magn. Reson*. 64, 547-552 (1985).
6. Shaka, A. J., Keeler, J., Frenkiel, T., and Freeman, R., *J. Magn. Reson*., 52, 335 (1983)
7. Bax, A., Griffey, R.H. and Hawkins, B.L., *J. Magn. Reson*., 55, 301(1983)
8. Bax, A. and Subramanian, S., *J. Magn. Reson*. 67, 565 (1986)
9. Cotter, R.J., Ed., "*Time-of-flight mass spectrometry*", American Chemical Society Washington, DC, 1994, p54.
10. Gaskell, S.J., *J. Mass Spectrom.* 32:677-688 (1997).

# CHAPTER 3

# MASS SPECTROSCOPY AND NUCLEAR MAGNETIC RESONANCE STUDIES OF THE MECHANISM OF AQUEOUS POLYMERIZATION OF MALEIC ACID [1]

[1] Guozhong Xu, Xudong Jia, Charles Yang, Jon Amster. To be submitted to *Macromolecules*

# INTRODUCTION

Mass spectrometry has found increasing use for the characterization and analysis of synthetic polymers [1]. Matrix-assisted laser desorption/ionization (MALDI) is a soft ionization technique that produces singly charged ions of very high mass with minimum fragmentation [2]. The technique provides information on the average molecular weight, molecular weight distribution, composition of end-groups and repeating units, composition distribution in copolymers, and even additives or impurities for a wide variety of polymers [1, 3, 4]. It has been also used to monitor polymerization and analyze free radical propagation rate coefficient [5], chain transfer coefficient [6], and mode of chain termination [7]. ESI [8] is another soft ionization technique for soluble synthetic polymers. ESI possesses high ionization efficiency and generates multiple charged ions for large biomolecules to allow the analysis of higher mass species in mass spectrometers with limited m/z range. The propensity for multi-charging increases the complexity of mass spectra for polydisperse synthetic polymers [1]. Even though the complex spectra can be deconvoluted in high resolution mass spectra such as those obtained from FT-ICR [9], ESI is generally used for low MW oligomers [10]. In this particular study, MALDI-TOF-MS and LC/ESI/MS are applied for the characterization of low molecular weight poly(maleic acid) and the elucidation of the mechanism of aqueous polymerization of maleic acid in the presence of hypophosphite.

Maleic acid has been commonly believed to be extremely difficult to homopolymerize [11]. The reluctance of maleic acid to polymerize is due to its severe steric hindrance and polar effects of the carboxylic acid groups. As a consequence, poly(maleic acid) (PMA), a versatile low molecular weight polymer with many practical

and potential uses, is conventionally prepared by hydrolysis of poly(maleic anhydride), which is synthesized by polymerization of maleic anhydride from organic solvents such as benzene and acetic anhydride. However, it has been recently reported that maleic acid was able to undergo free radical homopolymerization in the presence of sodium hypophosphite ($NaH_2PO_2$) [12]. The polymerization was monitored by FT-Raman spectroscopy. It was found that the carbon-carbon double bond of maleic acid disappeared when a solution of 40% maleic acid, 20% sodium hypophosphite, and 2.0% potassium persulfate ($K_2S_2O_8$) was heated at 90$^{o}$C. No characterization of the product polymer was performed. The resulted PMA was found to be more efficient for crosslinking cellulose than the current industrial product [13]. Characterizing the produced polymer and understanding of the mechanism of polymerization is invaluable for controlling the polymerization process and optimizing the product for different purposes.

It is expected that hypophosphite plays a key role in the polymerization of maleic acid. $^{31}$P-NMR should be very valuable for investigating the reactions of hypophosphite, defining the way that phosphorus incorporates into the PMA oligomers. Under appropriate conditions readily achieved in the NMR operation, the peak areas associated with various species are proportional to the relative distribution of phosphorus in the mixture [14]. So, $^{31}$P-NMR can generate quantitative information for various phosphorus-containing PMA oligomers. NMR and mass spectrometry together provide complementary information for characterization of the oligomers and elucidation of the polymerization mechanism.

The paper will focused on the characterization of poly(maleic acid) synthesized by aqueous polymerization in the presence of hypophosphite and elucidation of mechanism of polymerization by use of MALDI-TOF-MS, LC/MS, $^{31}P$ and $^{1}H$-NMR.

## EXPERIMENTAL SECTION

### Materials

Maleic acid (MA), sodium hypophosphite (SHP), ammonium hypophosphite (AHP), potassium persulfate (PPS), 2, 5-dihydroxy benzoic acid (DHB), and 1-hydroxy isoquinoline (HIQ) were purchased from Aldrich Chemical Co. (Milwaukee, WI) Ammonium persulfate (APS), HPLC-grade acetonitrile (ACN), and trifluoroacetic acid (TFA) came from J. T. Baker Inc. (Phillipsburg, NJ). All chemicals except acetonitrile were reagent grade and used without any further purification.

### Polymerization of Maleic Acid

PMA(1). In a three-neck flask equipped a condenser, a magnetic stirrer, and a $N_2$ inlet, 25.0 g maleic acid, 11.4 g $NaH_2PO_2$, and 61.1 g deionized water were added. The system was purged with $N_2$. The temperature was controlled by a circulating water bath. When the reaction mixture became a clear solution upon heating to 65$^{o}$C, 2.46 g $K_2S_2O_8$ was added in several portions during polymerization. The reaction was maintained at 65$^{o}$C for 7 hours and monitored by FT-Raman spectroscopy until the characteristic C=C stretch at 1650 $cm^{-1}$ and =C-H stretch at 3050 $cm^{-1}$ of maleic acid disappeared.

PMA(2) and PMA(3). In the 10 mL reaction vials with a small magnetic stirrer, maleic acid, $NH_4H_2PO_2$, $(NH_4)_2S_2O_8$, and deionized water were added. The vials were purged by $N_2$ through a syringe needle. The vials were loaded in a Pierce Reacti-Therm

Heating Stirring Module kept at 55°C. The reaction is monitored by FT-Raman spectroscopy until all maleic acid was consumed in around 7 hours. The additional amounts of reactants and molar ratios were shown in Table 3.1.

Table 3.1. The amounts and molar ratios of reactants for preparation of three PMA oligomers

| PMA | MA/$H_2PO_2^-$ | MA/$S_2O_8^{2-}$ | MA (g) | $NaH_2PO_2$ (g) | $NH_4H_2PO_2$ (g) | $K_2S_2O_8$ (g) | $(NH_4)_2S_2O_8$ (g) | Total solution (g) |
|---|---|---|---|---|---|---|---|---|
| 1 | 2:1 | 23:1 | 25.0 | 11.40 | N/A | 2.50 | N/A | 100 |
| 2 | 2.5:1 | 20:1 | 2.00 | N/A | 0.5724 | N/A | 0.1967 | 5.0 |
| 3 | 2:1 | 30:1 | 2.00 | N/A | 0.7155 | N/A | 0.1311 | 5.0 |

**Further Oxidation of Poly(maleic acid)**

For investigation of end-group and structure of the PMA oligomer, one of the above prepared samples, PMA(3) was further oxidized. In a 10 mL reaction vial with a small magnetic stirrer, 1.0 g PMA(3) solution (40%), 0.1815 g $(NH_4)_2S_2O_8$ were added. The molar ratio between maleic acid unit and the added persulfate was 4:1. The vial was heated on a Pierce Reacti-Therm Heating Stirring Module at 70°C for 7 hours.

**Sample Treatment for Mass Spectroscopic Analysis**

PMA(2) and PMA(3) were synthesized from ammonium salts and were analyzed by mass spectroscopy and NMR without further purification. PMA(1) was synthesized from sodium and potassium salts and was desalted by ion exchange. The ion exchange column was made of a PTFE tube of 50 cm length and 2.0 mm internal diameter packed with $HNO_3$-treated DOWEX 50WX4-200 acidic exchange resin (100-200 mesh, Aldrich) and rinsed with deionized water to pH 7.0. The tube was connected with a 0.25 μm Nylon syringe filter (Whatman) and a syringe. 15 μL PMA solution was dropped into the PTFE tube and then 3.0 mL water was injected slowly into the tube to elute the sample. By

testing with pH paper, the first and last portions of column eluent with neutral pH were discarded. About 1.5 mL of the middle part of the eluent shown on acidic pH, and was retained for analysis by MALDI-TOF-MS.

**MALDI-TOF-MS**

The matrix solution was prepared by dissolving 15.4 mg DHB and 4.35 mg HIQ in 1.0 mL ACN/$H_2O$ (1:1, v/v) [15]. The matrix also gave excellent signals for low molecular weight polycarboxylic acids [18]. The PMA(1) solution after ion exchange had a concentration around 4.0 mg/mL, and was used directly. PMA(2) and PMA(3) were diluted to 5.0 mg/mL with ACN/$H_2O$. 10 μL PMA solution and 10 μL matrix were premixed in a 0.25 mL tube, and 1.0 μL mixed solution was deposited on the MALDI sample probe and dried under dry air stream.

MALDI-TOF mass spectra were obtained on a Bruker Reflex time-of-flight (TOF) mass spectrometer equipped with delayed extraction optics and a pulsed $N_2$ laser emitting at 337 nm. All samples were analyzed in reflection mode and positive ions were analyzed. The laser attenuation was adjusted to slightly above the threshold value. The signal was accumulated for about 150 shots until an acceptable signal/noise ratio was obtained. Polyethylene glycol was used for external calibration.

**LC/MS**

PMA(2) and PMA(3) were analyzed by LC/ESI/MS using a Perkin Elmer Sciex API I Plus liquid chromatography-quadrupole mass spectrometer. Separation was performed at room temperature using a Kromasil $C_{18}$ column (Keystone, 250x1 mm, dp 5.0 μm, pore size 10 nm) with a flow rate of 30 μL/min, of which 20 μL of column eluent was split to the mass spectrometer. The samples were prepared in water at a

concentration about 0.4% (*w/w*). 20 μL solution was injected onto the LC column and eluted out in 0.1% TFA aqueous mobile phase. Mass spectral signals were obtained in a mass range of m/z 100-1500 with 4.0 kV spray potential. Positive mass spectral signals were obtained for all samples because it was found the samples gave better signals in positive mode than in negative mode. UV signals were recorded at 220 nm.

**NMR**

The PMA samples were made as concentrated as possible (~15-20%) in water and pH was adjusted to 9.0 with NaOH in order to optimize the signal separation and the longitudinal relaxation times [16,17]. All NMR measurements were made using a 5.0 mm sample tube with a coaxial capillary tube containing $D_2O$ as the lock solvent. The arrangement avoided spectral complexity caused by H-D exchange.

$^{1}H$, $^{31}P$, and 2D-$^{31}P$ NMR spectra were acquired at room temperature on a Bruker AMX400 multi-nuclear spectrometer operating at 400.13 MHz for proton and 161.98 MHz for phosphorus. Water signal was suppressed in $^{1}H$ experiments by presaturation. The $^{31}P$ was decoupled during $^{1}H$ acquisition by GARP[18] sequence with a 90 degree decoupling pulse of 70 μs, while $^{1}H$ was decoupled in $^{31}P$ experiments using Waltz [19] sequence with 90 degree pulse of 110 μs. 2D-HMQC (heteronuclear multi-quantum coherence) [20] was collected using $^{1}H$-$^{31}P$ J coupling of 490 Hz. Long range $^{1}H$-$^{31}P$ coupling of 10 Hz was used in 2D-HMBC (heteronuclear multi-bond correlation) [21] experiment. The chemical shift of $^{31}P$ spectra was referenced externally to 85% phosphoric acid.

# RESULTS AND DISCUSSION

## MALDI-MS

Characterization of molecular weight, analysis of end-groups and repeating unit are the first step toward the understanding of the mechanism of polymerization. MALDI-MS is the most powerful tool for end-group analysis and structure confirmation for synthetic polymers. Figure 3.1 shows the MALDI-TOF mass spectrum of PMA(2). The signals of PMA(2) are assigned in Table 3.2. A homologous series at m/z 205, 321, 437, 553, 669, and 785 is clearly observable. This series confirms the repeat unit of maleic acid, 116 Da. These signals can be expressed by following formula:

$$[M+Na]^+ = 116n+89 = 116n+66+23$$

where n is the degree of polymerization, 23 indicates the sodium-cationization, and 66 equals to the molecular weight of hypophosphorus acid $H_3PO_2$. Because the hypophosphite has two active protons, poly(maleic acid) has two possible structures, monoalkyl phosphinate, which has end-group $H_2PO_2-$, or dialkyl phosphinate, in which $-HPO_2-$ is located in the middle of oligomers with succinic acid repeating units at both sides, as shown in Scheme 3.1.

The signals at m/z 393, 509, and 625 m/z, which are 44 Da lower than the above principal peaks, result from the loss of $CO_2$. The peaks at m/z 459 and 575, which are 22 Da higher than the peaks at m/z 437 and 553, result from the substitution of a proton by a second Na. The peak at m/z 337, which is 16 mass units higher than peak m/z 321, suggests the existence of monoalkyl phosphonate poly(maleic acid) oligomers (Scheme 3.1) and is confirmed by $^{31}$P-NMR as shown below. The NMR data preclude the other possible interpretation of 16 Da, namely that $Na^+$ is replaced by $K^+$. The phosphonate

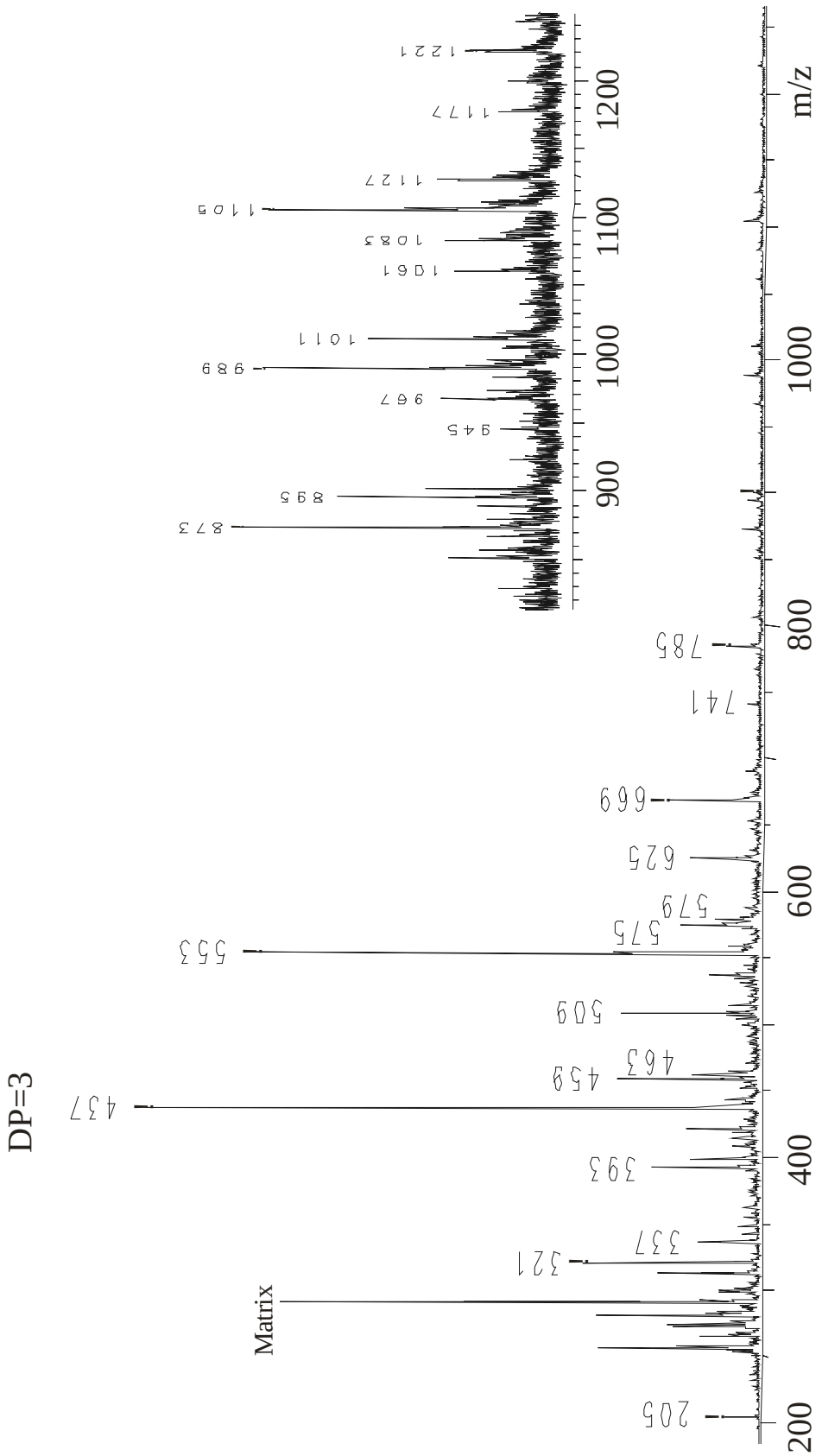


Figure 3.1 MALDI-TOF-MS spectrum of PMA(2)

Monoalkyl phosphinate

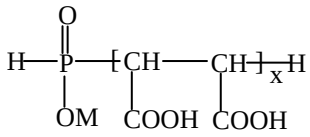

Dialkyl phosphinate

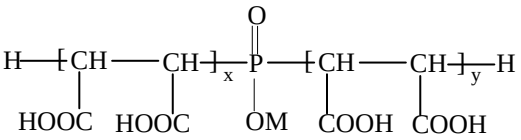

Monoalkyl phosphonate

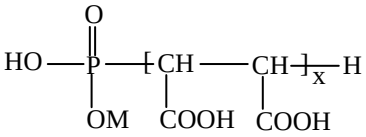

M = H, Na, or $NH_4$
x, y = 1, 2, 3, et al.

Scheme 3.1 Structure of poly(maleic acid) oligomers

may result either from the oxidation of phosphinate or from the free radical reaction of phosphite with maleic acid monomers as discussed below. The two peaks at m/z 463 and 579 are 26 mass units higher than m/z 437 and 553, or 90 mass units lower than m/z 553 and 669, respectively, possibly arise from the side reaction of the poly(maleic acid) oligomers as will be discussed below.

The weak signals at m/z 873, 989, 1105, and 1221 also exhibit a mass increment of 116 Da, and have a residual mass 61 or 167 Da. If these signals were generated from the oligomers with two end-groups as a result of recombination termination of growing chains, they should have a mass residual of 65+65+23=153 or 65+87+23=175 Da ($H_2PO_2^-$ = 65, $NaHPO_2^-$ = 87). These peaks instead appear to be MALDI artifact, from dimerization of analyte.

Table 3.2 Assignment of MALDI-TOF-MS signals of PMA(2)

| Mass | DP | Assignment |
|---|---|---|
| 205 | 1 | $H_2O_2P–(MA)–H + Na^+$ |
| 250-315 | | Matrix signals |
| 321 | 2 | $H–(MA)_x–PO_2H–(MA)_y–H + Na^+$, x+y=2 ; x, y=0, 1, 2 |
| 337 | 2 | $H_2O_3P–(MA)_2–H + Na^+$ |
| 393 | 3 | Peak 437-$CO_2$ |
| 437 | 3 | $H–(MA)_x–PO_2H–(MA)_y–H + Na^+$, x+y=3 ; x, y=0, 1, 2, 3 |
| 459 | 3 | $H–(MA)_x–PO_2H–(MA)_y–H + 2Na^+–H^+$, x+y=3 ; x, y=0, 1, 2, 3 |
| 463 | 4 | Peak 553-46-44 |
| 509 | 4 | Peak 553-$CO_2$ |
| 553 | 4 | $H–(MA)_x–PO_2H–(MA)_y–H + Na^+$, x+y=4 ; x, y=0, 1 to 4 |
| 575 | 4 | $H–(MA)_x–PO_2H–(MA)_y–H + 2Na^+–H^+$, x+y=3 ; x, y=0, 1 to 4 |
| 579 | 5 | Peak 669-46-44 |
| 625 | 5 | Peak 669-44 |
| 669 | 5 | $H–(MA)_x–PO_2H–(MA)_y–H + Na^+$, x+y=5 ; x, y=0, 1 to 5 |
| 691 | 5 | $H–(MA)_x–PO_2H–(MA)_y–H + 2Na^+–H^+$, x+y=5 ; x, y=0, 1 to 5 |
| 785 | 6 | $H–(MA)_x–PO_2H–(MA)_y–H + Na^+$, x+y=6 ; x, y=0, 1 to 6 |
| 873 | Dimer | 437x2-1, or 321+553-1 |
| 989 | Dimer | 437+553-1, or 321+669-1 |
| 1105 | Dimer | 553x2-1, 437+669-1, or 321+785-1 |
| 1221 | Dimer | 437+785-1, or 553+669-1 |

The MALDI-MS spectrum of PMA(1) is presented in Figure 3.2. The spectrum is similar to that of PMA(2) except that it has fewer high mass species. The lack of higher mass oligomers is attributed to more frequent chain transfer as result of more hypophosphite used, which will be discussed later.

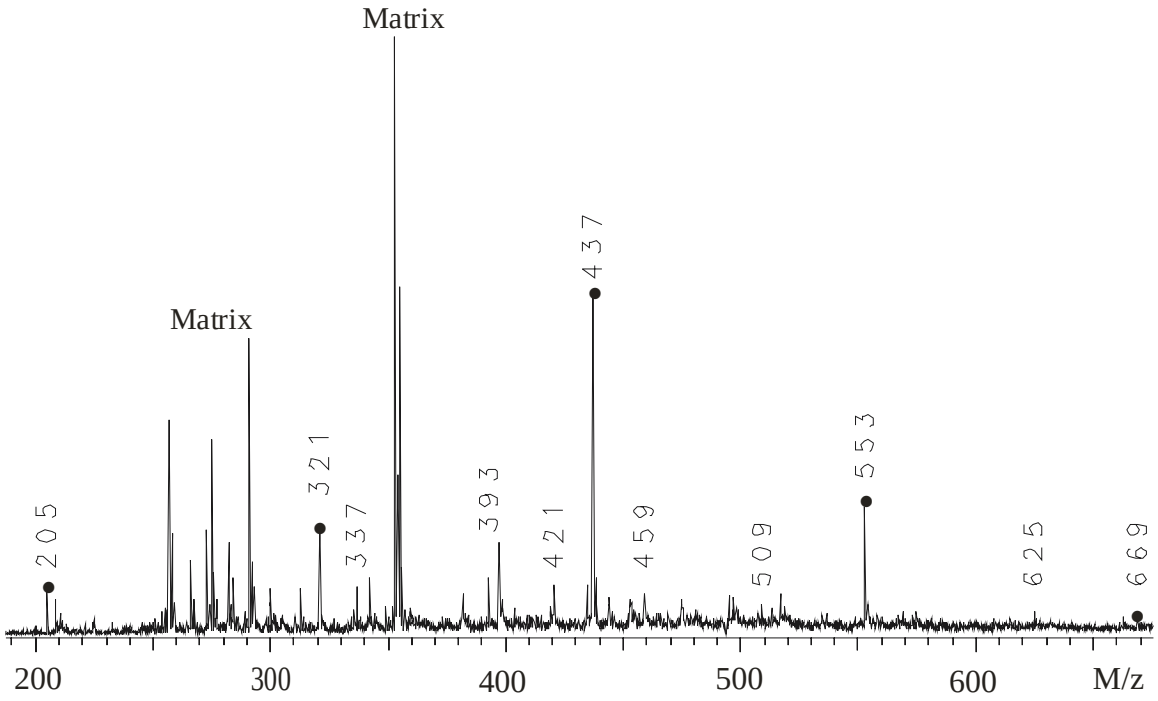


Figure 3.2 MADLI-TOF-MS spectrum of PMA(3) after ion exchange

**LC/MS**

Poly(maleic acid) oligomers have low molecular weights, and MALDI matrix may suppress the low mass signals. In the case of polycarboxylic acid, MALDI requires a relatively high concentration (>2.0 mg/mL) to produce the signal, some minor components produced during the polymerization may be missing in the MALDI spectrum. The liquid chromatography coupling to mass spectrometry is ideal for

separation and analysis of complex reaction products. When it is used for low MW oligomers, it will not only confirm the result of end-groups and repeating unit obtained from MALDI-MS, but also provides the information of side reactions taking place during polymerization. The LC/MS spectrum containing all signals of the PMA(2) components is presented in Figure 3.3.

The LC/MS data are consistent with the result of MALDI-TOF-MS. The homologous peaks at m/z 183, 299, 415, 531, and 647 with a mass spacing of 116 Da correspond to the poly(maleic acid) of degree of polymerization (DP) from 1 to 5. This series of signals have a mass residual of 67 Da, which confirms that poly(maleic acid) oligomers are either monoalkyl phosphinate or dialkyl phosphinate as shown in Scheme 3.1. The peaks at m/z 200, 316, 432, and 548 are 17 mass units higher than the first series, and result from the substitution of one proton by an ammonium ion. Those peaks that are 18 or 36 mass units lower than the first series are produced by loss of one or two water molecules. The peaks at m/z 199 and 315, which are 16 mass units higher than peaks at m/z 183 and 299 respectively, are monoalkyl phosphonates. The monoalkyl phosphonates can be produced either by reaction of phosphite radical with one or two maleic acid molecules, or by oxidization of corresponding monoalkyl phosphinates by $(NH_4)_2S_2O_8$, as will be discussed later. The assignment of the peaks is shown in Table 3.3.

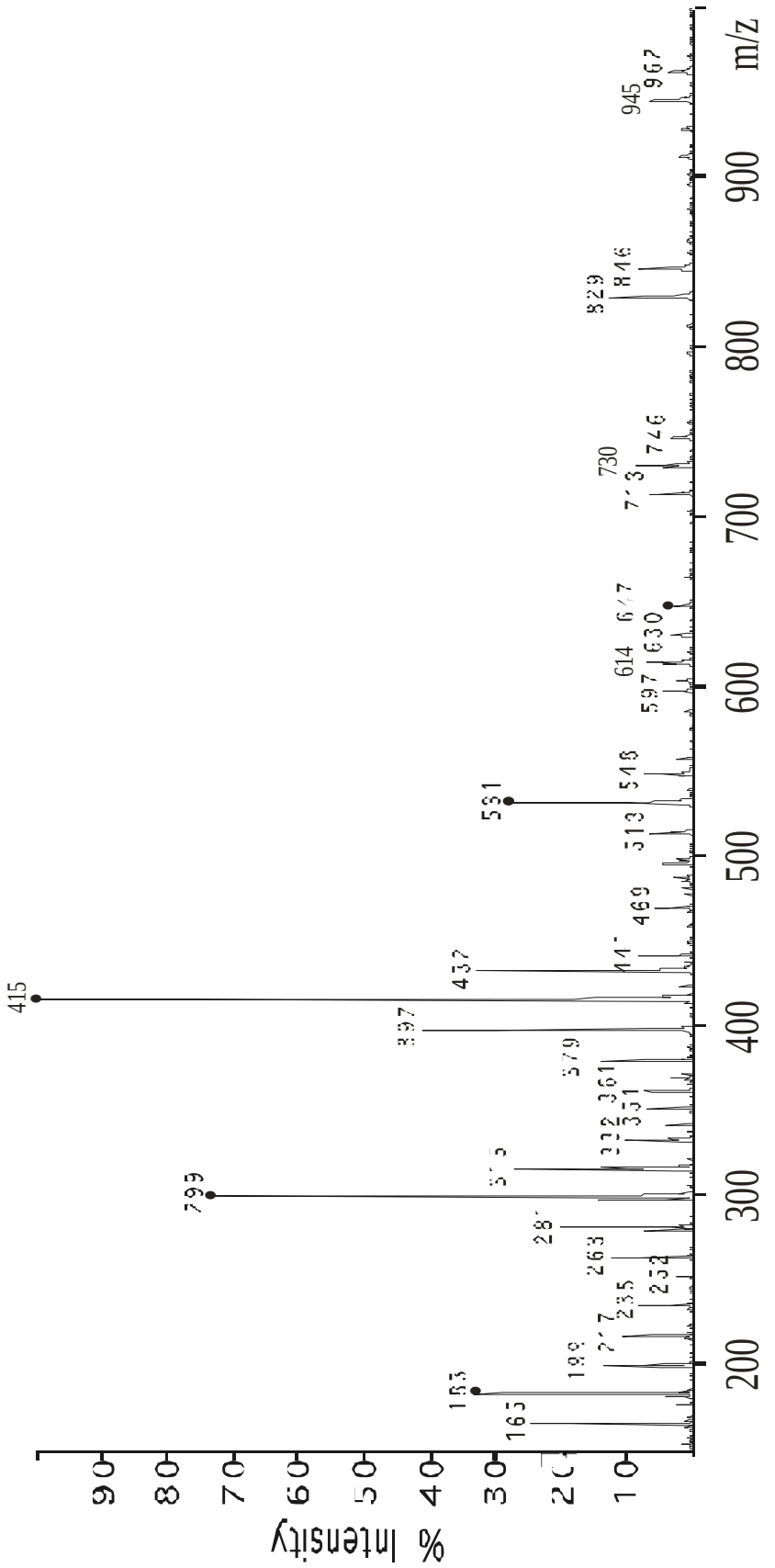


Fig 3.3 LC/MS spectrum of PMA(2)

Table 3.3 Assignment of LC/MS signals of PMA(2)

| Mass | DP | Assignment |
|---|---|---|
| 165 | 1 | Peak 183-$H_2O$ |
| 183 | 1 | $H_2O_2P$–(MA)–H + $H^+$ |
| 199 | 1 | $H_2O_3P$–(MA)–H + $H^+$ |
| 217 | 1 | 198+ $NH_4^+$ |
| 235 | 2 | Peak 299-46-$H_2O$ |
| 263 | 2 | Peak 299-2$H_2O$ |
| 281 | 2 | Peak 299-$H_2O$ |
| 299 | 2 | H–$(MA)_x$ –$PO_2H$–$(MA)_y$ –H + $H^+$, x+y=2; x, y=0, 1, 2 |
| 315 | 2 | $H_2O_3P$–$(MA)_2$–H + $H^+$ |
| 332 | 2 | 314 + $NH_4^+$ |
| 351 | 3 | Peak 415-46-$H_2O$ |
| 361 | 3 | Peak 415-3$H_2O$ |
| 379 | 3 | Peak 415-2$H_2O$ |
| 397 | 3 | Peak 415-$H_2O$ |
| 415 | 3 | H–$(MA)_x$ –$PO_2H$–$(MA)_y$ –H + $H^+$, x+y=3; x, y=0, 1, 2, 3 |
| 432 | 3 | 414+ $NH_4^+$ |
| 441 | 4 | Peak 531-46-$H_2O$ |
| 469 | 4 | Peak 531-$CO_2$-$H_2O$ |
| 513 | 4 | Peak 531-$H_2O$ |
| 531 | 4 | H–$(MA)_x$ –$PO_2H$–$(MA)_y$ –H + $H^+$, x+y=4; x, y=0, 1 to 4 |
| 548 | 4 | 530+ $NH_4^+$ |
| 597 | Dimer | 298x2+$H^+$ |
| 614 | Dimer | 298x2 + $NH_4^+$ |
| 630 | Dimer | 298+314 + $NH_4^+$ |
| 647 | 5 | H–$(MA)_x$ –$PO_2H$–$(MA)_y$ –H + $H^+$, x+y=5; x, y=0, 1 to 5 |
| 713 | Dimer | 414+298+$H^+$ |
| 730 | Dimer | 414+298+ $NH_4^+$ |
| 746 | Dimer | 414+314+ $NH_4^+$ |
| 829 | Dimer | 414x2+ $H^+$ |
| 846 | Dimer | 414x2+ $NH_4^+$ |
| 945 | Dimer | 414+530+ $H^+$ |
| 962 | Dimer | 414+530+ $NH_4^+$ |

**1D-$^{31}$P-NMR**

Hypophosphite plays a key role in the polymerization of maleic acid. Without hypophosphite, maleic acid does not polymerize but isomerizes to fumaric acid and precipitates out of the aqueous solution [22]. Therefore, $^{31}$P-NMR was used to investigate the reaction of hypophosphite. Both chemical shift and spin splitting provide valuable structural information for phosphorus-containing compounds [23]. Even though $^{31}$P chemical shifts have been observed over a range exceeding 1000 ppm, the phosphoryl derivatives, such as in the study, generally give signals within a narrow range going from -50 to 90 ppm [23].

The signals in a $^{31}$P-NMR spectrum may show fine structure due to spin-spin splitting as a result of resonance interaction between a given phosphorus nucleus with other magnetically active nuclei such as proton through the electronic structure in the molecule [23]. The effect of coupling is to split the individual peaks of $^{31}$P-NMR spectrum into smaller multiplets of the same total intensity. The multiplicity of a $^{31}$P peak due to the first order splitting is given by $(2nI+1)$, where $I$ is the nuclear spin of the coupled nuclei and equals to 1/2 for proton nuclei. The relative intensity of the (n+1) peaks is governed by the binominal distribution. The coupling constant J denotes the strength of interaction and provides bonding information for the phosphorus atoms in a compound. When a phosphorus atom is directly connected to a hydrogen, the coupling constant J is generally about 200 Hz for triply connected phosphorus, in the range of 400-700 Hz for quadruply connected phosphorus, and even higher for phosphorus exhibiting more than five nearest-neighbor atoms [23, 25]. The presence of one intermediate atom between two spin-coupled atoms greatly reduces the coupling constant

to the range of 15-30 Hz. The long range coupling usually results in unresolved line broadening in the $^{31}P$ spectra rather than the appearance of fine structure. The NMR spectra complicated by spin-spin splitting can be simplified by spin decoupling, which assists in the interpretation of spectra as well as provides additional information.

In Figure 3.4 are the $^{31}P$-NMR proton-coupling and broadband proton decoupling spectra of PMA(2). The satellites in both sides of decoupling peaks in proton-decoupling spectrum result from the incomplete decoupling. The broadband decoupling does not present any technique difficulty in $^{1}H$ and $^{13}C$-NMR. However, it is very difficult for $^{31}P$ owing to wide spectral range, largely different coupling constants (from several Hz to as high as several thousand Hz), and the possible electronic interference between observing and decoupling frequencies [26].

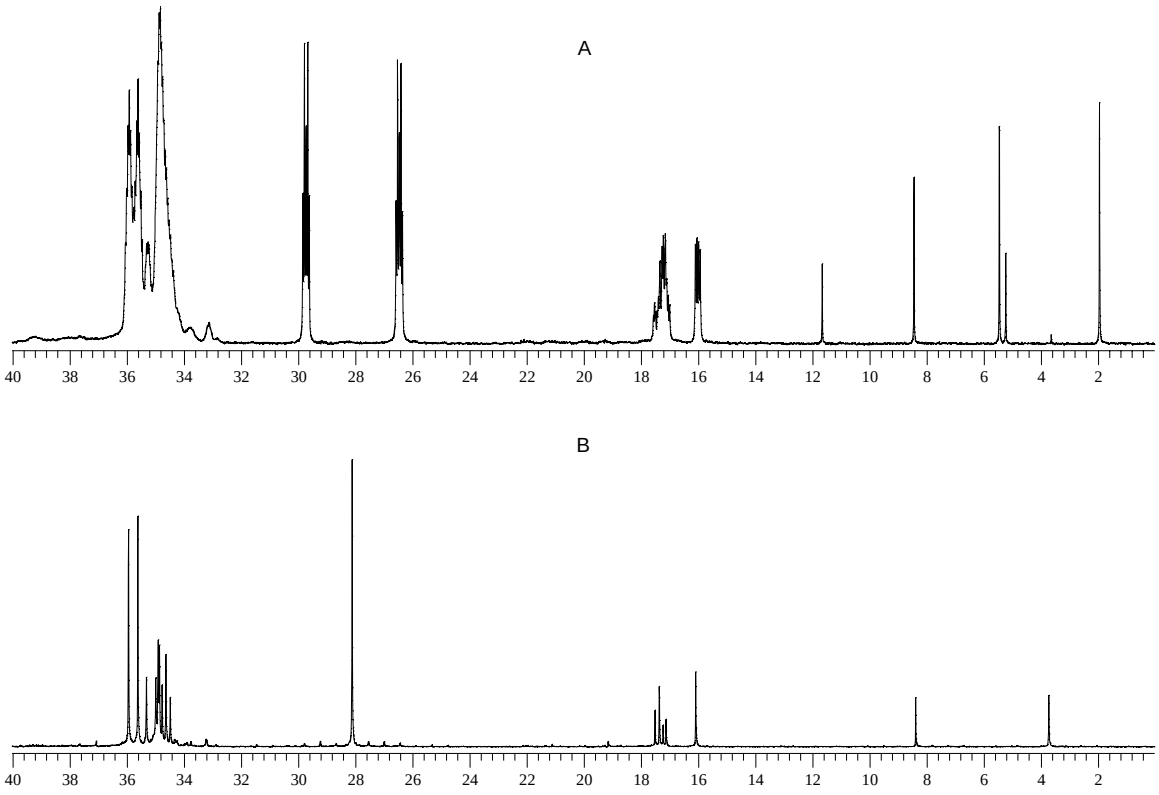


Figure 3.4 $^{31}P$-NMR spectra of PMA(2), Proton (A) coupling and (B) decoupling

The 1:2:1 triple peaks at δ 11.6, 8.4, and 5.2 ppm, which reduce to one peak at δ 8.4 ppm in proton-decoupling spectrum, belong to unreacted hypophosphite. The triple peaks with a large single bond coupling constant $^{1}J(P^{-}H)$ around 520 Hz are a result of strong coupling between the two directly bonded protons and the observing phosphorus atom. The 1:1 doublet peaks at δ 5.46 and 1.96 ppm with a $^{1}J(P\text{-}H)$ ~568 Hz, which become one peak at δ 3.71ppm in H-decoupling spectrum, are produced by phosphite. The weak single peak at δ 4.1ppm belongs to phosphate. The signal assignment of $H_2PO_2^{-}$, $HPO_3^{2-}$, and $PO_4^{3-}$ was confirmed by adding a drop of suspected ingredient to the sample tube, since it is very rare for resonance of two different compounds to be superimposed [27].

The two widely spaced (separation of 529 Hz) quintets at δ between 29.8 and 26.3 ppm collapse into a single peak at 28.1 ppm after proton decoupling. They are generated by a phosphorus atom with a directly connected proton. They are produced by monoalkyl phosphinate, and will be confirmed by 2D spectra and oxidation of the end-groups as shown later. The value of $^{1}J(P\text{-}H)$ in above phosphoryl compounds increases with the increasing electronegativity of proton, alkyl, and hydroxyl groups, as 520 Hz in hypophosphite, 529 Hz in monoalkyl phosphinate, and 568 Hz in phosphite.

The complex signals with chemical shifts between 32 to 40 ppm and between 15.8 to 17.8 ppm do not show any direct P-H coupling. They are simplified but still shown as multiplet peaks in the proton decoupling spectrum. The different peaks in H-decoupling spectrum correspond to phosphorus atoms with different molecular environment. The unresolved broadening lines in the chemical shift between 32 and 40 ppm are a result of long-range phosphorus-hydrogen coupling. These two groups of signals may be

produced by dialkyl phosphinate and monoalkyl phosphonate respectively, but may also by some kinds of inorganic phosphorus complex, which are commonly found in inorganic phosphorus system.

**2D-$^{31}$P-NMR**

To completely assign the signals of $^{31}$P-NMR spectra, 2D $^{31}$P-NMR was employed to analyze the correlation of phosphorus atoms and proton in the polymerization products. There are two groups of protons in the polymerization products, the protons directly bonded on the phosphorus atoms and those connected on the backbone carbon atoms of the poly(maleic acid) oligomers. In $^{1}$H-NMR, the phosphorus-bonded protons are deshielded and give signals at lower field with chemical shift between 5.0 to 8.0 ppm, whereas the saturated carbon-bonded protons produce signals at high field with chemical shift between 1.5 and 3.5 ppm. Because of the huge difference between single-bond P-H coupling constant (>500 Hz) and multi-bond coupling constant (<30 Hz), the correlation between phosphorus and proton through single bond and multi-bond is difficult to be observed at the same time. Therefore, two sorts of 2D-NMR experiments, Heteronuclear Multi-Quantum Coherence (HMQC) and Heteronuclear Multi-Bond Correlation (HMBC), were performed to investigate the directly and indirectly bonded phosphorus-proton coupling. The results were presented in Figures 3.5 and 3.6.

Figure 3.5 is the 2D HMQC $^{31}$P-NMR spectrum of PMA(2) with $^{1}$H-NMR spectrum on the top and proton decoupling $^{31}$P-NMR spectrum on the left side. It reveals the correlation between phosphorus atoms and their directly bonded protons. The proton signals are also widely split by directly connected phosphorus due to strong coupling.

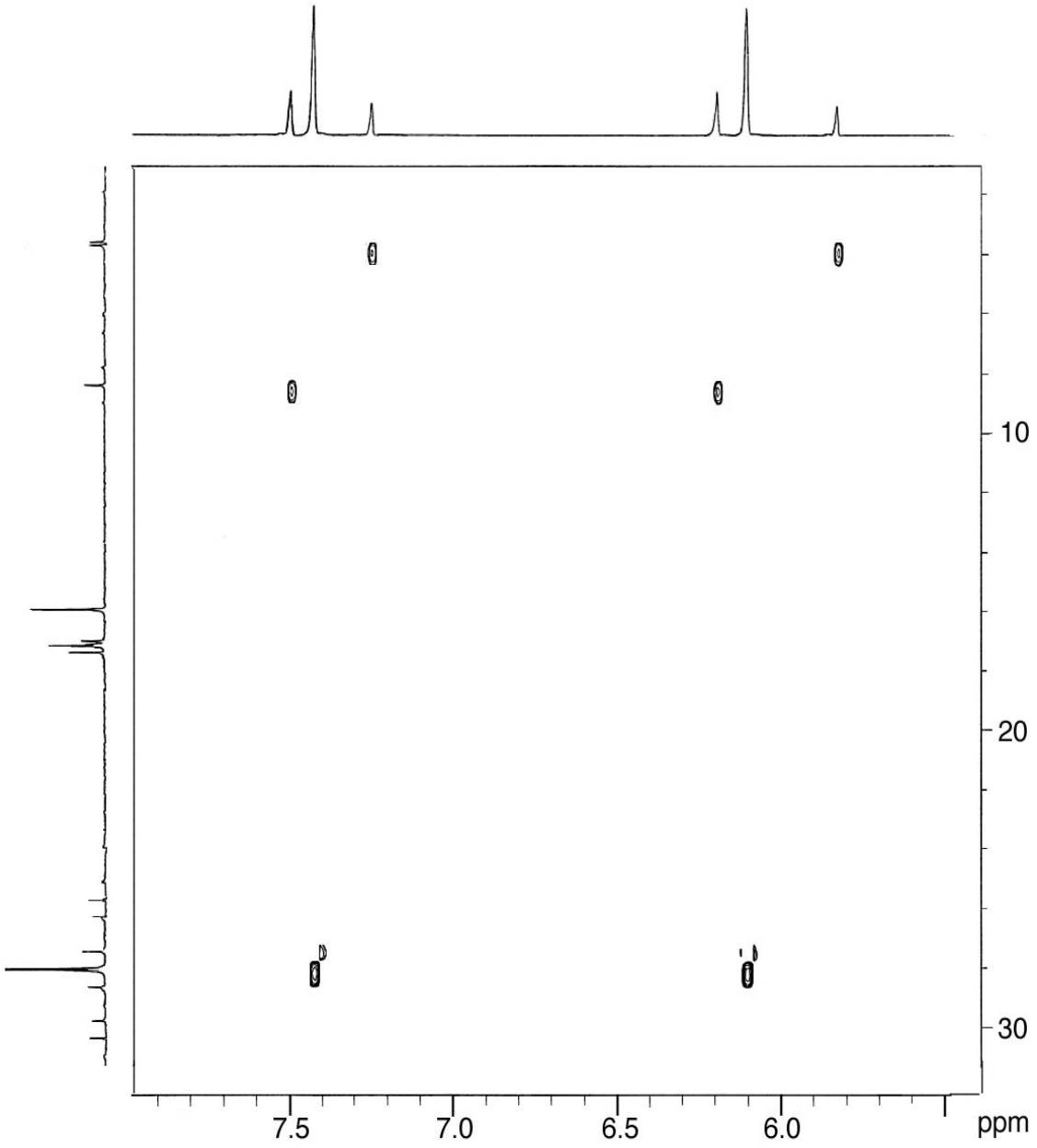


Figure 3.5 2D HMQC $^{31}$P-NMR of PMA(2)

Three couples of proton signals are found in $^{1}$H-NMR. The two proton peaks at δ 5.83 and 7.25 ppm, both coupled to phosphorus at δ 3.71 ppm, are protons on phosphite. The two $^{1}$H peaks at δ 6.20 and 7.49 ppm, coupled to phosphorus at δ 8.37 ppm, come from the two protons on hypophosphite. The another two proton peaks at δ 6.10 and 7.41ppm, coupled to phosphorus at δ 28.2 ppm, belong to monoalkyl phosphinate.

Figure 3.6 presents the 2D-HMBC $^{31}$P-NMR spectrum regarding the coupling between phosphorus with protons through more than one bonds, i.e., the protons bonded to backbone carbon atoms in the poly(maleic acid) oligomers. The $^{1}$H-NMR signals at chemical shift between 2.5 and 3.5 ppm are undoubtedly produced by protons connected to saturated backbone carbon atoms in the poly(maleic acid) oligomers. The detailed assignment of these proton signals is difficult owing to complexity. The coupling of phosphorus signal at δ 28.2 ppm to protons at δ 2.25, 2.5, and 2.70 ppm provides further evidence that this phosphorus belongs to the end-group of monoalkyl phosphinate oligomers. The phosphorus atoms with δ around 35 ppm, with no directly bonded protons, are also strongly coupled to these saturated protons of wide chemical shifts. So, this group of complicated phosphorus signals originate from the dialkyl phosphinate oligomers but not from inorganic phosphorus complex. The last groups of phosphorus signals at δ 15-18 ppm are also coupled to the carbon-bonded protons in the main chain of PMA oligomers, are produced by monoalkyl phosphonate oligomers. Overall, the $^{31}$P and $^{1}$H-NMR signals of PMA(2) are assigned in Table 3.4.

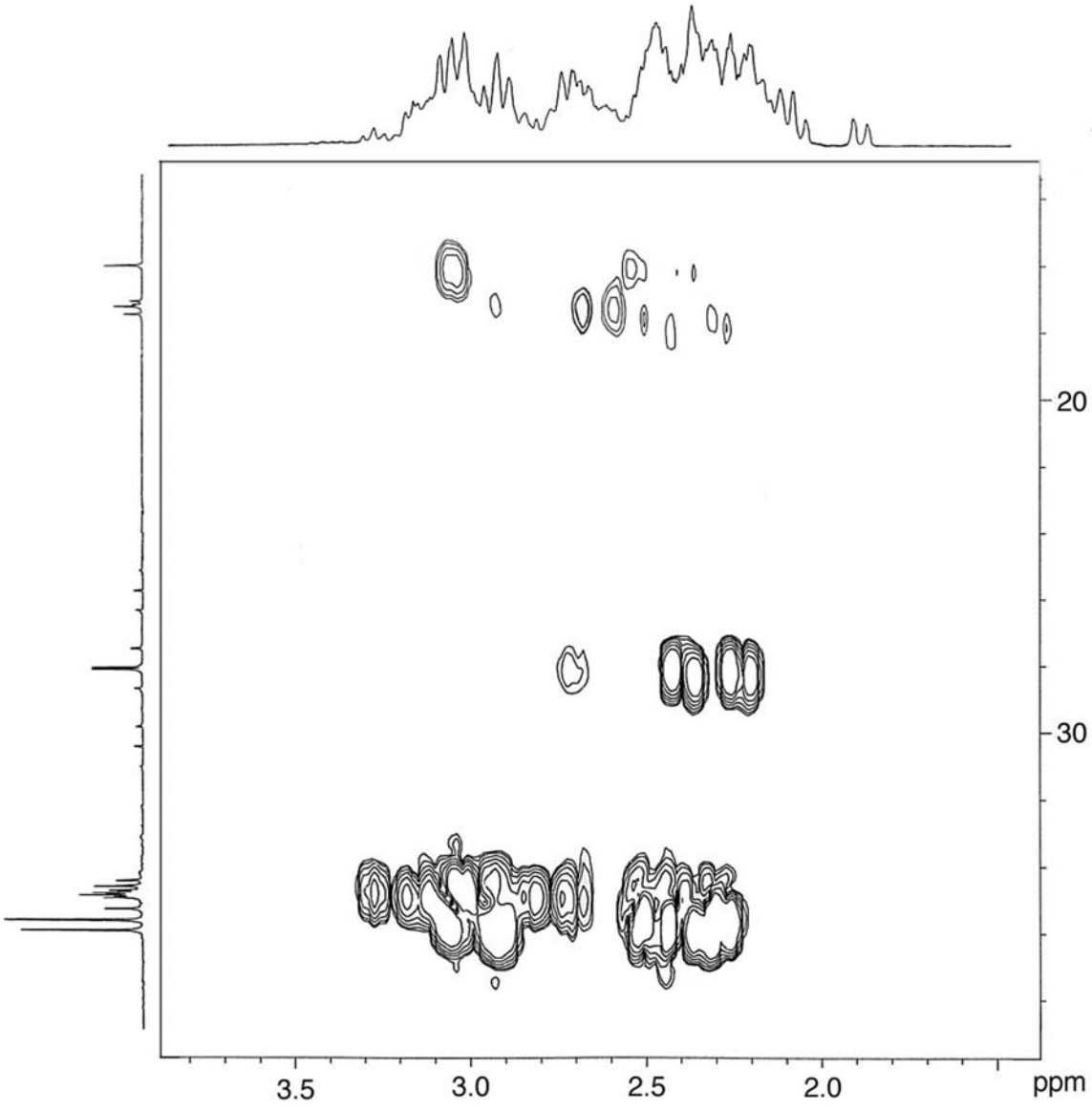


Figure 3.6 2D HMBC $^{31}$P-NMR of PMA(2)

Table 3.4 Assignment of $^{31}P$ and $^{1}H$-NMR signals of PMA(2)

| $^{31}P$ signals, δ (ppm) | $^{1}H$ signals, δ (ppm) | Species |
|---|---|---|
| 36.4-32.8, multi-peaks | | —$PO_2^+$— |
| 30.0-36.4, two quintets | 7.43, 6.01, doublet | $HPO_2^+$— end-group |
| 17.7-15.9, two groups of multi-peaks | | $PO_3^{2+}$ — end-group |
| 11.6, 8.42, 5.2, triplets | 15.0, 6.20, doublet | $H_2PO_2^+$ |
| 5.4, 1.9, doublets | 7.25, 5.83, doublet | $HPO_3^{2+}$ |
| 3.63, singlet | | $H_3PO_4^{3+}$ |
| | 1.8-3.4, multi-peaks | Saturated C–H |

**Composition of Polymerization Products**

$^{31}P$-NMR is useful for mixture analysis on the basis of peak areas, which are proportional to the distribution of associated phosphorus components. PMA(2) and PMA(3) were synthesized with MA/AHP (maleic acid to $NH_4H_2PO_2$) molar ratio of 2.5:1 and 2.0:1, respectively. The relative amounts of different species in the reaction products were analyzed quantitatively based on the $^{31}P$-NMR spectra and shown in Table 3.5.

The majority of product is dialkyl phosphinate. When hypophosphite was used at 50 mol % of maleic acid as in the case of PMA(3), only 6.8% of hypophosphite was left unreacted, 2.5% phosphorus was oxidized into phosphite, about 52.7% of phosphorus was incorporated into dialkyl phosphinate, 30.3% of phosphorus into monoalkyl phosphinate, and less than 5.0% into monoalkyl phosphonate. When the hypophosphite was decreased to 40 mol% of maleic acid, most hypophosphite was consumed, only 1.3% hypophosphite remained unreacted. The amount of monoalkyl phosphinate decreased to 16.5%, as a result of further reaction of the another P-H with free radical and maleic acid to produce more dialkyl phosphinate due to the lack of more reactive hypophosphite. Consequently, dialkyl phosphite increased to 69.4%. The amount of monoalkyl phosphonate also marginally increased.

Table 3.5 Molar distribution of reaction products according to the peak areas of $^{31}$P-NMR spectra. PMA(3)-2 is the result of PMA(3) after further oxidation with 1/4 molar number of ammonium persulfate at 70$^{o}$C for 7 hours

| Component | PMA(2) (%) | PMA25(3) (%) | PMA25(3)-2 (%) |
|---|---|---|---|
| Dialkyl phosphinate | 69.4 | 52.7 | 51.5 |
| Monoalkyl phosphinate | 16.5 | 30.3 | 0.6 |
| Monoalkyl phosphonate(1) | 7.3 | 5.0 | 35.8 |
| Monoalkyl phosphonate(2) | 3.3 | 2.7 | 3.3 |
| Hypophosphite | 1.3 | 6.8 | 0.0 |
| Phosphite | 2.2 | 2.5 | 5.9 |
| Phosphate | 0.005 | 0.0 | 2.9 |

**Free Radical Mechanism of Polymerization**

Radical initiation

The successful analysis of molecular weight distribution, end-group, repeating unit, and oligomer distribution by mass spectroscopy and NMR has provided solid basis for the analysis of mechanism of polymerization. Maleic acid does not polymerize in the absence of either hypophosphite or free radical initiator peroxide. Both hypophosphite and free radical are necessity for the polymerization. Mass spectral and NMR data support unambiguously that the phosphorus was permanently incorporated into poly(maleic acid) oligomers. The fact indicates that the oligomerization of maleic acid invokes the formation and reaction of phosphorus radicals.

Phosphorus compounds can be induced to form radicals directly by thermolysis or photolysis of P-P, P-H, P-Cl, P-O-C, or P-C bonds by gain or loss of an electron to give radical ions, or by interaction with UV, x-ray irradiation, or other radical producing compounds, such as peroxides and azo-compounds. Reactions of the last-named class include compounds containing P-H and P-Cl bonds [28].

Phosphines, substituted phosphines, hypophosphite, and phosphite possess one or more easily homolysed P-H bond. In the presence of radical initiators such as $(NH_4)_2S_2O_8$, they readily undergo homolysis of the P-H bond and react with alkenes by radical-chain addition to give organic phosphorus compounds characteristic of radical addition to the double bond [28, 29]. The generation and reaction of the phosphorus radicals with olefins have been explored widely for preparation of organic phosphorus compounds, and summarized by Sosnovsky [29], Harris and Stacey [30], and Cadgan [28]. Following mechanism was commonly accepted for the reaction of phosphine with olefins [28]:

$$PH_3 \xrightarrow[\text{or UV}]{\text{Peroxide}} \bullet PH_2$$

$$\bullet PH_2 + RCH{=}CH_2 \longrightarrow \bullet CHR{-}CH_2{-}PH_2$$

$$\bullet CHR{-}CH_2{-}PH_2 + PH_3 \longrightarrow RCH_2{-}CH_2{-}PH_2 + \bullet PH_2$$

$$RCH_2{-}CH_2{-}PH_2 \xrightarrow[\text{or UV}]{\text{Peroxide}} RCH_2{-}CH_2{-}\dot{P}H$$

$$RCH_2{-}CH_2{-}\dot{P}H + RCH{=}CH_2 \longrightarrow \bullet CHR{-}CH_2{-}PH{-}CH_2{-}CH_2R$$

$$\bullet CHR{-}CH_2{-}PH{-}CH_2{-}CH_2R + PH_3 \longrightarrow RCH_2{-}CH_2{-}PH{-}CH_2{-}CH_2R + \bullet PH_2$$

etc.

Hypophosphorus acid and hypophosphite generate free radical and react with olefins in the way similar to phosphine to produce di-n-alkyl phosphinic acid [28, 29]. Hydrogen abstraction from hypophosphorus acid to give $H_2PO_2^{\bullet}$ as a chain-carrying radical is the key step in the widely used reaction between diazonium and hypophosphorus acid. The producing $H_2PO_2^{\bullet}$ was used to initiate the polymerization of acrylonitrile [31]. Therefore, it is beyond doubt that hypophosphite reacts with persulfate to produce the radical $H_2PO_2^{\bullet}$, which commences the free radical chain reaction with

maleic acid and shows as end-group in poly(maleic acid) oligomers. This is supported by MALDI-MS and LC/MS data.

The free radical mechanism of the oligomerization of maleic acid in the presence of hypophosphite and persulfate is expressed in Scheme 3.2. Thermal homolysis of ammonium persulfate results in two sulfate negative radicals. The abstraction of a hydrogen from hypophosphite by $SO_4^{\bullet -}$ gives rise to the chain-carrying hypophosphite radical $H_2PO_2^{\bullet}$. Kornblum suggested following alternative structures for the hypophosphite radical [32]:

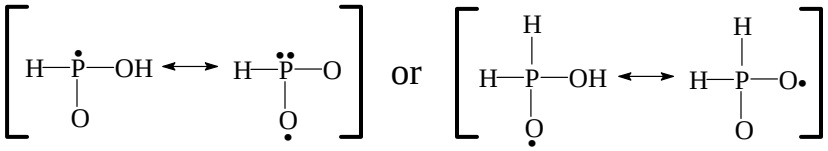


A B C D

Evidence from $^{31}$P-NMR eliminates the possibility of type C and D radicals. It should be type A rather than type B radical initiates the oligomerization. A phosphorus-carbon rather than a phosphorus-oxygen bond exists in the oligomer, because the hypophosphite ester type of end group would almost certainly hydrolyze much more readily than a phosphorus-carbon linkage [31].

Chain propagation and termination

As shown in the Scheme 3.2, the hypophosphite radical $H_2PO_2^{\bullet}$ attacks the maleic acid monomer, and oligomerization of maleic acid proceeds to through the ordinary addition mechanism.

Scheme 3.2. Proposed mechanism of aqueous polymerization of maleic acid

Initiation

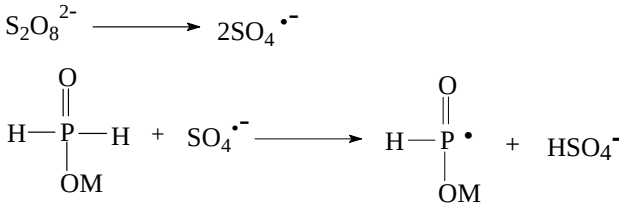

Chain propagation and termination by chain transfer

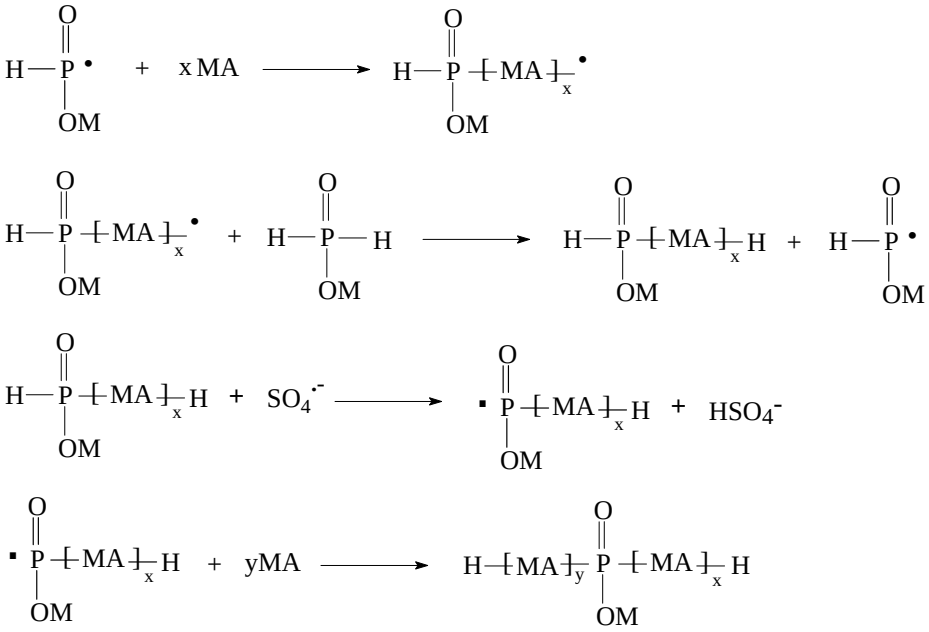

Scheme 3.2 (Continued)

Production of monoalkyl phosphonate

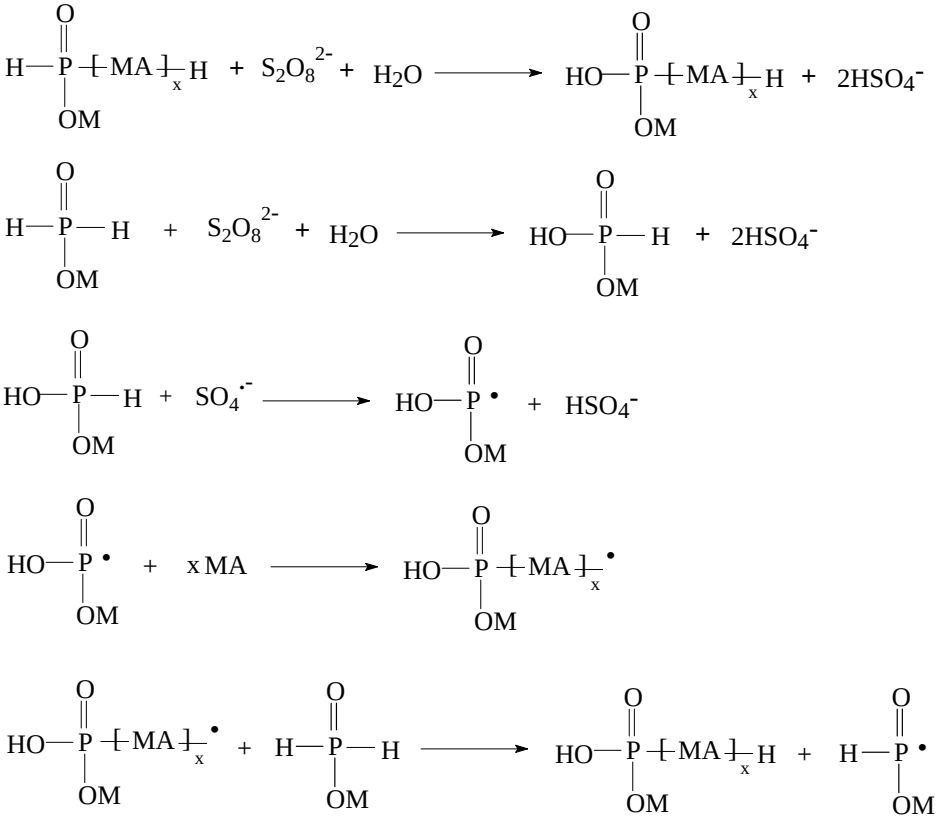

Chain termination by loss of •COOH

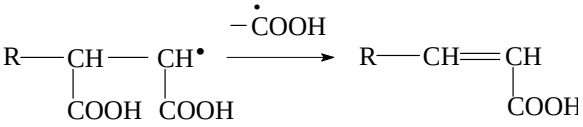

However, MALDI-TOF-MS and LC/MS data indicate that the aqueous polymerization of maleic acid only produces oligomers with a degree of polymerization (DP) less than 7. Meanwhile, when $NH_4H_2PO_2$ was used in an amount equal to half molar number of maleic acid, a very small amount of radical initiator $(NH_4)_2S_2O_8$, about 2.0-3.0 mol% of that of maleic acid, was able to initiate the reaction of all maleic acid. Theoretically, 3.0 mol% of persulfate should result in polymer with an average DP around 33 provided no new radical was produced by chain transfer. The extremely low DP indicates frequent chain transfer, which results in premature termination of growing chain and another active free radical, which is able to initiate another route of oligomerization of maleic acid, otherwise, maleic acid cannot be consumed completely.

Frequent chain transfer is reasonable in the oligomerization of maleic acid. It is attributed to the intrinsic inability of maleic acid to polymerize. The propagating oligomer radicals, due to strong electrostatic repulsion and steric crowding, hardly attack maleic acid monomer. The reluctantly growing oligomer radicals will readily absorb a proton from hypophosphite to terminate and generate a new hypophosphite radical $H_2PO_2^{\bullet}$, which starts another oligomerization of maleic acid.

The oligomers with a hypophosphite end-group have another P-H bond, which can also be fused by reacting with sulfate radical to form a phosphorus radical. The oligomer radical is able to attack one or several more maleic acid monomers and produce dialkyl phosphinate oligomers. The reactivity of monoalkyl phosphinate is seen by the amount of dialkyl phosphinate. From Table 3.4, one can find that relative amount of monoalkyl phosphinate decreased and that of dialkyl phosphinate increased when the amount of hypophosphite was reduced from 50mol% in PMA(3) to 40% in PMA(2).

Generation of monoalkyl phosphonates

The oligomerization of maleic acid in the presence of hypophosphite and persulfate also produces oligomers with phosphite end-group, shown as the peak at m/z 337 in MALDI-MS spectra and the peaks at m/z 199 and 315 in the LC/MS spectra. The monoalkyl phosphonate oligomers can be produced by the oxidation of hypophosphite end-group of monoalkyl phosphinate by persulfate, which will be discussed below.

Another source is the oligomerization initiated by phosphite directly. Phosphite is produced by a side reaction, the oxidation of hypophosphite by ammonium persulfate. Phosphite has a proton directly connected to phosphorus and is also able to produce a phosphite radical $PO_3^{2-\bullet}$ [28, 29]. The radical reacts with one or several maleic acid monomer to form the monoalkyl phosphonate oligomers with a very low degree of polymerization. The investigation of polymerization of maleic acid in the presence of phosphite will be discussed in future publication.

**Oxidation of the End-groups of Poly(maleic acid) Oligomers**

The structure of the ploy(maleic acid) was further investigated by end-group oxidation. PMA(3) was synthesized with a maleic acid/ammonium hypophosphite (MA/AHP) molar ratio of 2:1 and a maleic acid/ammonium persulfate (MA/APS) molar ratio of 30:1. Raman spectrum showed that polymerization was complete with no maleic acid left. The reaction product was further oxidized with ammonium persulfate in amount of one fourth of molar number of maleic acid at 70$^{o}$C for 7 hours.

Figure 3.7 shows the $^{31}$P-NMR spectra of PMA (3) before (A) and after (B) further oxidation. The reaction can be quantitatively expressed by the change of peak area as

shown in Table 3.5. The reducing ability of phosphorus compounds decreases by the order of hypophosphite > monoalkyl phosphinate > phosphite. After further oxidation, the amount of dialkyl phosphinate remained unchanged. However, all residual hypophosphite was oxidized to phosphite and phosphate. The signal of monoalkyl phosphinate almost disappeared, while that of monoalkyl phosphonate increased to a similar extent. This is a direct evidence that the monoalkyl phosphinate oligomers were oxidized to monoalkyl phosphonate by persulfate.

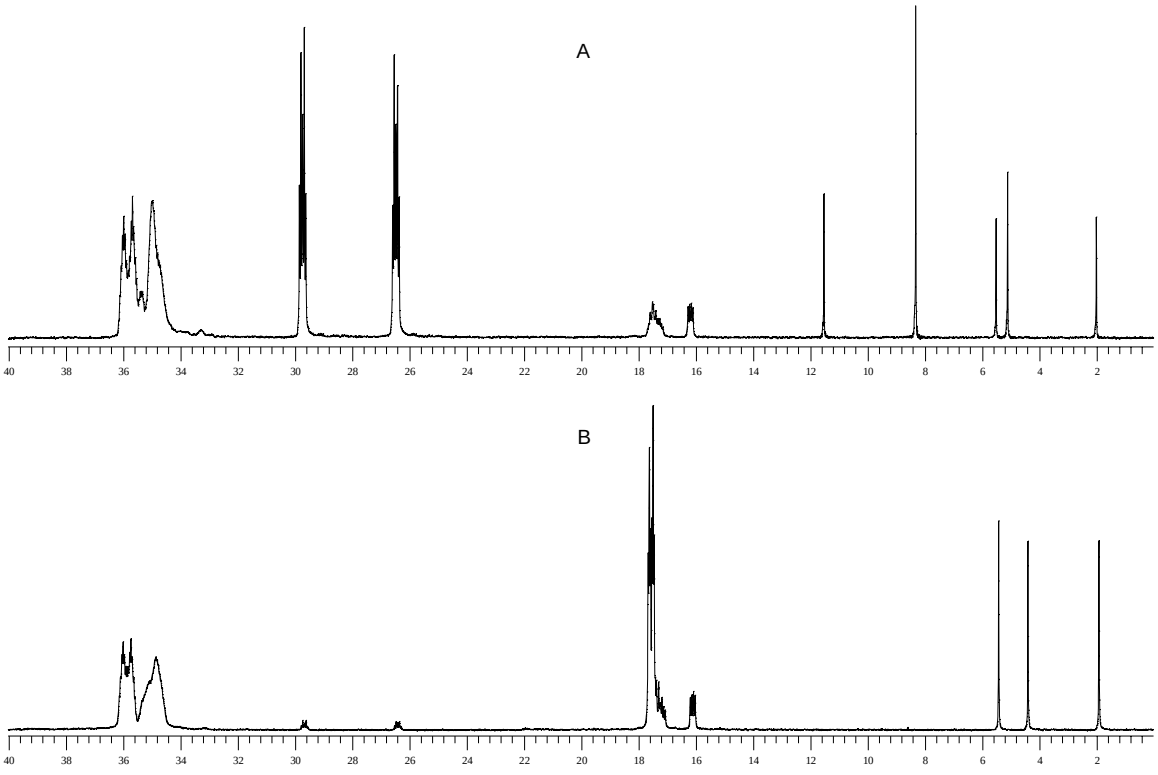


Figure 3.7 $^{31}$P-NMR spectra of PMA(3), before (A) and after (B) further oxidation with ammonium persulfate

$^{1}$H-NMR presented in Figure 3.8 provides a consistent result with $^{31}$P-NMR. The peaks assignment is shown in Table 3.4. The proton signals of hypophosphite at δ 7.50 and 6.20 ppm almost disappeared, and those of monoalkyl phosphinate oligomer end-groups at δ 7.43 and 6.11 ppm are significantly decreased. In contrast, the peaks of phosphite at δ 7.25 and 5.83 ppm increased.

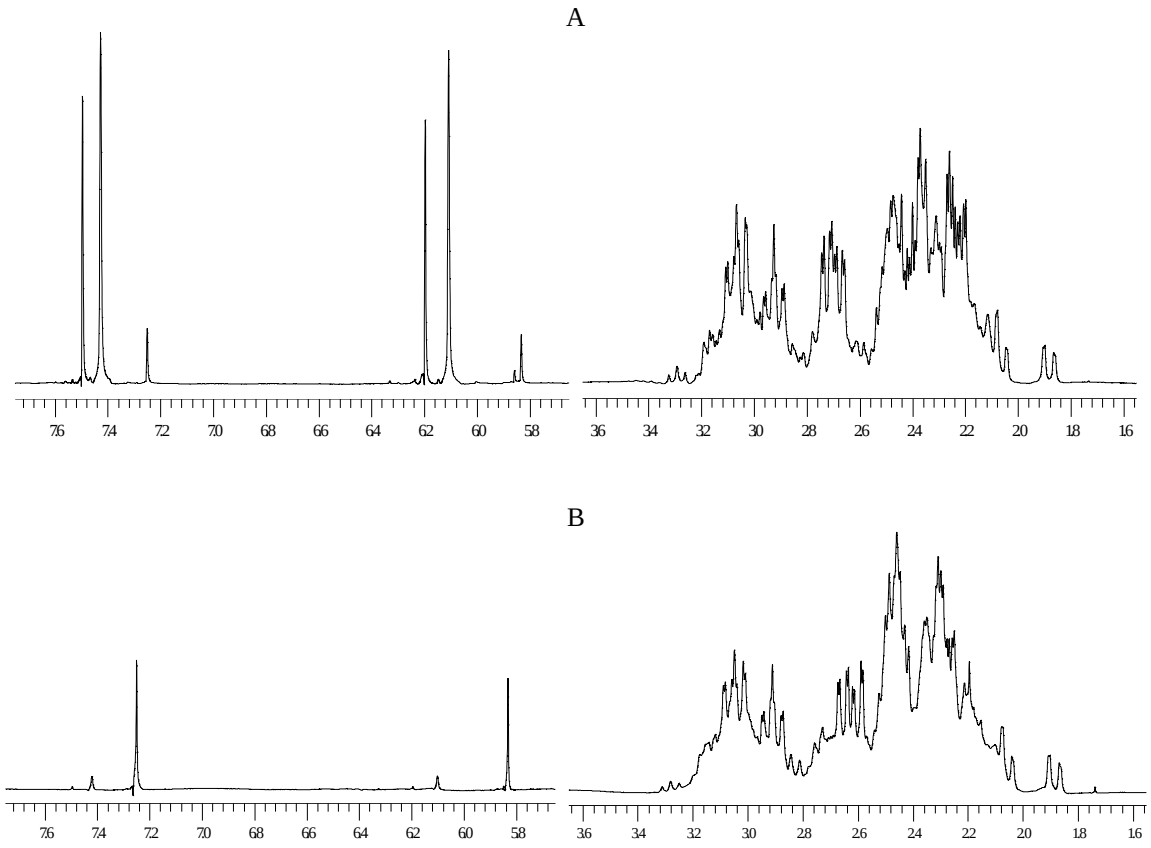


Figure 3.8 $^{1}$H-NMR spectra of PMA(3) before (A) and after (B) further oxidation

The oxidation of end-group is confirmed by mass spectrometry. Figure 3.9 presents the LC/MS spectra of PMA(3) before (A) and after (B) oxidation. The signal of monoalkyl phosphinate oligomer (DP=1) at m/z 183 and its related signals at m/z 165

(by loss of a $H_2O$), 200 and 217 (both are ammonium adducts) almost disappeared, while peak of monoalkyl phosphonate at m/z 199 and its related signals at m/z 181 (loss of $H_2O$) and m/z 216 (ammonium adduct) came out at high intensity. The phenomenon is the direct result of oxidation of end-group of phosphinate oligomer (DP=1) and formation of phosphonate. The peak at m/z 299 of phosphinate oligomer (DP=2) and peak at m/z 315 of phosphonate only changed slightly. Therefore, for PMA(3) prepared in the use of hypophosphite at half molar number of monomer, most of the monoalkyl phosphinate oligomers contain only one maleic acid repeat unit, i.e., DP=1.

The oxidation of end-group is also demonstrated by the dimer formation. The peak at m/z 498 before oxidation is the dimer $182+298+NH_4^+$, and is replaced by the peak at m/z 497, the dimer $198+298+H^+$, after oxidation. The peak at m/z 614 before oxidation is the dimer $182+414+NH_4$, and is replaced by the peak at m/z 613, the dimer of $198+414+H^+$, after oxidation

**Side Reaction**

It is reasonable for side reactions to take place during the oligomerization of maleic acid. The reaction product PMA(2) was analyzed by LC/ESI/MS. Figure 3.10 presents the UV, TIC chromatograms, and the corresponding mass spectra. There are four peaks in UV chromatogram and three peaks in TIC. The third peak in UV chromatogram appears as a shoulder of the second peak in TIC. The first two peaks are the major species of PMA oligomers, the first peak has a relatively lower MW than the second one. The oligomers of lower MW eluted out the column faster than those of higher MW. The last two peaks in the UV chromatogram result from side reactions during polymerization.

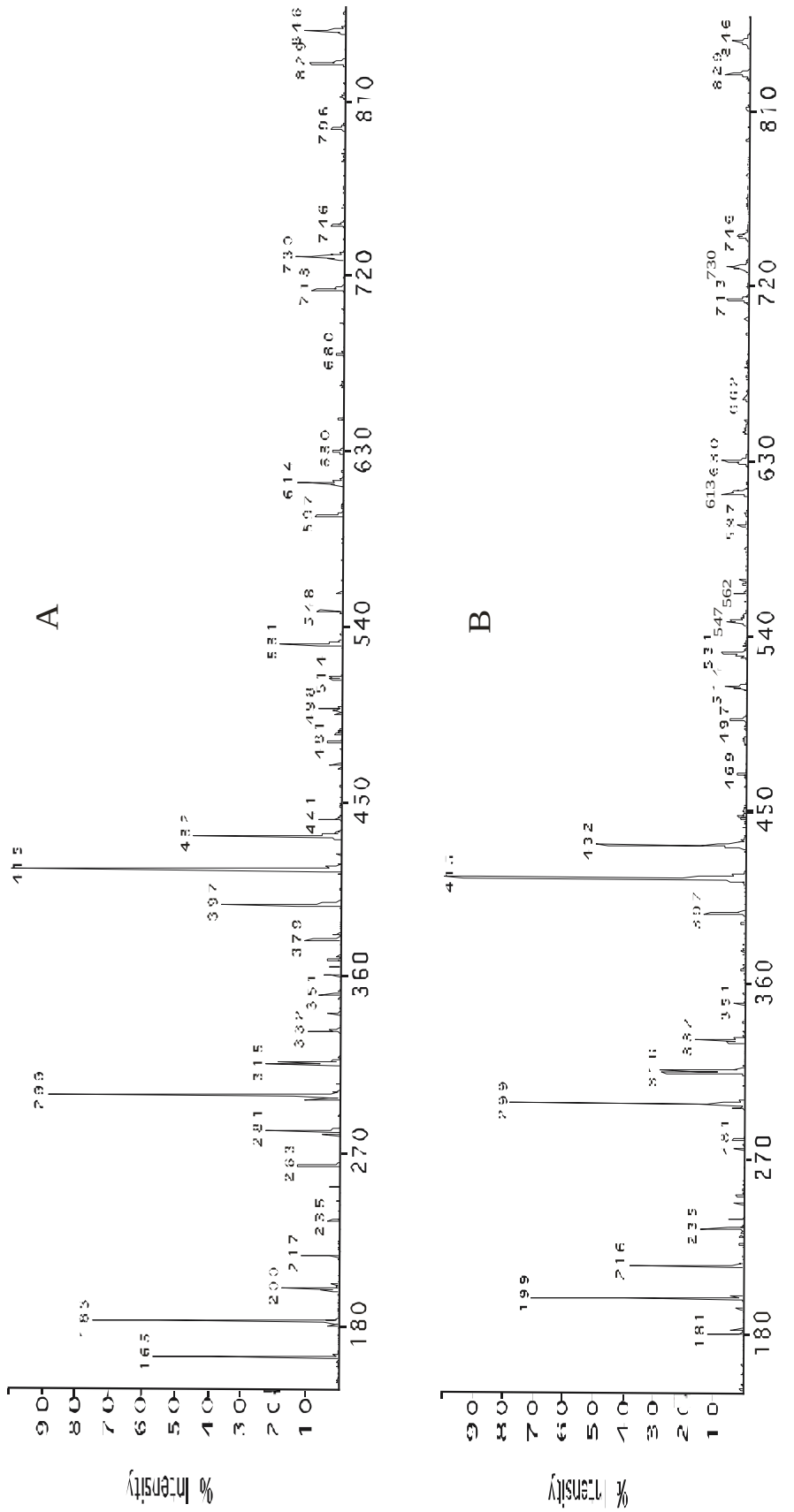


Figure 3.9 LC/MS spectra of PMA(3) before (A) and after (B) further oxidation

The mass spectrum corresponding to the last peak in the chromatogram is shown in Figure 3.10(C). The Peak at m/z 369 is 46 Da lower than the peak at m/z 415 (DP=3). It possibly originated from the termination of propagation radicals by loss of one •COOH as shown in Scheme 3.2. Further loss of one $H_2O$ led to the peak at m/z 351. The peak at m/z 235, 116 Da lower than the peak at m/z 351, also resulted from the same termination and loss of one $H_2O$. The peak at m/z 469 is 62 mass units lower than the peak at m/z 531 (DP=4), may result from the loss of one $CO_2$ and one $H_2O$. It could also be the dimer of the peak at m/z 235. The peak at m/z 585 is 116 Da higher than the peak at m/z 469, and should have the same source.

The mass spectrum corresponding to the third peak in UV chromatogram is presented in the Figure 3.10(D). The peak at m/z 585 is 46 Da lower than the peak at m//z 531 (DP=4) due to the chain termination through the loss of •COOH. The peak at m/z 441 is 90 Da lower than the peak at m/z 531 and 44 Da lower than the peak at m/z 485, should be produced by further loss of one $H_2O$ from m/z 485. Like the peak at m/z 441, the peak at m/z 557 is also 90 Da lower than m/z 647 (DP=5), and should have the similar source. The components of these peaks contain carbon-carbon double bonds. This is the reason why they produce weak ion signal in TIC but exhibit intense UV absorbance.

Decarboxylation described above is commonly found in polymerization of polycarboxylic acid. When maleic anhydride was polymerized in organic solvent, $CO_2$ was released [34]. In most cases reported, elemental analyses have failed to correspond to the expected empirical formula, $C_4H_4O_4$. The resulted polymer was high in carbon and hydrogen and deficient in oxygen. The produced poly(maleic acid) contained about

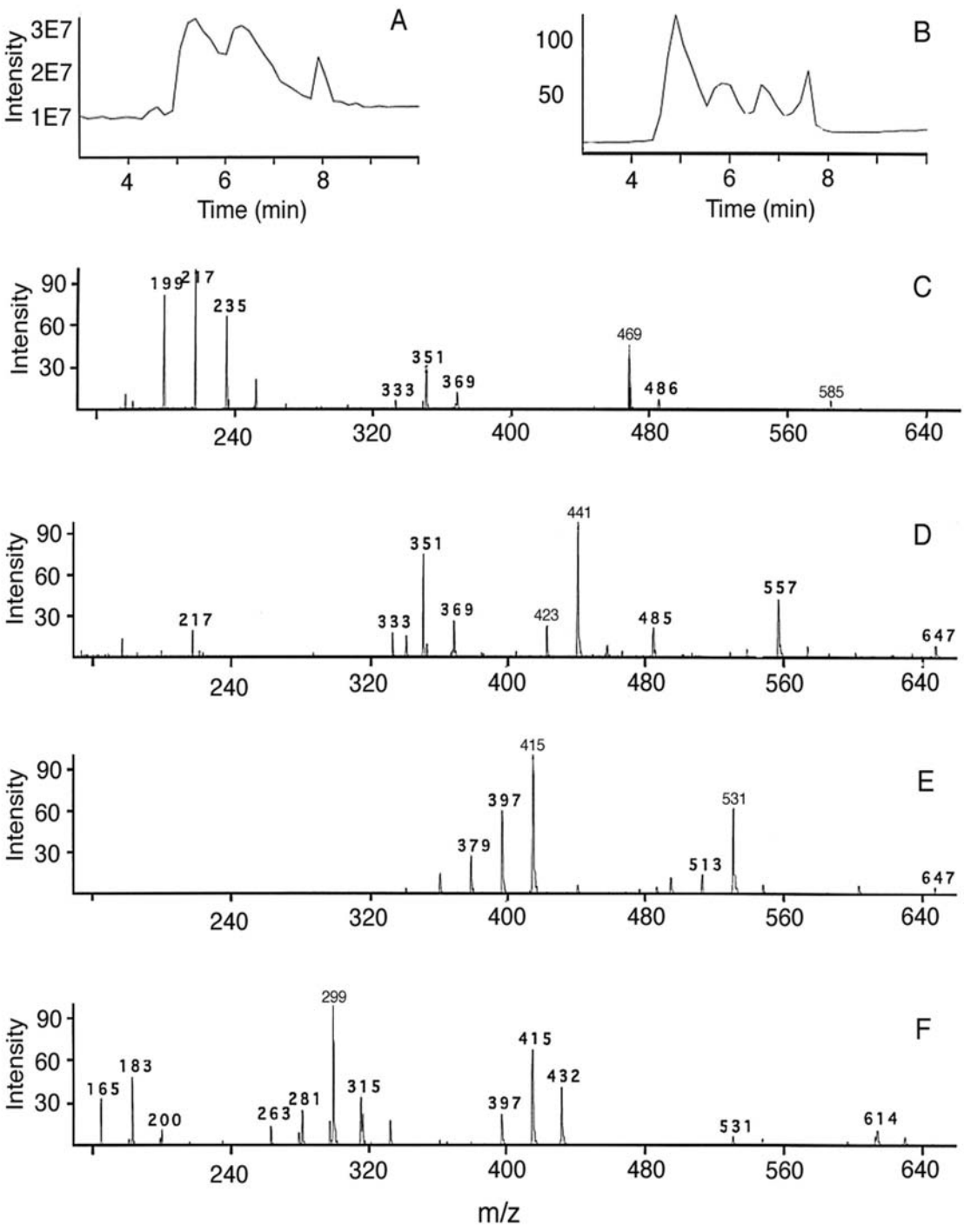


Figure 3.10 LC/MS spectra of PMA(2). TIC (A), UV(B) chromatographs, and mass spectra corresponding to chromatograph peak 1 (C), 2(D), 3(E), 4(F).

2.5-4.0% decarboxylated MA. Another case is itaconic acid [35]. During the free radical polymerization of itaconic anhydride and itaconic acid in bulk or in solution, a substantial amount of carbon dioxide was split off and subsequent reactions failed to give the repeating itaconic structure.

The first and second peaks in chromatograph are related to the major species of PMA oligomers. The small MW oligomers were eluted out before large components, as shown in Figure 3.10 (E) and (F).

## CONCLUSION

MALDI-TOF-MS and LC/ESI/MS have been successfully applied for analysis of molecular weight and end-groups of poly(maleic acid) oligomers prepared by aqueous polymerization of maleic acid in the presence of hypophosphite and free radical initiator. The distribution of different phosphorus-containing species and end-groups of the oligomers have also been quantitatively investigated by $^{31}P$ and $^{1}H$-NMR. The insight from mass spectroscopy and NMR analysis has provided complimentary information and led to the understanding of the mechanism of aqueous polymerization of maleic acid.

Maleic acid undergoes free radical homopolymerization in the presence of hypophosphite and free radical initiator. Abstraction of a hydrogen atom from hypophosphite to produce a hypophosphite radical is the key step in the polymerization. The hypophosphite radical attacks maleic acid monomer and commences the oligomerization. The propagation radicals hardly attack more monomers owing to strong electronic repulsion and steric hindrance. They readily extract a proton from hypophosphite to terminate and produce another hypophosphite radical, which starts

another route of oligomerization. The frequent chain transfer leads to very low degree of polymerization below 6 even though only catalytic amount of the radical initiator was used. The propagation chain may also be terminated by loss of •COOH.

The hypophosphite end-group of the monoalkyl phosphinate PMA oligomers is able to produce another radical and thus the oligomers grow in another end of chain and produce dialkyl phosphinate oligomers, which account for the major species of the oligomers. As the amount of hypophosphite decreased, the amount of monoalkyl phosphinate decreased while amount of dialkyl phosphinate increased as a result of further reaction of monoalkyl phosphinate.

Monoalkyl phosphonate oligomers were also produced in the polymerization either by oxidation of monoalkyl phosphinate oligomers or by the reaction of phosphite radical with maleic acid. Phosphite was produced by the oxidation of hypophosphite. By loss of its directly connected proton, phosphite was also able to produce a phosphorus radical and attack one or more maleic acid monomers to produce monoalkyl phosphonate oligomers.

## REFERENCES

1. Hanton, S. D., *Chem. Rev*. 101(2):527-569 (2001)
2. Karas, M., Bachmann, D., Bahr, U., Hillenkamp, F., *Int. J. Mass Spectrom. Ion Proc.* 78:53 (1987)
3. Nielen, M.W.F., *Mass Spectr. Rev*. 18:309-344 (1999)
4. Liu, J.S., Loewe, R.S., McCullough R.D., *Macromolecules* 32(18):5777-5785 (1999)
5. Eschewer, J., Karnack, J., *Macromolecules* 29(13):4536-4543 (1996)

6. Kapfenstein, H.M, Davis, T.P., *Macrom. Chem. Phys*. 199(11):2403-2408 (1998)
7. Zammit, M. D., Davis, T. P., Haddleton, D. M., Sudmdaby, K. G., *Macromolecules* 30(7):1915-1920 (1997)
8. Cole, R.B., "*Electrospray ionization mass spectrometry: fundamentals, instrumentation, and applications*", John Wiley & Sons, 1997.
9. Lorenz, S.A., Maziarz III, E.P., Wood, T.D., *Applied Spectroscopy* 53(1):18A-36A (1999)
10. Vonk, E.C, Langeveld-Voss, B.M.W., van Dongen, J.L.J., Janssen, R.A.C., Cramers, C.A., *J. Chromatography* A 911:13-26(2001).
11. Trivedi, B.C., Culbertson, B. M. "*Maleic Anhydride*", Plenum Press, New York and London, 1982
12. Yang, C.Q., Gu, X., *J. Appl. Polym. Sci.* 81(1):223-228(2001)
13. Mao, Z., Yang, C.Q., *Textile Res. J.* (Submitted).
14. Crutchfield, M.M., Dungan, C.H., Letcher, J.H., Maker, V., Van Wazer, J.R., "*$^{31}P$ nuclear magnetic resonance*", John Wiley & Sons, 1967
15. Mohr, M.D, Börnsen, K.O, Widmer, H. M., *Rap. Comm. Mass Spectr*. 9:809-814 (1995)
16. Xu, G., Mize, T., Yang, C. Q., Amster, I. J., *Proc. 49th ASMS Conf Mass Spectrom & Allied Topics*, Chicago, IL (2001)
17. Glonek, T., Wang, P. J., Van Wazer, J. R., *J. Am. Chem. Soc*. 98:7968 (1976)
18. Shaka, A. J., Barker, P. B., and Freeman, R., *J. Magn. Reson*. 64, 547-552 (1985).
19. Shaka, A. J., Keeler, J., Frenkiel, T., and Freeman, R., *J. Magn. Reson*., 52, 335 (1983).

20. Bax, A., Griffey, R.H. and Hawkins, B.L., *J. Magn. Reson*., 55, 301(1983)

21. Bax, A. and Subramanian, S., *J. Magn. Reson*. 67, 565 (1986).

22. Van Wazer, J.R., "High resolution nuclear magnetic resonance", in "*Analytical chemistry of phosphorus compounds*", John Wiley & Sons, 1972.

23. Bentrude, W.G., Setzer, W.N., "Stereospecificity in $^{31}$P-element couplings: proton-phosphorus couplings", in "*Phosphorus-31 NMR spectroscopy in stereochemical analysis*", J.G. Verkade and L.D. Quin Ed., VCH Publishers, Deerfield Beach, FA, 1987

24. Van Wazer, J.R., Letcher, J.H., "Interpretation of experimental $^{31}$P NMR chemical shifts and some remarks concerning coupling constants", in "*$^{31}$P nuclear magnetic resonance*", M.M. Crutchfield, C.H. Dungan, J.H. Letcher, V. Maker, J.R. Van Wazer Ed., John Wiley & Sons, 1967

25. McFarlane, W., "Special experimental techniques in phosphorus NMR spectroscopy", in "*Phosphorus-31 NMR spectroscopy in stereochemical analysis*", J.G. Verkade and L.D. Quin Ed., VCH Publishers, Deerfield Beach, FA, 1987

26. Stanislawski, D.A., Van Wazer, J. R., *Anal. Chem*. 52:96-101 (1980)

27. Gadogan, J.I.G., "Radical reaction of phosphorus compounds", in "*Advances in free-radical chemistry*", Vol. 2, G.H.Williams Ed., Academic Press, 1967.

28. Sosnovesky, G., "*Free radical reactions in preparative organic chemistry*", Macmillan Co., New York, 1964, pp153-192

29. Harris, J. F., Stacey, F.W., *Org. Reactions* 13:158 (1963)

30. Warson, H., *Makromol. Chem*. 105:228-245 (1967)

31. Kornblum, N., Cooper, G.D., and Taylor, J.E., *J. Am. Chem. Soc*. 72:3013 (1950)

32. Culbertson, B.M., "Maleic acid and fumaric polymers", in "*Encyclopedia of polymer science and technology*", Editor-in-chief, J. I. Kroschwitz, Vol.9, John Wiley & Sons, New York, 1987

33. Tate, B. E., "Itaconic acid and derivatives", in "*Kirk-Othmer Encyclopedia of Chemical Technology*", 4th, Executive editor, Jacqueline I. Kroschwitz ; Editor, Mary Howe-Grant, Wiley, New York, 1991.

# CHAPTER 4

# AQUEOUS POLYMERIZATION OF SIX VINYL DICARBOXYLIC ACIDS AND TRICARBOXYLIC ACIDS INVESTIGATED BY MALDI-TOF-MS, $^{31}$P-NMR, AND FT-RAMAN [1]

[1] Guozhong Xu, Xudong Jia, Charles Yang, and Jon Amster
To be submitted to *Macromolecules*

## INTRODUCTION

The polymers of monoethylenically dicarboxylic acids have been in general industrial uses such as water treating agents, detergent additives, dispersing agents, chelating agents, corrosion inhibitors, crosslinking agents, fiber coupling agents [1], paper wet strength agents [2], et al. Poly(maleic acid) (PMA) has also been developed for the new generation of non-formaldehyde durable-press finish of cotton fabrics [3]. Typical monoethylenically dicarboxylic acids include maleic acid, fumaric acid, and itaconic acid. Homopolymers of theses ethylenically dicarboxylic acids have more carboxylic acid groups available for reaction and should possess higher efficiency for above mentioned industrial uses than their copolymers. However, most of current industrial polycarboxylic acids are homopolymers or copolymers of maleic acid, because of the difficulty in preparing the homopolymers of these monoethylenically dicarboxylic acids.

Monoethylenically dicarboxylic acids are extremely difficult to homopolymerize under the normal conditions used for most vinyl monomers such as acrylic acid, because of the high steric hindrance and polar effect of the two carboxylic acid groups [1]. Maleic acid (MA) is the most common vinyl dicarboxylic acid. It was so far reported to homopolymerize in the presence of polyvinylpyrrolidone (PVP), which formed a charge-transfer complex with maleic acid [4]. The produced PMA was a complex with PVP and could not be separated without decomposition. In order to separate PMA from PVA, the polymer complex was completely methylated with diazomethane. About 50-60% PMA was separated as methyl ester, which was found to have a low molecular weight about 400-500 Dalton. As result of difficult polymerization of MA, PMA has been

conventionally prepared by hydrolysis of poly(maleic anhydride), which is synthesized from maleic anhydride from organic solvents [1].

Itaconic acid (IA) is relatively easier to homopolymerize than the maleic acids [3]. IA underwent polymerization in 0.5 N hydrochloric acid aqueous solution under the initiation of persulfate. PIA was obtained with 35% yield after reaction at 50$^{o}$C for 68 hours [5]. PIA can be also prepared by hydrolysis of poly(itaconic anhydride), which is synthesized from itaconic anhydride in organic solvents [6]. The homopolymers and copolymers of itaconic acid or itaconic anhydride give out copious amount of carbon dioxide during polymerization and produce polymers of complicate structure under mild conditions [6, 7].

Fumaric acid (an isomer of maleic acid), mesaconic acid (an isomer of itaconic acid), 3-butene-1, 2, 3-tricarboxylic acid, and trans-aconictic acid are even more difficult in homopolymerization. So far there appears no report of homopolymerization for these unsaturated carboxylic acids. The general reluctance of polymerization of vinyl multicarboxylic acids is due to sever steric hindrance and strong polar effect of carboxylic acid groups in the monomers.

Recently, it was reported that maleic acid underwent polymerization in the presence of sodium hypophosphite and potassium persulfate [8]. When a solution of 40% maleic acid, 20% sodium hypophosphite, and 2.0% potassium persulfate ($K_2S_2O_8$) was heated at 90$^{o}$C for several hours, the characteristic Raman band of unsaturated C=C stretch at 1648 cm$^{-1}$ and =C-H stretch at 3062 cm$^{-1}$ of maleic acid disappeared. No characterization of the produced polymers was performed.

In this paper, we confirm the polymerization of maleic acid and itaconic acid in the presence of hypophosphite and persulfate, characterize the polymers by matrix-assisted-laser desorption/ionization time-of-flight mass spectroscopy (MALDI-TOF-MS) and $^{31}$P-NMR spectroscopy. Moreover, the new initiation system is further exploited to initiate the homopolymerization of other vinyl multicarboxylic acids in water. The structures of the monomers are shown in Scheme 4.1.

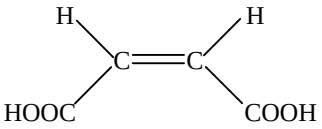


Maleic Acid (MA)
MW=116.01

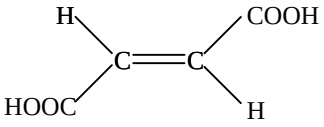


Fumaric Acid (FA)
MW=116.01

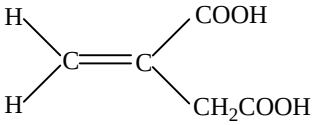


Itaconic Acid (IA)
MW=130.1

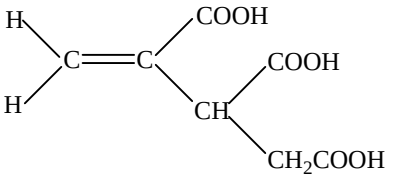


3-Butene-1,2,3-tricarboxylic Acid (BTA)
MW=188.1

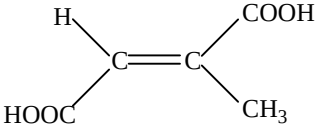


Mesaconic Acid (MSA)
MW=130.1

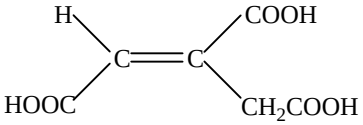


Trans-aconictic Acid (TAA)
MW=174.1

Scheme 4.1 Structure of vinyl multicarboxylic acids

# EXPERIMENTAL SECTION

## Materials

Maleic acid (MA), fumaric acid (FA), itaconic acid (IA), mesaconic acid (MSA), trans-aconictic acid (TAA), ammonium hypophosphite (AHP), 2, 5-dihydroxy benzoic acid (DHB), and 1-hydroxy isoquinoline (HIQ) were purchased from Aldrich Chemical Co. (Milwaukee, WI). 3-butene-1, 2, 3-tricarboxylic acid (BTA) was supplied from Lancaster Synthesis Inc. (Windham, NH). Ammonium persulfate (APS) and HPLC-grade acetonitrile (ACN) came from J. T. Baker Inc. (Phillipsburg, NJ). All chemicals except acetonitrile were reagent grade and used without further purification.

## Polymerization

The polymerization was carried out in a 10 mL reaction vials with a small magnetic stirrer. The unsaturated monomer (MA, FA, IA, BTA, MSA, or TAA), $NH_4H_2PO_2$, $(NH_4)_2S_2O_8$, and deionized water were added to the vial in a ratio listed in Table 4.1. The vials were purged by $N_2$ through a syringe needle and loaded on a Pierce Reacti-Therm Heating Stirring Module, which was kept at specific temperatures. For MA, FA, and IA, all $(NH_4)_2S_2O_8$ was added at the beginning of reaction. In the case of BTA, MSA, and TAA, the polymerization was slow, and $(NH_4)_2S_2O_8$ was added as two or three portions at the beginning and in the course of reaction. The polymerization is monitored by FT-Raman spectroscopy until all monomers disappeared. The temperature and reaction time were also shown in Table 4.1.

## FT-Raman

All Raman spectra were acquired in a Nicolet 950 FT-Raman spectrometer with a liquid sample accessory and a Ge detector cooled down with liquid $N_2$. All spectra were

recorded with a resolution 8 $cm^{-1}$, and 128 scans were cumulated to improve the spectral quality. During polymerization, about 0.15 mL of solution was transferred to Raman sample tube for spectral acquiring to monitor the extent of polymerization.

Table 4.1 The weight and molar ratios of reactants for polymerization of different monomers

| | Monomer (g) | $NH_4H_2PO_2$ (g) (Acid/AHP) | $(NH_4)_2S_2O_8$ (g) (Acid/APS) | Water (g) | Temperature ($^oC$) | Time (hours) |
|---|---|---|---|---|---|---|
| PMA | 2.000 | 0.7155 (2:1) | 0.1311 (30:1) | 2.8467 | 55 | 7 |
| PFA | 2.000 | 0.7151 (2:1) | 0.3932 (10:1) | 1.8917 | 95 | 0.4 |
| PBTA | 1.4617 | 0.3224 (2:1) | 0.5319 (10:3) | 3.3803 | 75 | 30 |
| PIA-1 | 2.400 | 0.7658 (2:1) | 0.4210 (10:1) | 2.4132 | 90 | 0.5 |
| PIA-2 | 3.000 | 0.1914 (10:1) | 0.2631 (20:1) | 4.0455 | 75 | 2 |
| PMSA | 1.200 | 0.3828 (2:1) | 0.6315 (10:3) | 3.6050 | 75 | 33 |
| PTAA | 2.000 | 0.4769 (2:1) | 0.4631 (10:1.8) | 2.2610 | 55 | 28 |

**MALDI-TOF-MS**

The matrix solution was prepared by dissolving 15.4 mg DHB and 4.35 mg HIQ in 1.0 mL ACN/$H_2O$ (1:1, v/v) [9]. The mixed matrix gave excellent signals for low molecular weight polycarboxylic acids [10]. All samples were analyzed directly without any purification. All samples were made into 10.0 mg/mL solution with ACN/$H_2O$. Then 5.0 μL sample solution and 10 μL matrix were premixed in a 0.25 mL tube, and 1.0 μL mixed solution was dropped on the MALDI sample probe and dried under dry air stream.

MALDI-TOF mass spectra were obtained on a Bruker Reflex Time-of-Flight (TOF) mass spectrometer equipped with delayed extraction optics and a pulsed $N_2$ laser emitting at 337 nm. Positive ion signals were acquired for all samples using reflection mode. The laser attenuation was adjusted to slightly higher than the threshold value. The signal was

accumulated for 100-200 shots until acceptable signal/noise ratio was obtained. Polyethylene glycol was used for external calibration.

**$^{31}$P-NMR**

Proton coupling and decoupling $^{31}$P-NMR spectra were acquired at room temperature on a Bruker AMX400 multi-nuclear spectrometer operating at 61.98 MHz for phosphorus. In proton decoupling measurements, $^{1}$H was decoupled using Waltz sequence with 90-degree pulse of 110 μs [11]. All spectra were collected with a spectral width of 100 ppm and 32 scans. All samples were made in water with a concentration about 15-20%, and pH was adjusted to 9.0 with NaOH in order to optimize the signal separation and the longitudinal relaxation times [12, 13]. All NMR measurements were made in a 5.0 mm sample tube with a coaxial capillary containing the lock solvent $D_2O$. The arrangement avoided spectral complexity caused by H-D exchange. The chemical shift of $^{31}$P spectra was referenced externally to 85% phosphoric acid.

## RESULTS AND DISCUSSION

### Polymerization of Maleic Acid and Characterization of PMA

Raman

The Raman spectra of aqueous solutions of $(NH_4)_2S_2O_8$, $(NH_4)_2SO_4$, and $NH_4H_2PO_2$ are presented in Figure 4.1 (A), (B), and (C) respectively. In the spectrum of $(NH_4)_2S_2O_8$, the bands at 1075 and 835 $cm^{-1}$ are the $S_2O_8^{2-}$ symmetric stretch and S=O stretch. After $(NH_4)_2S_2O_8$ decomposes into $SO_4^{2-}$, these two peaks will disappear and the stretching mode of $SO_4^{2-}$ at 980 $cm^{-1}$ appears (Figure 4.1(B)). These three peaks were used to monitor the reaction of $(NH_4)_2S_2O_8$ during the polymerization. In the spectrum (C) of $NH_4H_2PO_2$, the intense peak at 1044 $cm^{-1}$ is due to P–O stretch, and the

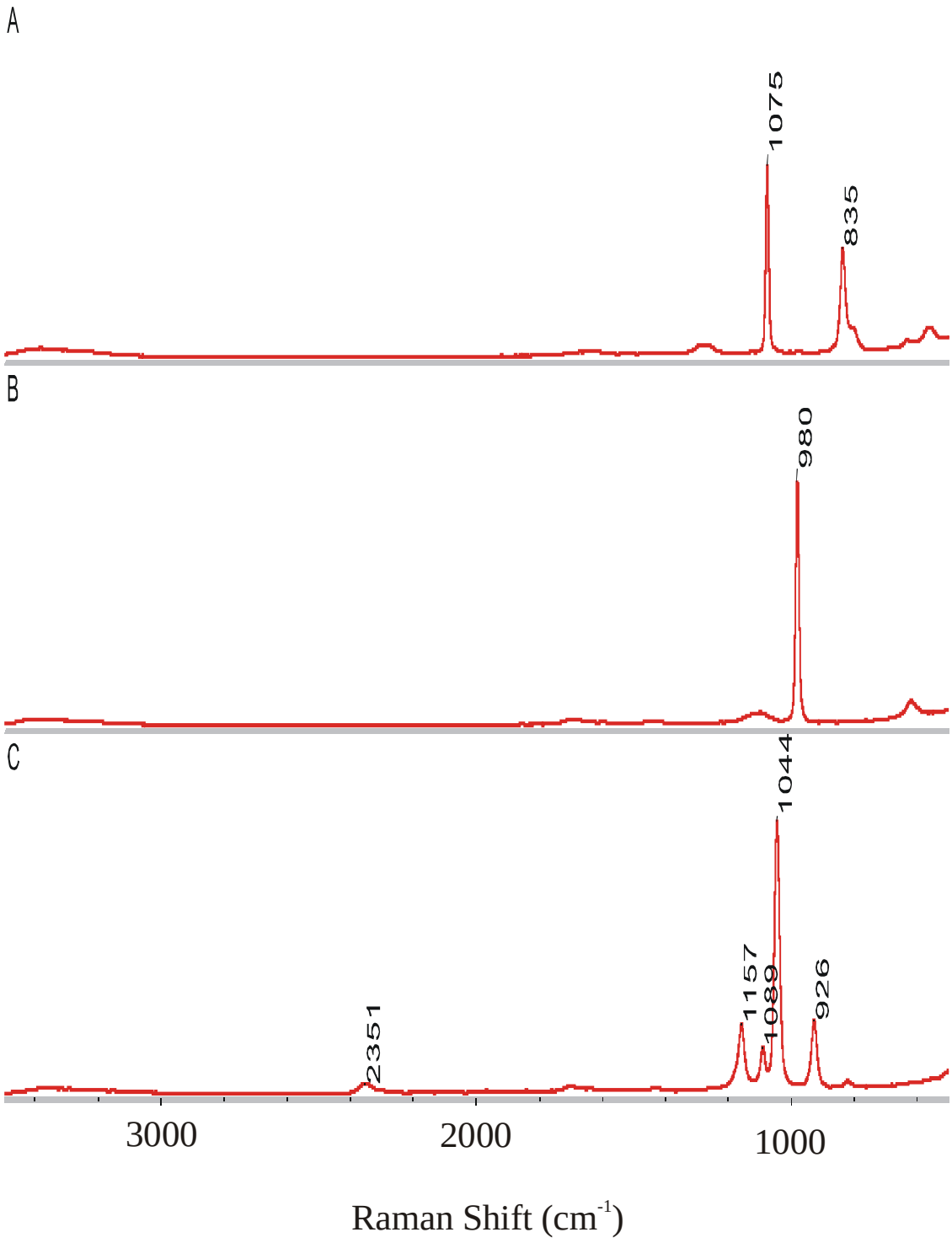


Figure 4.1 Raman spectra of (A) $(NH_4)_2S_2O_8$ , (B) $(NH_4)_2SO_4$ , and (C) $NH_4H_2PO_2$ in water

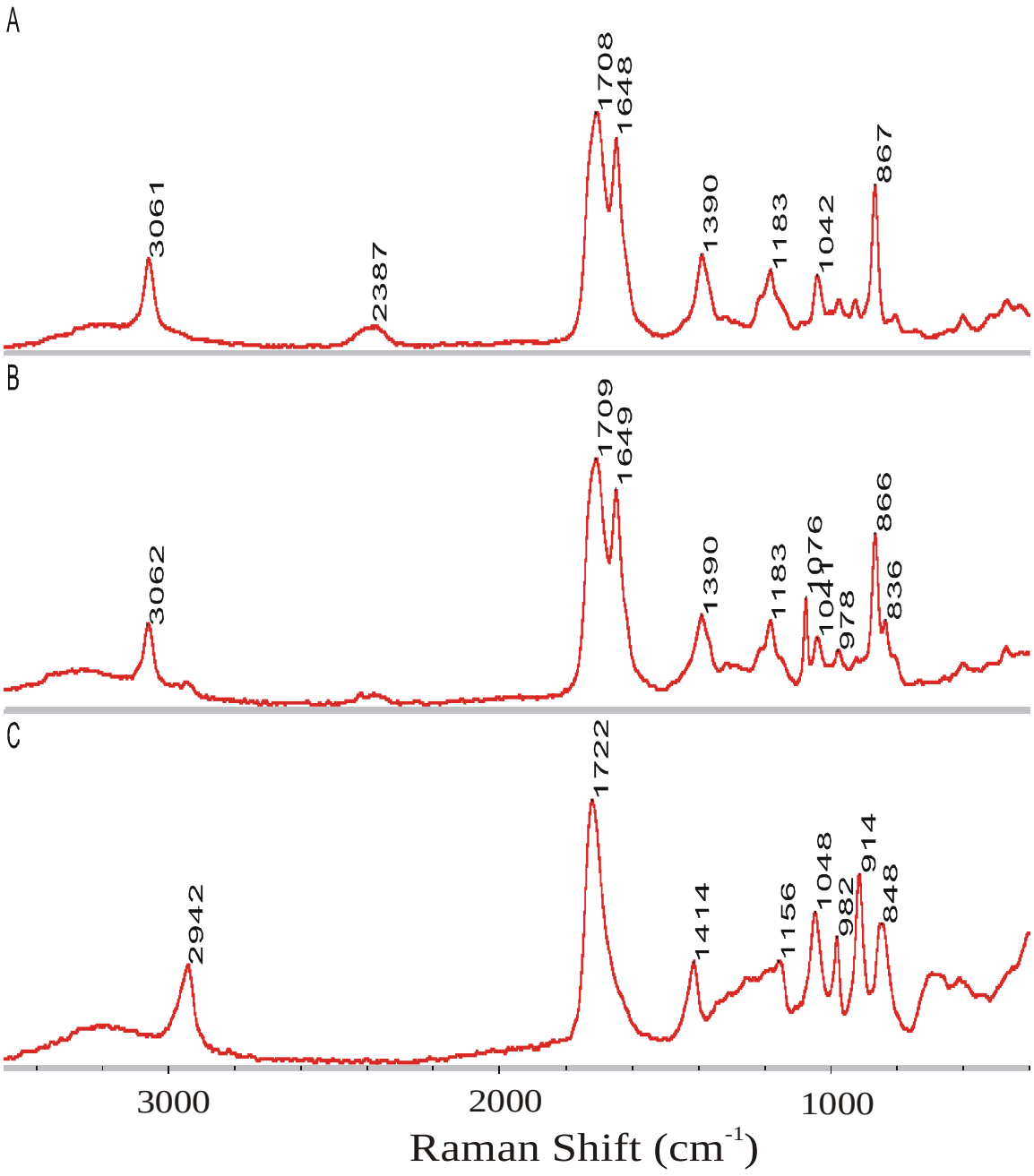


Figure 4.2 Raman spectra of (A) aqueous solution of 40% MA and 14.3% $NH_4H_2PO_2$; and the mixture of 40% MA, 14.3% $NH_4H_2PO_2$ , and 2.62% $(NH_4)_2S_2O_8$ (molar ratio MA/AHP/APS = 30:15:1) after reaction at 55°C for (B) 20 min, and (C) 7 hours

Table 4.2 The frequencies and assignment of Raman shift of PMA system

| Compound | Raman Shift ($cm^{-1}$) | Assignment |
|---|---|---|
| $S_2O_8^{2-}$ | 1075 | $S_2O_8^{2-}$ symmetric stretch |
| | 835 | S–O stretch |
| $SO_4^{2-}$ | 980 | $SO_4^{2-}$ symmetric stretch |
| $H_2PO_2^-$ | 2351 | $PH_2$ symmetric stretch |
| | 1157 | $PH_2$ scissor |
| | 1089 | $PH_2$ wag |
| | 1043 | $PO_2$ symmetric stretch |
| | 926 | $PH_2$ twist |
| Maleic acid | 3062 | =C–H stretch |
| | 1709 | C=O (unsaturated carboxylic acid) stretch |
| | 1648 | C=C stretch |
| | 1390 | combination of C–O stretch and in-plane O–H deformation (dimmer, unsaturated carboxylic acid) |
| | 1183 | =C–C stretch |
| | 867 | =C–H out-of-plane deformation |
| PMA | 2942 | saturated C–H stretch |
| | 1722 | C=O (saturated carboxylic acid) stretch |
| | 1056 | saturated C–C–C stretch |
| | 1414 | combination of C–O stretch and in-plane –O–H deformation (dimmer, saturated carboxylic acid) |
| | 914 | OH...O out-of-plane deformation |

broad peak at 2351 $cm^{-1}$ is owing to P–H stretch [14]. The Raman shift signals of maleic acid system are assigned in Table 4.2.

It is seen from Figure 4.2 that maleic acid underwent polymerization in the presence of $NH_4H_2PO_2$ and radical initiator $(NH_4)_2S_2O_8$. Figure 4.2(A) is the Raman spectrum of mixed solution of 40 wt% maleic acid (MA) and 14.3 wt% $NH_4H_2PO_2$ (molar ratio MA/ $NH_4H_2PO_2$ = 2/1). The stretching modes of unsaturated =C–H and the alkene (C=C) of maleic acid appear at 3061 and 1648 $cm^{-1}$, respectively [15, 16]. The strong peak at 867 $cm^{-1}$ is produced by the out-of-plane deformation of unsaturated =C–H of maleic acid

[17]. Because the carboxylic acid carbonyl is conjugated to C=C, the frequency of its stretching mode is lowered to 1709 $cm^{-1}$. The broad peak at 2387 $cm^{-1}$ is produced by P-H stretch of hypophosphite. Figure 4.2(B) is the Raman spectrum of mixture of MA, $NH_4H_2PO_2$, and $(NH_4)_2S_2O_8$ (molar ratio MA/AHP/APS=30:15:1) after reaction at 55$^oC$ for 20 min. The sharp peak at 1076 $cm^{-1}$ is the characteristic band of $(NH_4)_2S_2O_8$. After reaction for overnight about 7 hours, another Raman spectrum was recorded and shown as Figure 4.2 (C). The characteristic peak of $S_2O_8^{2-}$ at 1076 $cm^{-1}$ was replaced by the characteristic peak of $SO_4^{2-}$ at 982 $cm^{-1}$. This phenomenon indicates that $S_2O_8^{2-}$ decomposed completely into $SO_4^{2-}$ after reacted overnight. More importantly, the alkene C=C stretch at 1649 $cm^{-1}$ and unsaturated =C–H stretch at 3062 $cm^{-1}$ disappeare completely, while the intense peak of saturated C–H stretch at 2942 $cm^{-1}$ emerges. The spectral change unequivocally demonstrates that the unsaturated maleic acid was polymerized into saturated compounds. Meanwhile, the stretch of carboxylic acid carbonyl is shifted back to normal position at 1722 $cm^{-1}$ because COOH is not longer conjugated to C=C after polymerization. The peak at 1390 $cm^{-1}$ in Figure 4.2(A) and (B) is due to the combination of C–O stretch and –O–H in-plane deformation of the dimmer of MA [16, 17]. After polymerization, the band moves back to a higher frequency at 1414 $cm^{-1}$. The out-of-plane deformation of unsaturated =C–H at 866 $cm^{-1}$ is also replaced by the saturated OH...O out-of-plane deformation at 912 $cm^{-1}$. It is meaningful to find that the stretching bond of P–H at 2387 $cm^{-1}$ disappears and the stretching mode of P-O increases in intensity and frequency to 1048 $cm^{-1}$ after polymerization. This result indicates that P–H of hypophosphite directly participated in the polymerization

MALDI-MS

The molecular weight distribution and end-group of poly(maleic acid) was characterized by MALDI-TOF-MS. Figure 4.3 is MALDI-TOF-MS spectrum of PMA. A homologue series at m/z 205, 321, 437, 553, 669, and 785 is clearly observed with a peak-to-peak increment 116 mass units, which confirms the repeat unit of maleic acid. These signals can be expressed by following formula:

$$[M+Na]^+ = 116n+89 = 116n+66+23$$

where n is the number of repeating unit, 23 is due to sodium-cationization, and mass residual 66 is equal to the molecular weight of hypophosphorus acid $H_3PO_2$. Polymer chains corresponding to these peaks have two possible structures as supported by $^{31}$P-NMR spectra and shown in Scheme 2.2. One is monoalkyl phosphinate, which has $H_2PO_2-$ and H as two end-groups of oligomer chains. Another is dialkyl phosphinate, in which $-HPO_2-$ is located in the middle of oligomer with two hydrogens as end-groups.

The weak signals at m/z 393, 509, and 625, which are 44 Da lower than the above principal peaks, result from the loss of $CO_2$. The peaks at m/z 459 and 575, which are 22 Da higher than the peaks at m/z 437 and 553, result from the substitution of one H by a second Na. The peak at m/z 337, which is 16 Da higher than peak at m/z 321, is due to monoalkyl phosphonate oligomers (Scheme 4.2) and is confirmed by $^{31}$P-NMR signals at $\delta$ 16-18 ppm as shown below.

The MALDI-TOF data indicate a very low degree of polymerization (DP) of PMA. The low DP is attributed to slow propagation of growing chains and frequent chain transfer to hypophosphite. The polymerization has been also investigated by LC/MS and

2D-$^{31}$P-NMR, and will be published in another paper [18]. A mechanism has been proposed and simply shown in Scheme 4.2.

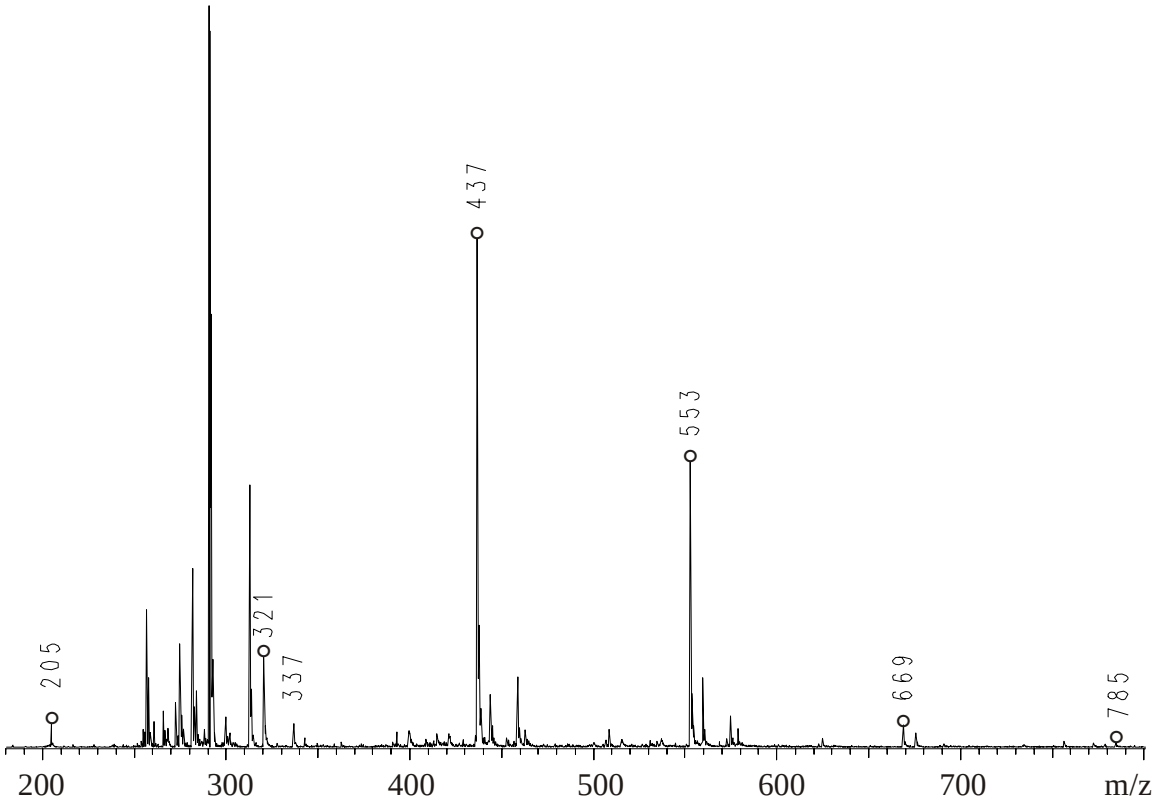


Figure 4.3 MALDI-TOF-MS spectrum of PMA

Hypophosphite $MH_2PO_2$ produces a radical $MHPO_2^{\bullet}$ by extraction of a hydrogen atom in the presence of radical initiator such as $(NH_4)_2S_2O_8$. $MHPO_2^{\bullet}$ initiates the polymerization of maleic acid. However, chain propagation is difficult due to the electronic repulsion between growing radical and maleic acid monomer and steric crowding of maleic acid. The growing chains terminate by radical transfer to $MH_2PO_2$. The chain transfer results in premature chain termination and a new radical $MHPO_2^{\bullet}$ capable of initiating another round of oligomerization. The ease of chain transfer is

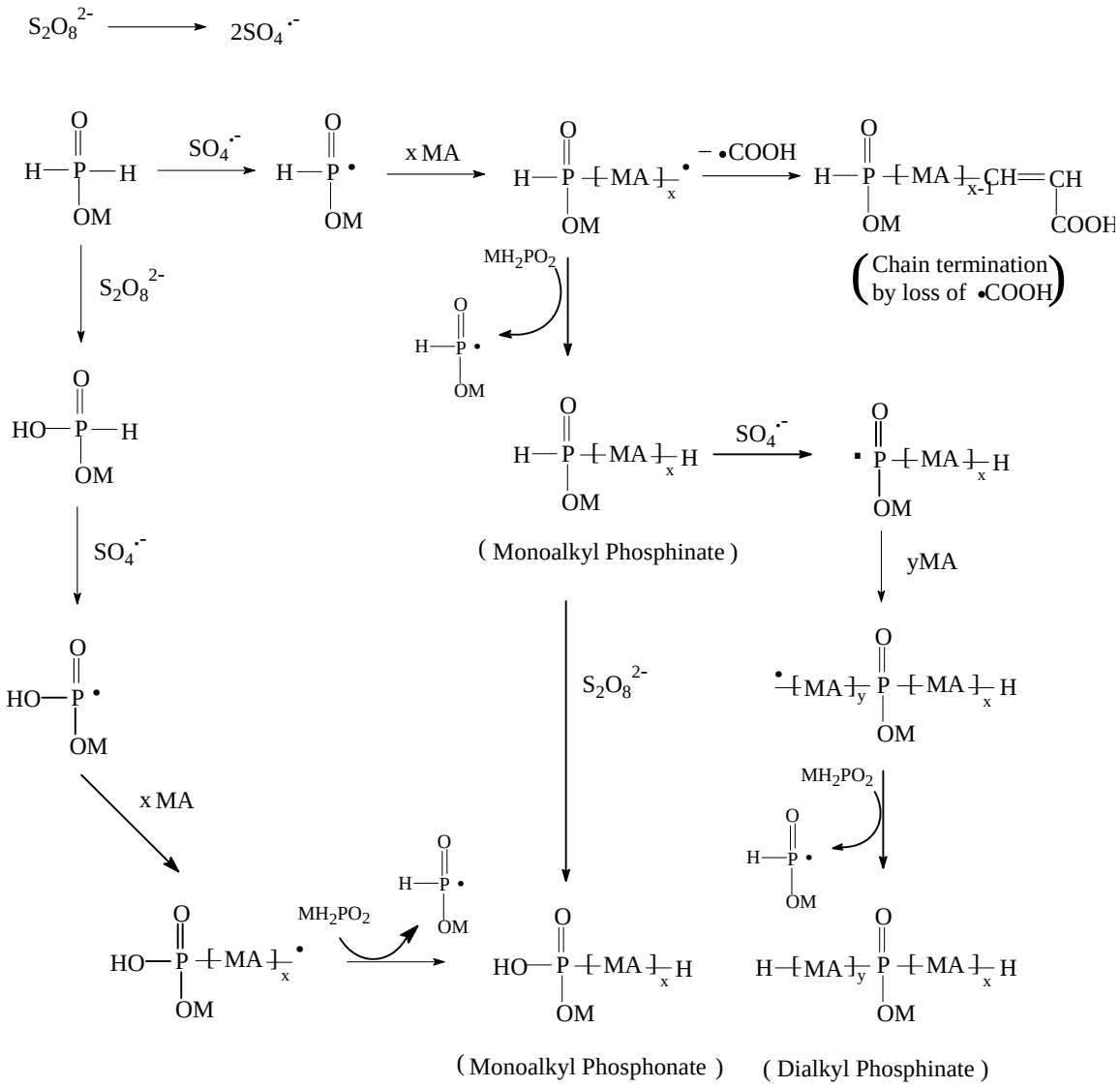


Scheme 4.2 The suggested mechanism of aqueous polymerization of maleic acid

supported by the fact that 3.3 mol% radical initiator $(NH_4)_2S_2O_8$ is able to complete the polymerization but result in a degree of polymerization less than 6. Growing oligomer chains may also terminate by loss of •COOH and produce an unsaturated end-group. The end-group of resulting phosphinate oligomers has another P-H, which is also able to produce a phosphorus radical and reacts with more maleic acid to produce dialkyl phosphinate oligomers. The side reaction, oxidation of hypophosphite, produces phosphite, which is also able to form a radical and react with maleic acid and thus leads to the formation of monoalkyl phosphonate. Another source of monoalkyl phosphonate oligomers is the oxidation of monoalkyl phosphinate oligomers.

$^{31}$P-NMR

Both chemical shift and coupling constant of $^{31}$P-NMR spectra provide valuable structural information for phosphorus-containing compounds. Figure 4.4 presents $^{31}$P-NMR proton-coupling (A) and broadband proton decoupling (B) spectra of PMA.

The satellites in both sides of decoupling peaks in H-decoupling spectrum result from the incomplete decoupling [19]. The 1:2:1 triple peaks at δ 11.56, 8.35, and 5.14 ppm in the H-coupling spectrum reduce to one peak at δ 8.35 ppm in H-decoupling spectrum, are owing to the unreacted hypophosphite, which accounts for 6.8% of total phosphorus. The large coupling constant $^1$J(P–H) around 520 Hz is due to the strong interaction between the phosphorus atom with its directly bonded proton. The 1:1 doublet peaks at δ 5.54 and 2.04 ppm with a $^1$J(P-H) ~568 Hz, which become one peak at δ 3.79 ppm in H-decoupling spectrum, are produced by phosphite, which resulted from the oxidation of hypophosphite by persulfate. The assignment of $H_2PO_2^-$ and $HPO_3^{2-}$ was confirmed by adding a drop of suspected ingredient to the sample tube.

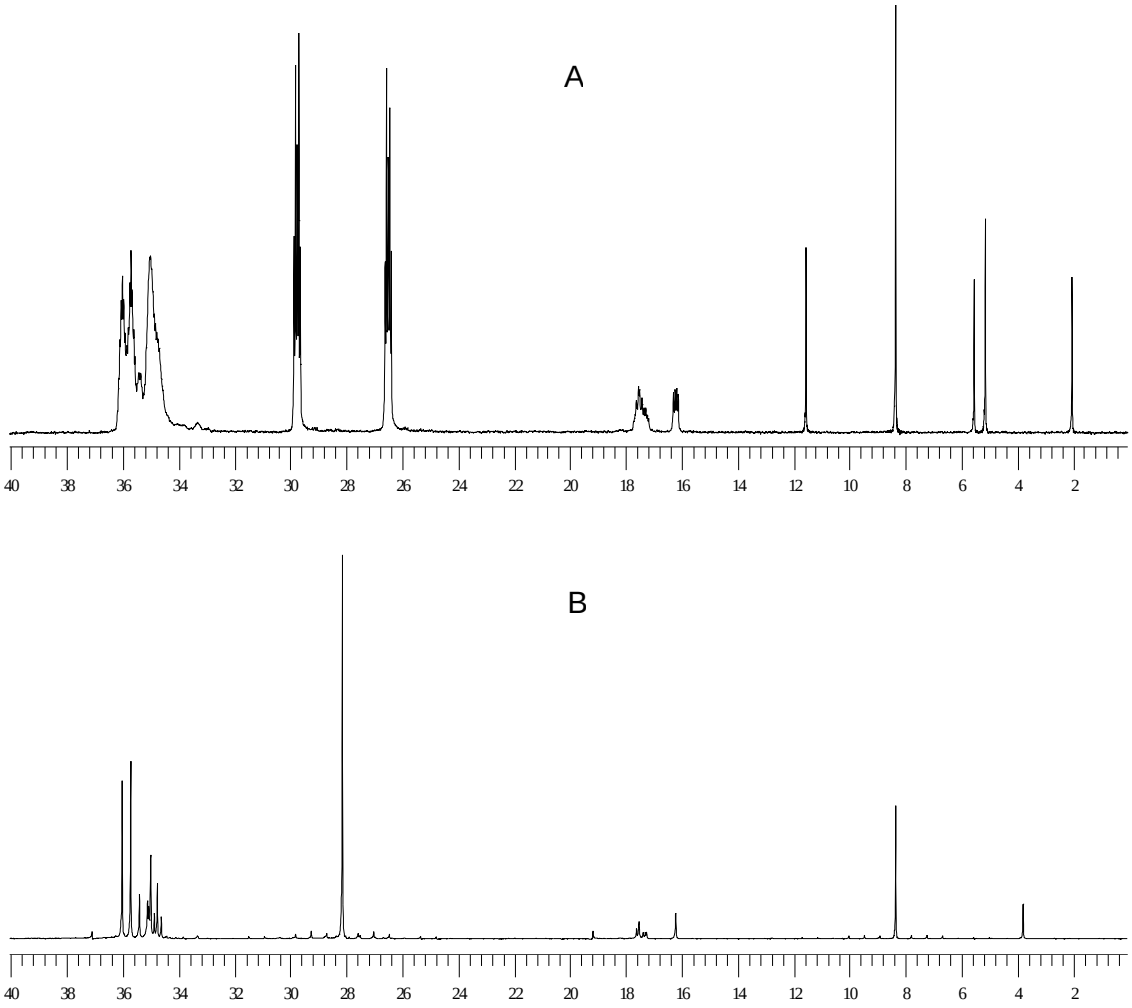


Figure 4.4 $^{31}$P-NMR spectra of PMA, (A) proton coupling and (B) proton decoupling

The PMA oligomers have also been investigated by 2D HMQC and HMBC $^{31}$P-NMR spectroscopy [18], and it has been found that all signals between δ 15 to 40 ppm are coupled to protons on the saturated backbone of the oligomers. In the $^{31}$P-NMR spectra shown Figure 4.4 , the broad signals at δ 32-40 ppm do not show any P-H bond, should be produced by dialkyl phosphinate oligomers. They are broadened and complicated by multi-bond P-H coupling. The two widely spaced ($^{1}$J(P–H) 529 Hz)

quintets between δ 26 and 30 ppm collapse into a single peak at δ 28.14 ppm after proton decoupling, thus belong to a phosphorus with a directly connected proton. It is confirmed by end-group of PMA oligomers as shown in MALDI-TOF-MS spectrum. The two groups of signals between δ 15.8 to 17.8 ppm without directly connected proton are generated by monoalkyl phosphonate oligomers, which may be produced from the oxidation of monoalkyl phosphinate oligomers or from the free radical reaction of phosphite with maleic acid. When PMA is further oxidized by $(NH_4)_2S_2O_8$, the signals between δ 26 to 30 ppm disappeared while the signals between δ 15.8 to 17.8 ppm significantly increased, as a result of oxidation of end-group [18].

The molar distribution of different species in the reaction products is analyzed quantitatively based on the peak areas of $^{31}$P-NMR spectra and shown in Table 4.3. About 52.7 mol% of phosphorus was incorporated into dialkyl phosphinate oligomers, 30.3% into monoalkyl phosphinate oligomer, and 7.7% into monoalkyl phosphonate oligomers.

Table 4.3 The molar percentage of different species in the polymerization products according to the peak areas of $^{31}$P-NMR spectra.

| Species | PMA(%) | PFA(%) | PBTA (%) | PIA-1(%) | PMSA(%) | PTAA(%) |
|---|---|---|---|---|---|---|
| Dialkyl phosphinate | 52.7 | 76.8 | 32.9 | 37.0 | 44.7 | 19.4 |
| Monoalkyl phosphinate | 30.3 | 6.8 | 25.0 | 10.6 | 6.1 | 64.3 |
| Monoalkyl phosphonate | 7.7 | 13.6 | 16.6 | 1.0 | 39.3 | 4.6 |
| Hypophosphite | 6.8 | 0.0 | 1.7 | 34.0 | 0 | 2.2 |
| Phosphite | 2.5 | 2.7 | 22.8 | 17.3 | 7.6 | 9.3 |
| Phosphate | 0.0 | 0.1 | 0.9 | 0.0 | 2.3 | 0.1 |

**Polymerization of Fumaric Acid and Characterization of Poly(fumaric acid)**

Raman

Raman spectroscopic study demonstrates that fumaric acid polymerized in the presence of hypophosphite very quickly. Fumaric acid has very limited solubility in water (in 100 g water, 0.63 g at 25$^{o}$C, 9.8 g at 100$^{o}$C), so a spectrum of solid fumaric acid (Figure 4.5(A)) is used for comparison. The intense peak at 1686 $cm^{-1}$ is due to the overlap of stretching modes of alkene C=C and carboxylic acid carbonyl. When fumaric acid, $NH_4H_2PO_2$, $(NH_4)_2S_2O_8$ and water were mixed together and heated to 95$^{o}$C, fumaric acid dissolved gradually in about 30 min, then a Raman spectrum of the clear solution was acquired and presented in Figure 4.5 (B). One finds that alkene C=C stretch at 1686 $cm^{-1}$ disappears and carboxylic acid carbonyl shifts back to higher frequency at 1721 $cm^{-1}$, the normal position of saturated carboxylic acid carbonyl. Meanwhile, the unsaturated = C–H stretch at 3069 $cm^{-1}$ is replaced by saturated C–H stretch at 2942 $cm^{-1}$. The phenomenon indicates that fumaric acid polymerized completely and very quickly in the presence of hypophosphite.

$^{31}$P-NMR

$^{31}$P-NMR spectra of the poly(fumaric acid) (PFA) are presented in Figure 4.6. The spectra are similar to those of poly(maleic acid) as shown in Figure 4.4. The relative molar ratios of different species are listed in Table 4.3. Nearly all hypophosphite was reacted. Only about 2.8% of hypophosphite was oxidized to phosphite and phosphate. Dialkyl phosphinate oligomers were the major products and accounted for 76.8% of phosphorus. About 6.8% of phosphorus was incorporated into monoalkyl phosphinate oligomers, and 13.6% into monoalkyl phosphonate oligomers.

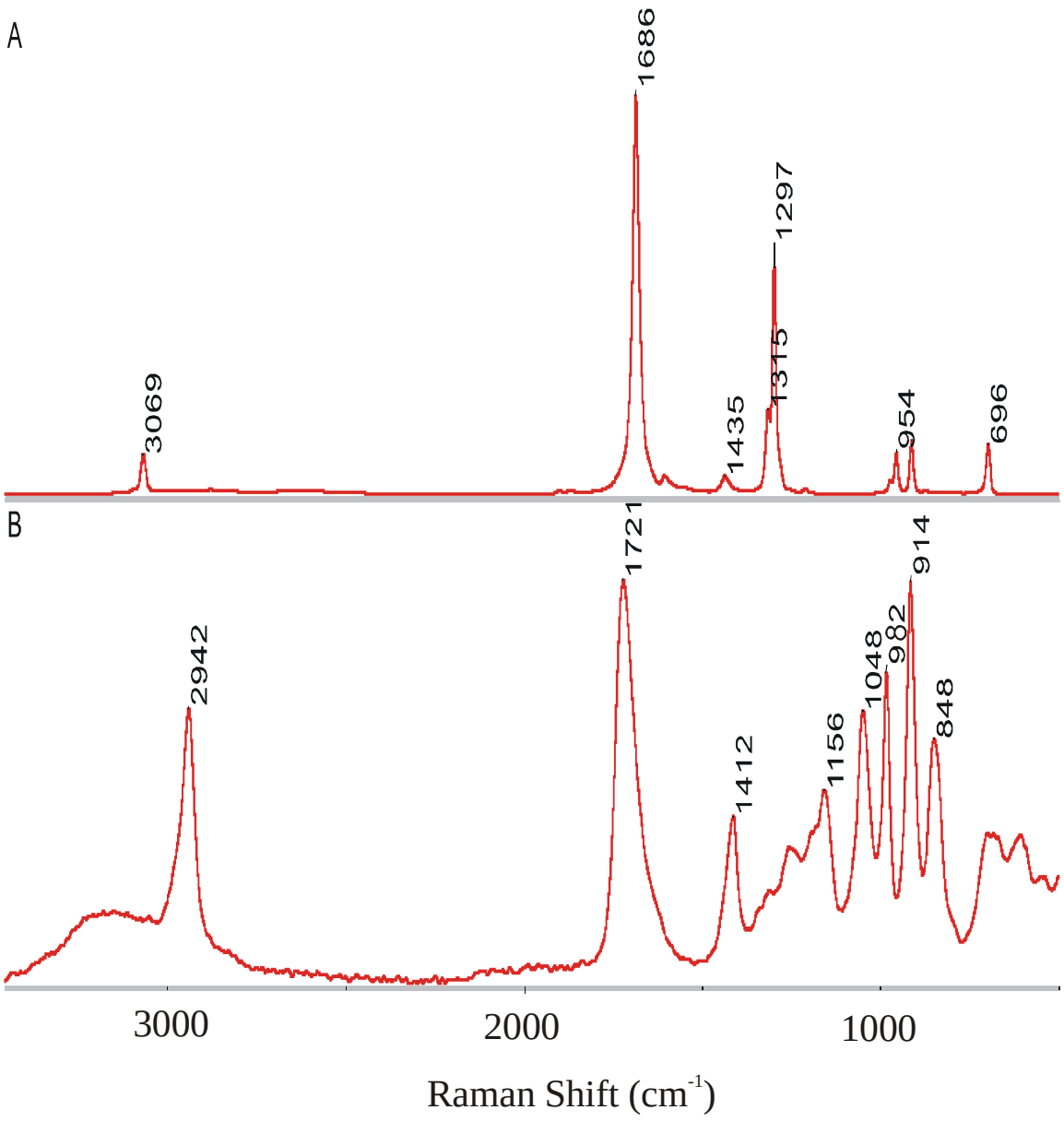


Figure 4.5 Raman spectra of (A) solid fumaric acid and (B) mixture of 40% FA, 14.3% $NH_4H_2PO_2$ , and 7.86% $(NH_4)_2S_2O_8$ (molar ratio FA/AHP/APS = 10:5:1) after reaction at 95$^{o}$C for 20 min

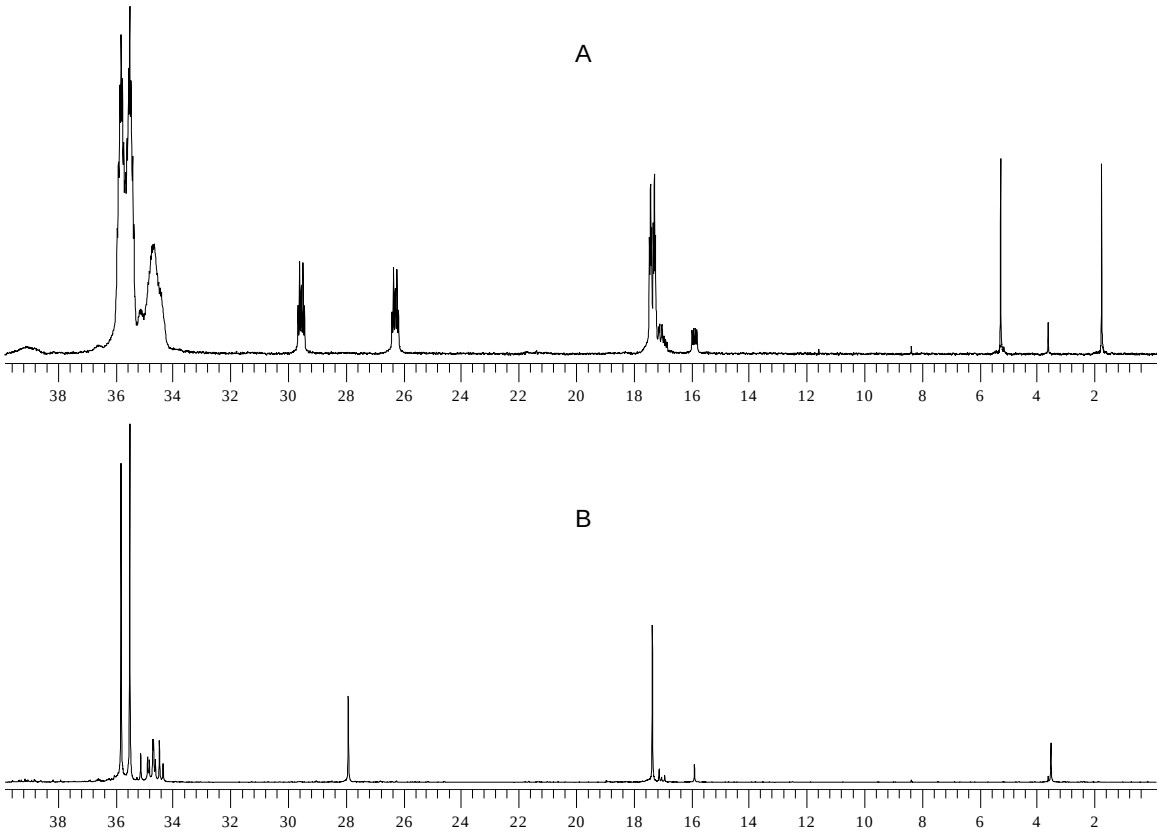


Figure 4.6 $^{31}$P-NMR of PFA, (A) proton coupling and (B) proton decoupling

MALDI-TOF-MS

MALDI-TOF-MS spectrum of PFA is shown in Figure 4.7. The spectrum is also similar to that of PMA. The homologue series of peaks at m/z 205, 321, 437, 553 have a mass increment of 116 Da, which confirms the repeating unit of fumaric acid, and a mass residual of 89 Da. As in the case of poly(maleic acid), the mass residual indicates this series of signals are produced by phosphinate oligomers with 1, 2, 3, and 4 repeating units. Most of these oligomers are dialkyl phosphinate, as shown in NMR data. One can

also find two weak peaks at m/z 221 and 337, which are 16 mass units higher than the peaks at m/z 205 and 321, respectively. They belong to monoalkyl phosphinate oligomers, which account for 13.6 mol% of phosphorus. The low degree of polymerization suggests that a phosphorus radical generally only reacted with no more than three fumaric acid monomers before it terminated by chain transfer.

The signal at m/z 321 is more intense and the peak at m/z 553 is weaker than their counterparts in PMA. The signal at m/z 669 corresponding to degree of polymerization 5 is very weak and the peak at m/z 785 corresponding to degree of polymerization 6 does not show out in PFA. This result suggests that the average molecular weight of PFA is even lower than that of PMA. The chain propagation in the case of fumaric acid was even more difficult than that in maleic acid.

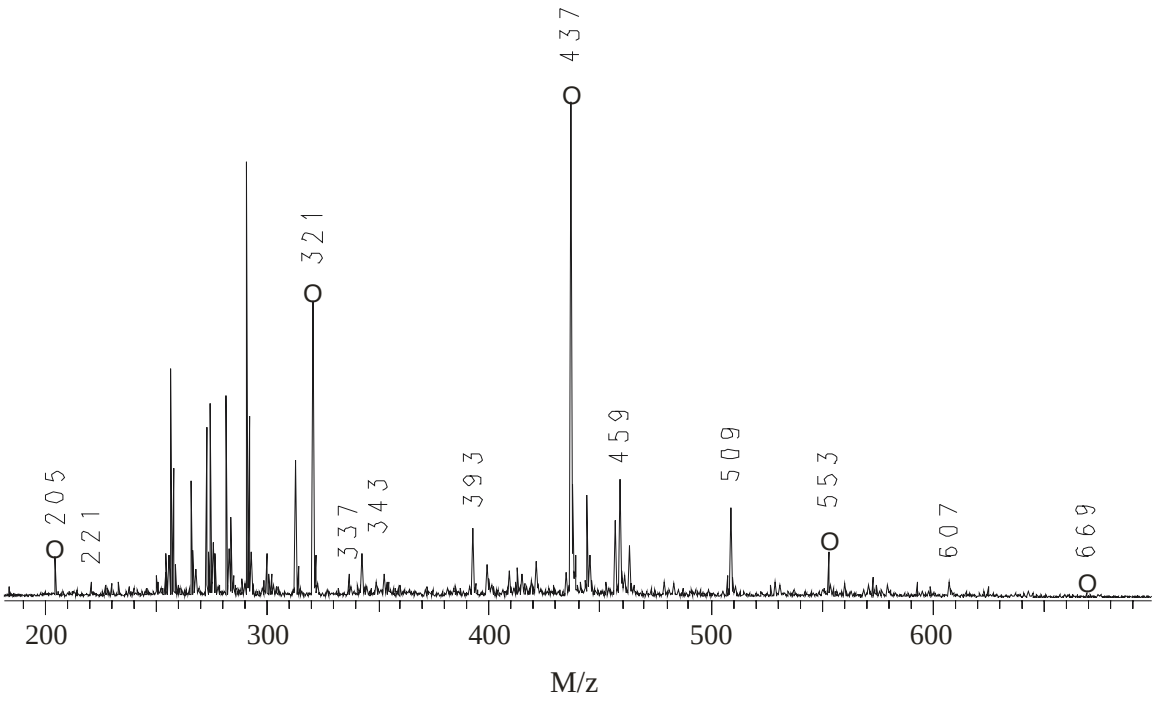


Figure 4.7 MALDI-TOF-MS spectrum of PFA

Still remained to be explained is the fast reaction of fumaric acid. Raman spectrum revealed that polymerization completed once fumaric acid dissolved in water at 95$^{o}$C in about 30 min. Fumaric acid is probably more vulnerable to attack by $HPO_2^{\bullet -}$. Meanwhile, radical $HPO_2^{\bullet -}$ was generated more quickly at high temperature.

**Polymerization of 3-Butene-1, 2, 3-tricarboxylic Acid and Characterization of PBTA**

Raman

The polymerization of 3-butene-1,2,3-tricarboxylic acid (BTA) is also demonstrated by Raman spectra in Figure 4.8. Spectrum (A) corresponds to 26% BTA aqueous solution. The asymmetric and symmetric stretching modes of =C–H appear at 3117 and 3006 $cm^{-1}$, respectively, while the stretching mode of saturated C–H appears at 2938 $cm^{-1}$. The peaks at 1707 and 1638 $cm^{-1}$ result from the stretching modes of carboxylic acid carbonyl and alkene C=C. The radical initiator $(NH_4)_2S_2O_8$ was added in three portions of 0.1773 g with a total amount of 0.5319 g. An amount of 0.3224 g $NH_4H_2PO_2$ and the first portion of $(NH_4)_2S_2O_8$ were added at the beginning of reaction. A Raman spectrum was acquired after 14 hours and shown in Figure 4.8(B). One finds that unsaturated =C–H stretch at 3117 and 3006 $cm^{-1}$ almost disappear completely and the saturated C–H stretch at 2935 $cm^{-1}$ significantly increases. The intense carboxylic acid carbonyl C=O stretch band shifts from 1707 $cm^{-1}$ to 1714 $cm^{-1}$. It suggests that the carboxylic acid groups are no longer conjugated to C=C. The change of the above Raman signals is the evidence of polymerization of BTA.

It is interesting to find that two peaks at 1834 and 1770 $cm^{-1}$ emerge out. These two peaks look like the asymmetric and symmetric stretching modes of anhydride. However,

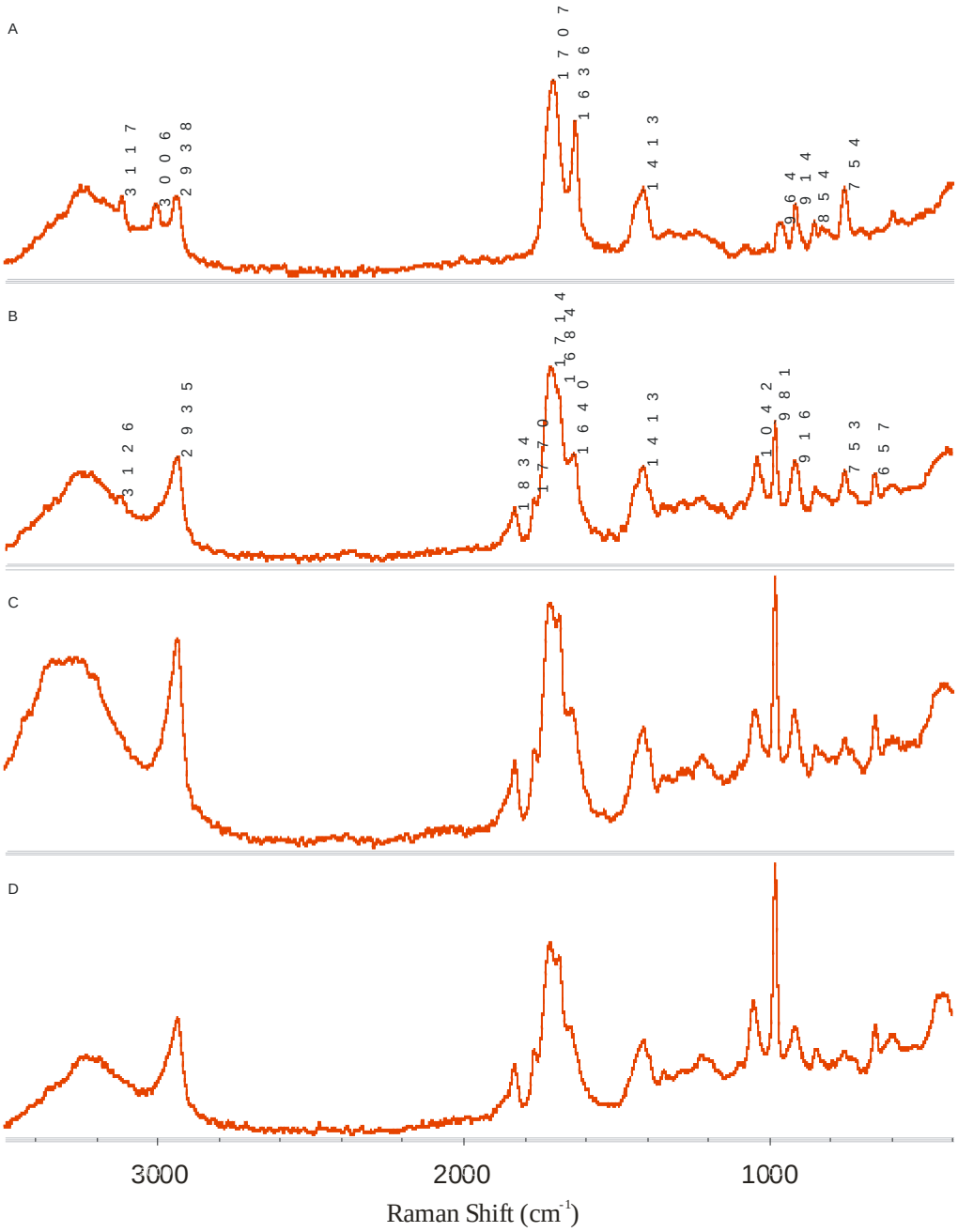


Figure 4.8 Raman spectra of (A)aqueous solution of 3-butene-1, 2, 3-tricarboxylic acid; (B) mixture of BTA, $NH_4H_2PO_2$ , and first portion of $(NH_4)_2S_2O_8$ after reaction for 14 hours; (C) after adding 2nd portion of $(NH_4)_2S_2O_8$ and reaction for 10 more hours; (D) after adding 3rd portion of $(NH_4)_2S_2O_8$ and reaction for another 5 hours

how did anhydride form in aqueous solution? Was it due to the formation of stable cyclic structure in the concentrated solution? The C=C stretch at 1638 $cm^{-1}$ reduces into a weak peak at 1640 $cm^{-1}$. The new weak band at 1684 $cm^{-1}$ is possibly generated by carboxylic acid carbonyl conjugated with C=C, which was produced by chain termination through the loss of COOH and formation of unsaturated chain end as in the case of maleic acid. This will be supported by MALDI-TOF mass spectrum. When the second portion of $(NH_4)_2S_2O_8$ was added, and the reaction proceeded for 10 more hours, another Raman spectrum was recorded and shown in Figure 4.8(C). After the third portion of $(NH_4)_2S_2O_8$ was added, and reaction continued for another 5 hours, a Raman spectrum was acquired again and shown in Figure 4.8(D). Once can find that addition of more $(NH_4)_2S_2O_8$ only brought about minor change in the Raman spectra. The C=C stretch at 1640 $cm^{-1}$ further shrinks while the weak band at 1684 $cm^{-1}$ increases slightly. The Raman spectra need more investigation.

Table 4.4 The frequencies and assignment of Raman shift of PBTA

| Compound | Raman Shift ($cm^{-1}$) | Assignment |
|---|---|---|
| BTA | 3117 | $=CH_2$ asymmetric stretch |
| | 3006 | $=CH_2$ symmetric stretch |
| | 2938 | saturated C–H stretch |
| | 1707 | carboxylic acid C=O (conjugated to C=C) stretch |
| | 1636 | C=C stretch |
| | 1413 | combination of C–O stretch and –O–H deformation (dimmer, unsaturated carboxylic acid) |
| PBTA | 2931 | saturated –C–H asymmetric stretch |
| | 1834 | saturated symmetric C=O (anhydride) stretch? |
| | 1770 | saturated asymmetric C=O (anhydride) stretch? |
| | 1714 | carboxylic acid C=O stretch |
| | 1684 | carboxylic acid C=O stretch (conjugated to C=C) |

$^{31}$P-NMR

The $^{31}$P-NMR spectra of PBTA shown in Figure 4.9 are somewhat different from those of PMA and PFA. The relative ratios of phosphorus incorporated into different oligomers or oxidized to phosphite or phosphate are listed in Table 4.3. The broad and complex signals at δ 39-44 ppm are due to dialkyl phosphinate oligomers, which only account for 32.9 mol% of phosphorus. The two couples of multiplets between δ 26 and 33 ppm reduce into two single peaks at δ 30.4 and 28.3 ppm in the H-decoupling spectrum. They belong to monoalkyl phosphinate PBTA oligomers, which possibly have different numbers (most possibly one or two) of BTA repeating units. These monoalkyl

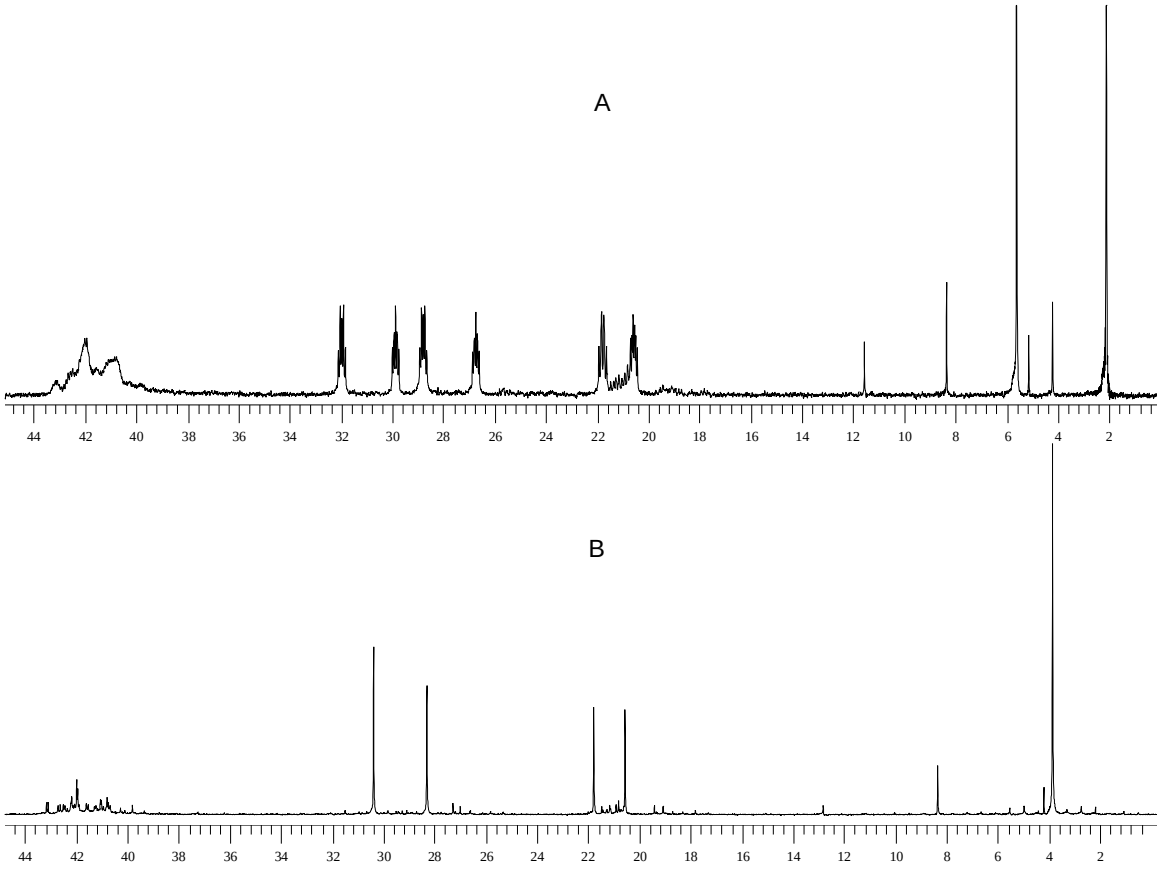


Figure 4.9 $^{31}$P-NMR spectra of PBTA, (A) proton coupling and (B) proton decoupling

phosphinate oligomers account for 25 mol% of phosphorus. The two groups of peaks at δ 20 to 22 ppm, which change into two single peaks at 21.7 and 20.6 ppm in H-decoupling spectrum, account for 16.6 mol% of phosphorus and should belong to monoalkyl phosphonate oligomers.

About 25.4 mol% phosphorus was not incorporated into PBTA oligomers. Only 1.7% hypophosphite remained unreacted. About 22.8% hypophosphite was oxidized into phosphite and 0.9% into phosphate. Phosphite was produced in an amount of 10 times of that in the case of poly(maleic acid) and poly(fumaric acid), possibly because more $(NH_4)_2S_2O_8$ was added and longer time was used for polymerization of BTA than for MA and FA.

MALDI-TOF-MS

More evidence of polymerization of BTA comes from the mass spectrum. The MALDI-TOF-MS spectrum of PBTA is presented in Figure 4.10. Analysis of the homologue peaks at m/z 465, 653, 841, and 1029 reveals that the masses of each peak can be expressed by (188n+66+23) where 188 is the molecular weight of monomer BTA, n is the number of repeat units, and 23 is due to sodium cationization. Like PMA, PBTA chains corresponding to these peaks have two possible structures. One is monoalkyl phosphinate, in which the oligomer chains are ended with $H_2PO_2-$ and H. Another is dialkyl phosphinate, in which $-HPO_2-$ is located in the middle of oligomer chains with two protons as end-groups. The peaks at m/z 443, 631, and 819 corresponding to (188n+66+1) refer to the same oligomer chains ionized by attaching a proton. The peak at m/z 481 can be expressed as (188×2+66+16+23). It corresponds to the monoalkyl phosphonate oligomers with two repeat units and having $H_2PO_3-$ and hydrogen as end-

groups, because NMR data eliminates the interpretation of the 16 Da as substitution of $Na^+$ by $K^+$. From the above information, we can conclude that BTA homopolymerized to produce oligomers of degree of polymerization less than 6.

One can also find a peak of medium intensity at m/z 397, which is 46 mass units lower than the peak at m/z 443. It is consistent with Raman band at 1684 $cm^{-1}$ and provides the evidence that some oligomers were produced through chain termination by loss of •COOH, which is similar to the case of maleic acid as shown in Scheme 4.2. The peak at m/z 353 is 44 mass units lower than the peak at m/z 397, and is possible due to further loss of a $CO_2$.

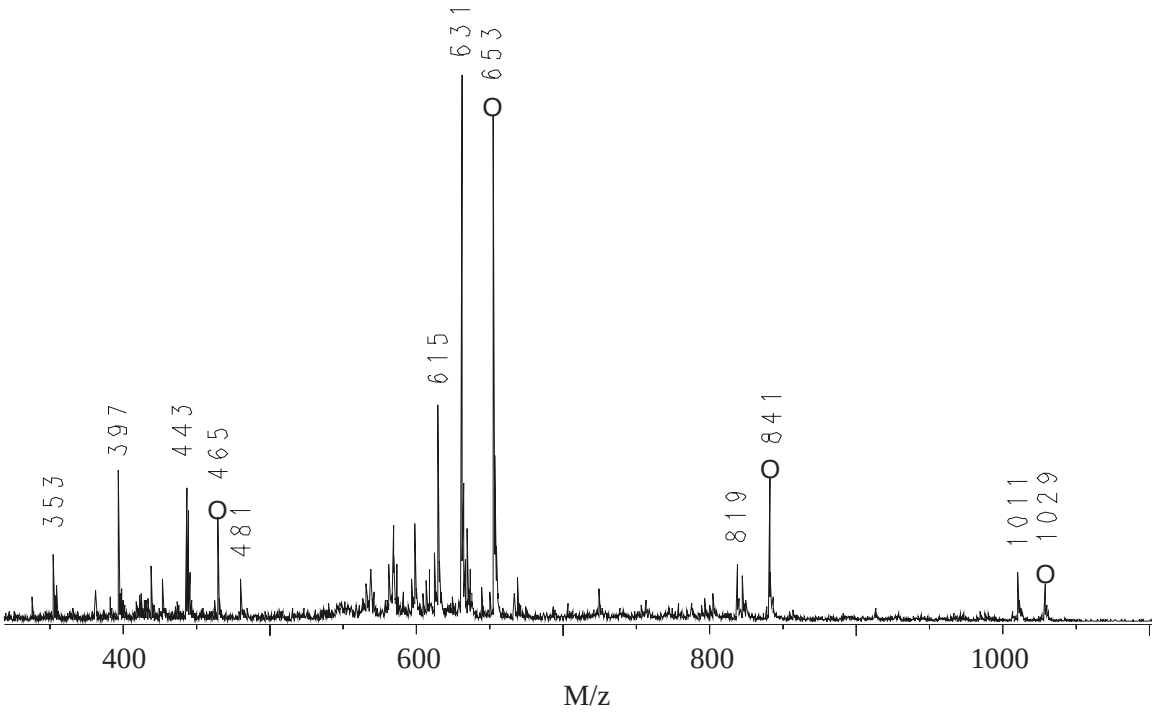


Figure 4.10 MALDI-TOF-MS spectrum of PBTA

Table 4.5 Assignment of MALDI-TOF-MS signals of PBTA

| Mass (m/z) | DP | Assignment |
|---|---|---|
| 353 | 2 | Peak 443-46-$CO_2$ |
| 397 | 2 | Peak 443-46 |
| 443 | 2 | $H–BTA_x–PO_2H–BTA_y–H + H^+$, x+y = 2, x, y = 0, 1, 2 |
| 465 | 2 | $H–BTA_x–PO_2H–BTA_y–H + Na^+$, x+y = 2, x, y = 0, 1, 2 |
| 481 | 2 | $H_2PO_3–BTA_x–H + Na^+$, x = 2 |
| 631 | 3 | $H–BTA_x–PO_2H–BTA_y–H + H^+$, x+y = 3, x, y = 0, 1, 2, 3 |
| 653 | 3 | $H–BTA_x–PO_2H–BTA_y–H + Na^+$, x+y = 3, x, y = 0, 1, 2, 3 |
| 819 | 4 | $H–BTA_x–PO_2H–BTA_y–H + H^+$, x+y = 4, x, y = 0, 1 to 4 |
| 841 | 4 | $H–BTA_x–PO_2H–BTA_y–H + Na^+$, x+y = 3, x, y = 0, 1 to 4 |
| 1011 | 5 | Peak 1011-$H_2O$ |
| 1029 | 5 | $H–BTA_x–PO_2H–BTA_y–H + Na^+$, x+y = 3, x, y = 0, 1 to 5 |

**Polymerization of Itaconic Acid and Characterization of Poly(itaconic acid)**

Raman

A mixture of 2.40 g itaconic acid, 0.7658 g $NH_4H_2PO_2$ and 2.41g $H_2O$ were heated to 90$^o$C to dissolve itaconic acid. A Raman spectrum was acquired for the initial clear solution and shown in Figure 4.11(A). The asymmetric and symmetric $=CH_2$ stretches appear at 3116 and 3007 $cm^{-1}$, respectively. The C=C stretch shows at 1643 $cm^{-1}$. The bands at 2368 and 1042 $cm^{-1}$ are due to the P–H and P–O stretches in hypophosphite, respectively. After addition of 0.4210 g $(NH_4)_2S_2O_8$ (molar ratio IA/AHP/APS = 10:5:1) and the polymerization proceeded at 90$^o$C for 30 min, another Raman spectrum was recorded and shown in Figure 4.11(B). The spectrum demonstrates that itaconic acid polymerized completely in 30 min. The unsaturated =C–H stretched at 3115 and 3006 $cm^{-1}$ disappear completely, while an intense saturated C–H stretch emerges at 2943 $cm^{-1}$. The C=C stretch at 1643 $cm^{-1}$ also disappears completely, while the stretch of

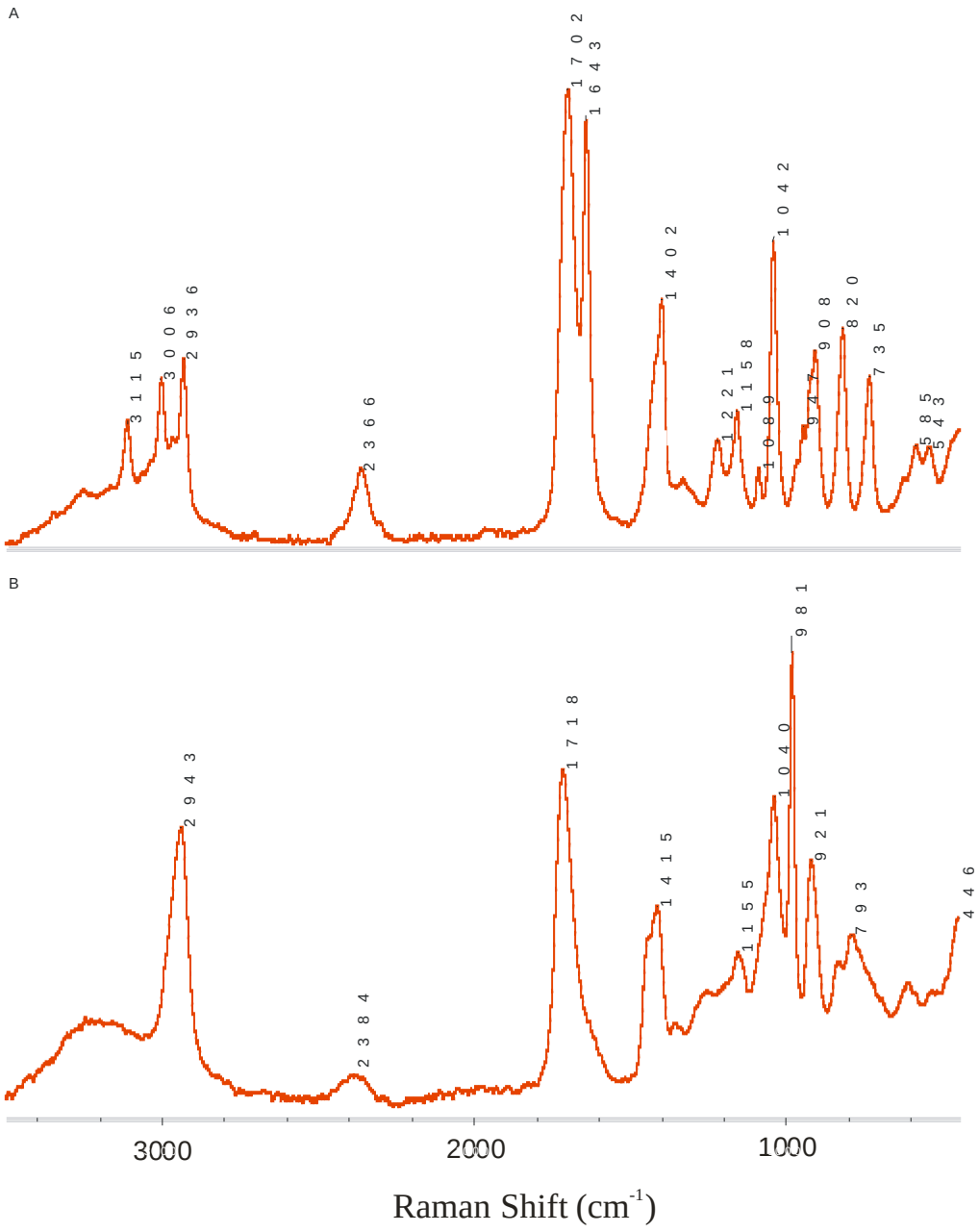


Figure 4-11 Raman spectra of (A) mixture of itaconic acid and $NH_4H_2PO_2$ in water; (B) mixture of itaconic acid, $NH_4H_2PO_2$ , and $(NH_4)_2S_2O_8$ after reaction for 30min

carboxylic acid carbonyl of IA at 1702 $cm^{-1}$ shifts to higher frequency at 1718 $cm^{-1}$ because carboxylic acid is no longer conjugated to C=C after polymerization. The strong peak at 981 $cm^{-1}$ is produced by S=O stretch of $SO_4^{2-}$.

Unlike all polymerization discussed above, the $PH_2$ symmetric stretch at 2377 $cm^{-1}$, $PH_2$ scissor at 1155 $cm^{-1}$ are still observable after polymerization. The result suggests that a lot of hypophosphite remained unreacted after polymerization.

Table 4.6 The frequencies and assignment of Raman shifts of PIA-1

| Compound | Raman Shift ($cm^{-1}$) | Assignment |
|---|---|---|
| Itaconic acid | 3115 | asymmetric $=CH_2$ stretch |
| | 3006 | symmetric $=CH_2$ stretch |
| | 2966 | asymmetric $-CH_2-$ stretch |
| | 2936 | symmetric $-CH_2-$ stretch |
| | 1702 | carboxylic acid C=O stretch |
| | 1643 | C=C stretch |
| | 1402 | combination of C–O stretch and –O–H deformation (dimmer, unsaturated carboxylic acid) |
| $H_2PO_2^-$ | 2366 | $PH_2$ symmetric stretch |
| | 1158 | $PH_2$ scissor |
| | 1042 | $PO_2$ symmetric stretch |
| PIA | 2943 | asymmetric stretch mode of $-CH_2-$ |
| | 1718 | stretch mode of C=O (saturated carboxylic acid) |
| | 1415 | combination of C–O stretch and –O–H deformation (dimmer, saturated carboxylic acid) |

$^{31}$P-NMR

The $^{31}$P-NMR spectrum of PIA-1 is illustrated in Figure 4.12. It is impressed that the signals of PIA oligomers are very weak compared with those of hypophosphite and phosphite. The relative amounts of different phosphorus-containing products according to the peak areas are listed in Table 4.3. There are 34.0 mol% of hypophosphite and

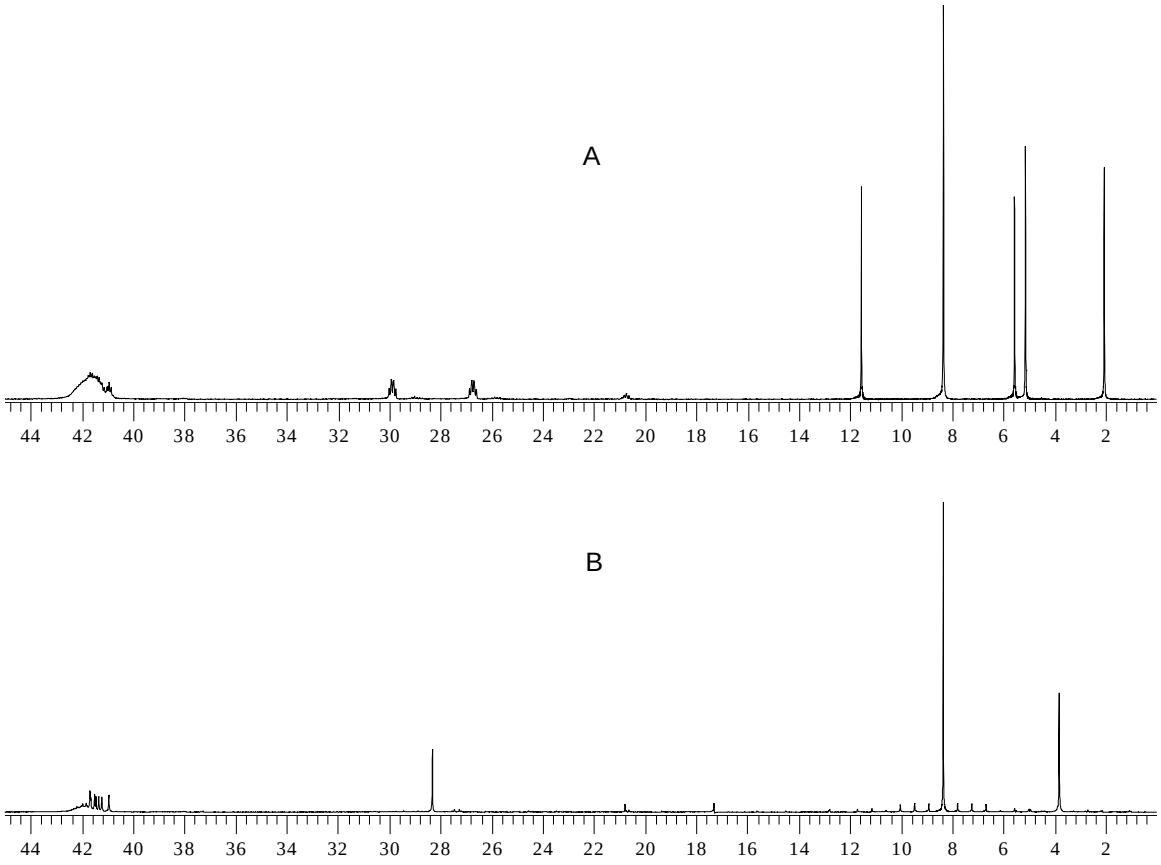


Figure 4.12 $^{31}$P-NMR spectra of PIA, (A) proton coupling and (B) proton decoupling

17.3 mol% of phosphite in the reaction product. This is consistent with the Raman data. Dialkyl phosphinate oligomers at δ 40-43 ppm and monoalkyl phosphinate oligomers at δ 26-31 ppm accounts for 37% and 10.6 mol% of total phosphorus, respectively. Only 1.0% monoalkyl phosphonate oligomers with δ 20-21 ppm was produced even though there was 17.3 mol% phosphite in the system. Only small amount of monoalkyl phosphonate was produced due to two possible reasons. Hypophosphite is more reactive for producing radical and initiating polymerization than phosphite, and a substantial amount of extra hypophosphite was available in the system. Another reason is the limited

oxidation of monoalkyl phosphinate oligomers by persulfate as result of short reaction time and small amount of persulfate used.

MALDI-TOF-MS

The MALDI-TOF-MS spectrum of the aforesaid PIA-1 is presented in Figure 4.13. One can find a well distributed homologous signals at m/z 479, 609, 869, 999, 1129, 1259, 1389, and 1519 with a mass increment of 130 Da. These signals can be expressed as (130n+66+23), where 130 is the mass of itaconic acid, n is the number of repeat unit, and 23 is due to sodium-cationization. Mass residual 66 indicates that these oligomers are phosphinate, as supported by the previous NMR data. There is another series of signals that are 22 Da lower than the first series of peaks. They are produced by proton ionization instead of sodium cationization. No mass signals of monoalkyl phosphonate oligomers, which are 16 mass units higher than phosphinate oligomers, are found in the spectrum. This result is consistent with $^{31}$P-NMR data.

The degree of polymerization (DP) of PIA is higher than that of PMA, PFA, and PBTA. The higher DP value suggests that chain transfer during polymerization of IA was less frequent than that in the cases of MA, FA, and BTA. In other word, itaconic acid is easier to polymerize than MA, FA, and BTA, because its 1, 1-disubstituted ethylene structure is steric preferred to 1, 2-substituted counterpart for polymerization.

According to our study, the amount of hypophosphite is critical to the polymerization of maleic acid. If the amount of hypophosphite is used in less than 33 mol% of maleic acid monomer, polymerization is difficult, slowly, and requires much more amount of persulfate for complete reaction of maleic acid. In order to investigate the effect of additional amount of $NH_4H_2PO_2$, IA was polymerized with a

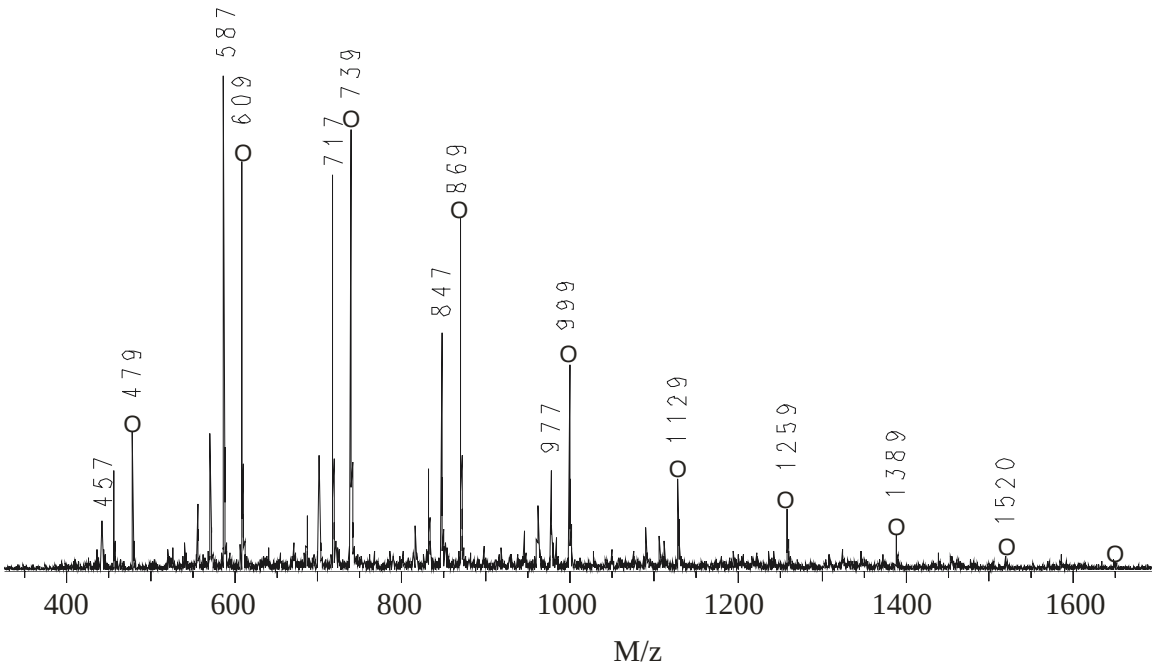


Figure 4.13 MALDI-TOF-MS spectrum of PIA-1

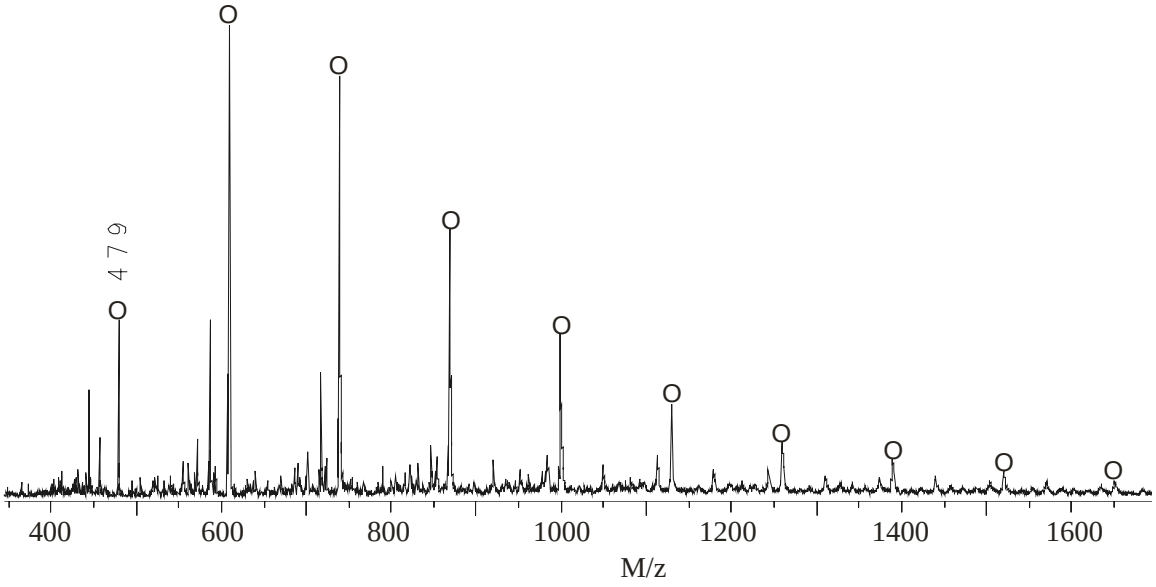


Figure 4.14 MALDI-TOF-MS spectrum of PIA-2

smaller amount of $(NH_4)_2S_2O_8$. The concentration of itaconic acid was identical to the previous one (PIA-1), but the molar ratio of IA/AHP/APS was 10/1/0.5 instead of 10:5:1. The polymerization was performed at 75°C instead of 90°C in order to reduce the decomposition rate of $(NH_4)_2S_2O_8$. A Raman spectrum was acquired after reaction for 2 hours, and it was found the polymerization was complete.

The MALDI-TOF-MS spectrum of the second PIA (PIA-2) is shown in Figure 4.14. The molecular weight distribution is similar to PIA-1. However, if considering the intensity of the homologue signals by proton ionization in PIA-1, one can find that the MW distribution of PIA-2 move to higher mass compared with PIA-1. For polymerization of itaconic acid, the growing chain can terminate through chain transfer to hypophosphite, but may also transfer to itaconic acid monomer by abstraction of an α-methylenic hydrogen and formation of stabilized allylic radicals [3, 6]. Therefore, even though chain transfer to hypophosphite was reduced by using a smaller amount $NH_4H_2PO_2$, the degree of polymerization of PIA was still limited by chain transfer to IA monomer.

**Polymerization of Mesaconic Acid and Characterization of PMSA**

Raman

Mesaconic acid (MSA) is also able to polymerize in the presence of hypophosphite. A reaction vial containing 1.2 g mesaconic acid and 3.6 g water was heated to 75°C to dissolve MSA, and a Raman spectrum was recorded and shown in Figure 4.15 (A). The unsaturated C=C stretch appears at 1652 $cm^{-1}$ with a peak height more than twice of that of C=O stretch at 1710 $cm^{-1}$. The weak band at 3078 $cm^{-1}$ belongs to the unsaturated

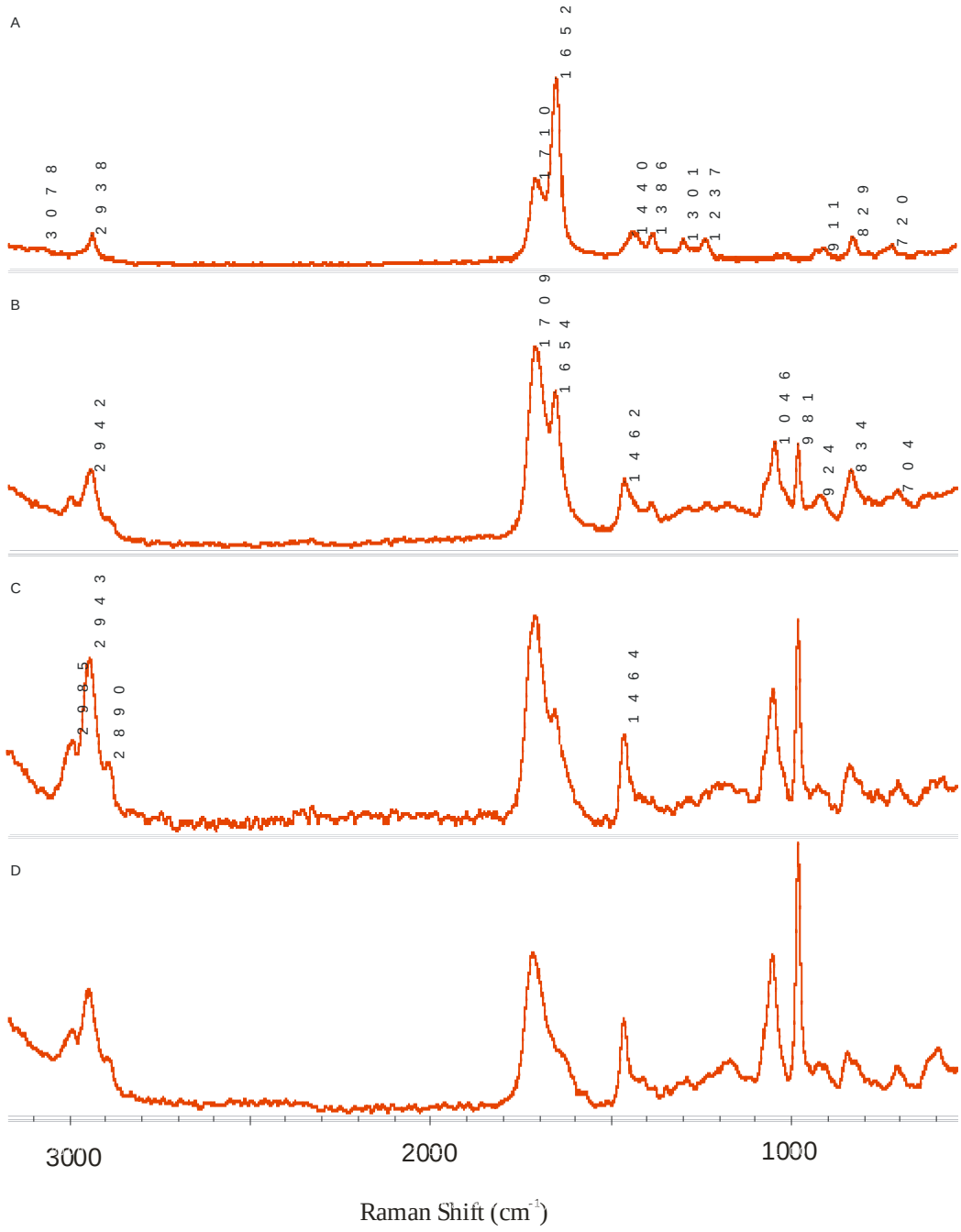


Figure 4.15 Raman spectra of (A) mesaconic acid in water; (B) mixture of mesaconic acid, $NH_4H_2PO_2$ , and first portion of $(NH_4)_2S_2O_8$ after reaction for 14 hours; (C) after adding 2nd portion of $(NH_4)_2S_2O_8$ and reaction for 12 more hours and (D) after adding 3rd portion of $(NH_4)_2S_2O_8$ and reaction for another 5 more hours

=C–H stretch. Three equal portions of 0.2105 g $(NH_4)_2S_2O_8$ (total 0.6315 g) were added during polymerization. The molar ratio of MSA/AHP/APS was 10:5:3.

When 0.3828 g $NH_4H_2PO_2$ and the first portion of $(NH_4)_2S_2O_8$ were to MSA solution, the reaction vial was maintained at 75$^oC$ for 14 hours, and then a Raman spectrum was acquired and shown in Figure 4.15(B). One finds that the relative heights of bands at 1654 and 1709 $cm^{-1}$ are inversed. The intensity of C=C band is reduced significantly.

After the second portion of $(NH_4)_2S_2O_8$ was added and reacted for another 12 hours, the third Raman spectrum was obtained and presented in Figure 4.15 (C). Then the third portion of $(NH_4)_2S_2O_8$ was added and reacted for 5 more hours, and the last Raman spectrum was recorded and shown in Figure 4.15(D). It is seen that the intensity of C=C stretch at 1654 $cm^{-1}$ further reduced and almost disappeared as reaction was completed.

Raman dada also indicate that MSA polymerized more slowly than MA, FA, and IA, and required more $(NH_4)_2S_2O_8$ for complete polymerization. The reluctance of polymerization arises from the severe steric hindrance of the tri-substituted monomer structure.

$^{31}$P-NMR

The $^{31}$P-NMR spectra of the poly(mesaconic acid) are presented in Figure 4.16. Similar to the NMR spectra of other oligomers, the NMR signals at δ between 32 to 39 ppm are produced by phosphorus atoms without directly bonded proton, and should belong to dialkyl phosphinate oligomers. The four multiplets at δ 25 to 31 ppm, which become two single peaks at δ 26.9 and 28.6 ppm after proton decoupling, are produced by monoalkyl phosphinate oligomers. The signals between δ 15 and 23 ppm, which do

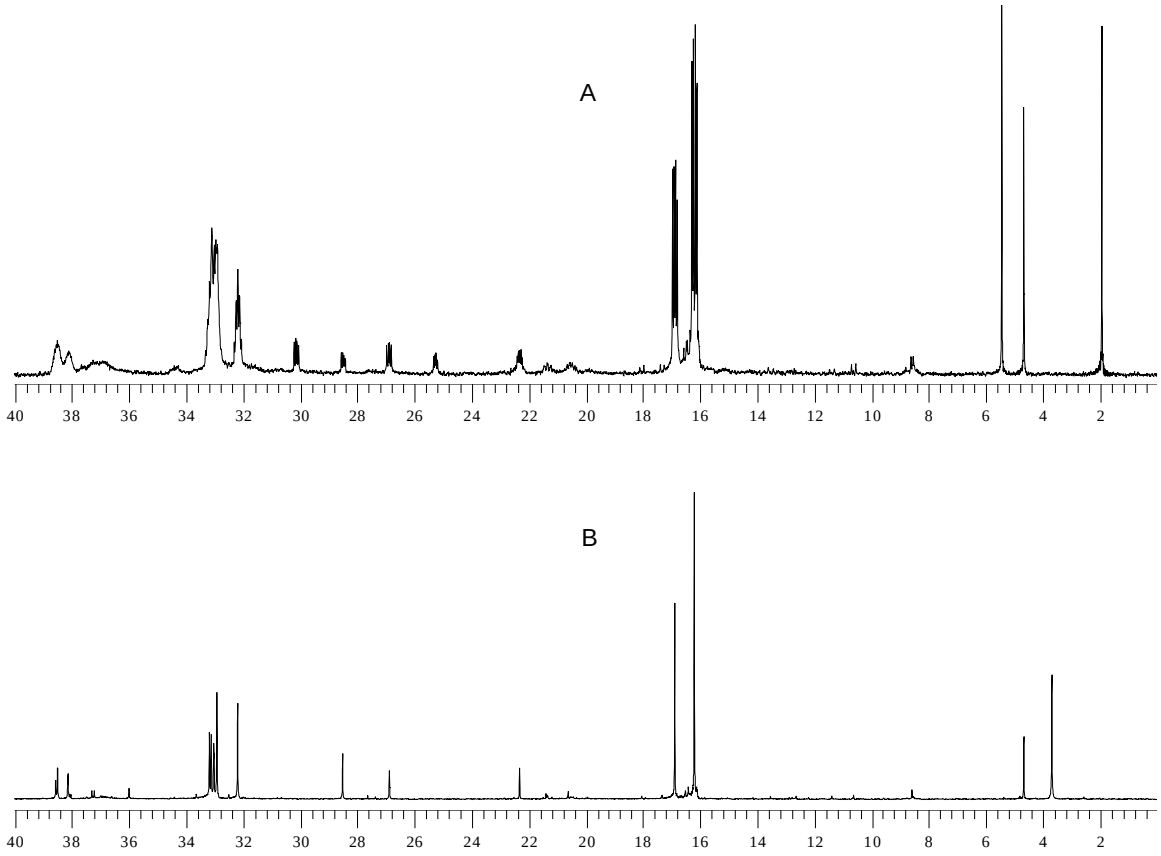


Figure 4.16 $^{31}$P-NMR spectrum of poly(mesaconic acid), (A) proton coupling and (B) proton decoupling

not show any directly connected proton, should be generated by monoalkyl phosphonate oligomers.

The long reaction time and the use of relatively large amount of $(NH_4)_2S_2O_8$ affected the molar distribution of the reaction products and led to side reactions and complex NMR spectra. Dialkyl phosphinate oligomers account for 44.7% of total phosphorus. There is only 6.1 mol% of monoalkyl phosphinate oligomers and no unreacted hypophosphite left in the reaction products. However, there is large amount of monoalkyl phosphonate oligomers, which account for about 39.3 mol% phosphorus in

the system. This is a result of oxidization of monoalkyl phosphite. The weak signals at δ 7-14 ppm and 18-24 ppm are possibly due to side reactions.

**Polymerization of Trans-aconictic Acid and Characterization of PTAA**

Raman

The Raman spectrum of aqueous solution of 2.0 g trans-aconictic acid (TAA) and 0.4769 g $NH_4H_2PO_2$ in 2.2610 g $H_2O$ (molar ratio TAA/AHP=2:1) is shown in Figure 4.17(A). The C=C stretch at 1659 $cm^{-1}$ and unsaturated =C–H stretch at 3084 $cm^{-1}$ are used to monitor the polymerization. The peak at 2364 $cm^{-1}$ is due to the $PH_2$ symmetric stretch of $NH_4H_2PO_2$. An amount of 0.4631 g $(NH_4)_2S_2O_8$ was added as two portions of 0.2621 g and 0.2010 g. Figure 4.17(B) is the Raman spectrum acquired after addition of 0.2621 g $(NH_4)_2S_2O_8$ and reaction at 55$^oC$ for 8 hours and addition of the second portion of persulfate (0.2010 g ). One can find that the characteristic peaks of TAA at 3084 and 1659 $cm^{-1}$ are only slightly reduced. After further reacted at 55$^oC$ for 20 hours, another Raman spectrum was acquired as shown in Figure 4.17(C). No $(NH_4)_2S_2O_8$ left, but about one fifth of monomer still survived as estimated by the area of C=C band at 1658 $cm^{-1}$. The polymerization is not complete. If more $(NH_4)_2S_2O_8$ had added and the reaction had been carried out for a longer time, TAA monomer should react completely.

$^{31}$P-NMR

The $^{31}$P-NMR spectra of the PTAA are shown in Figure 4.18. The spectra look similar to those of PBTA. The molar percentages of different species based on the peak area are also presented in Table 4.3. One can find that two groups of monoalkyl phosphinate oligomers are the major products and accounts for 64.3 mol% of phosphorus.

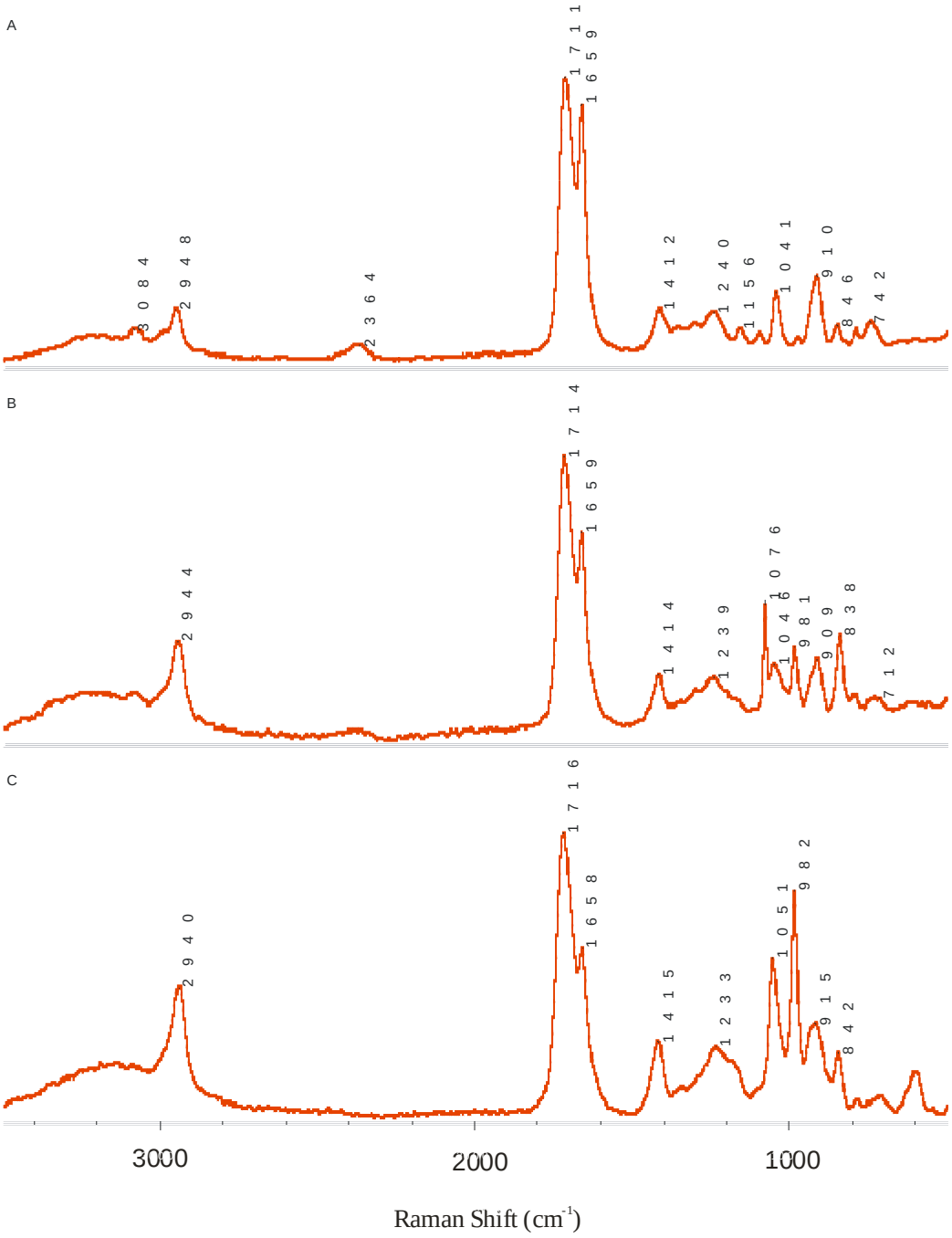


Figure 4.17 Raman spectra of (A) mixture of trans-aconictic acid and $NH_4H_2PO_2$ in water; (B) mixture of trans-aconictic acid, $NH_4H_2PO_2$ , and first portion of $(NH_4)_2S_2O_8$ after reaction for 8 hours; (C) after adding 2nd portion of $(NH_4)_2S_2O_8$ and reaction for 20 more hours

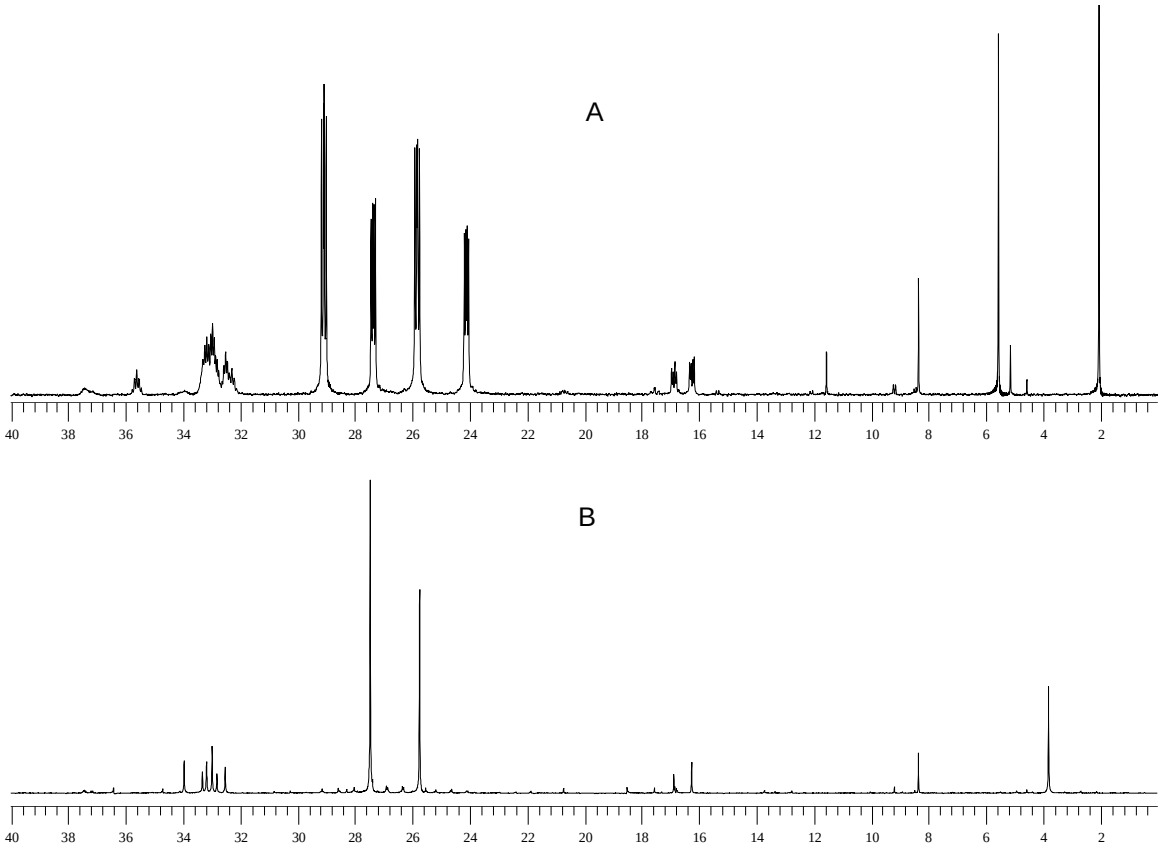


Figure 4.18 $^{31}$P-NMR spectrum of poly(trans-aconictic acid), (A) proton coupling and (B) proton decoupling

Dialkyl phosphinate oligomers accounts for 19.4%. Monoalkyl phosphonate oligomers only account for 4.6% of phosphorus. About 2.2% hypophosphite remained unreacted, and 9.3% was oxidized to phosphite.

## CONCLUSION

Maleic acid, fumaric acid, itaconic acid, 3-butene-1, 2, 3-tricarboxylic acid, mesaconic acid, and trans-aconictic acid are all able to homopolymerize in water in the presence of hypophosphate and persulfate. Fumaric acid and itaconic acid polymerized

faster than other monomers, while mesaconic acid and trans-aconictic acid polymerized slowly due to their tri-substituted ethylene structure. $^{31}$P-NMR spectroscopy indicated that phosphorus was permanently incorporated into oligomers as end-groups or in the middle of oligomer chains, it also provided quantitative information about the composition of reaction products.

The end-groups and molecular weight of the oligomers were determined by MALDI-TOF-MS. When hypophosphite was used in half molar concentration of monomers, polymerization of the aforementioned monomers except itaconic acid only produced oligomers of degree of polymerization less than 6. Itaconic acid was able to polymerize to a higher degree of polymerization than other monomers. However, the degree of polymerization of poly(itaconic acid) did not change much with the additional amount of hypophosphite possibly due to chain transfer to monomer.

## REFERENCES


1. Trivedi, B.C., Culbertson, B. M. "*Maleic anhydride*", Plenum Press, New York and London, 1982
2. Xu, G., Yang, C.Q., *J. Appl. Polym. Sci.* 74: 907-912 (1999)
3. Yang, C.Q., *U.S. Patent* 6,165,919 (2000), Assigned to Research Foundation of The University of Georgia
4. Sato, T., Nemoto, K., Mori, S., Otsu, T., *J. Macromol. Sci.-Chem.* A13(6):751-766 (1979)
5. Marvel, CS., Shepherd, T.H., *J. Org. Chem*. 24: 599-605(1959)
6. Tate, B.E., *Adv. Polym. Sci*. 5:214-232 (1967)

7. Tate, B. E., "Itaconic acid and derivatives", in "*Kirk-Othmer Encyclopedia of Chemical Technology*", 4th, Executive editor, Jacqueline I. Kroschwitz ; Editor, Mary Howe-Grant. Wiley, New York, 1991.
8. Yang, C.Q., Gu, X., *J. Appl. Polym. Sci.* 81(1):223-228(2001)
9. Mohr, M.D, Börnsen, K.O, Widmer, H. M., *Rap. Comm. Mass Spectr.* 9:809-814 (1995)
10. Xu, G., Mize, T., Yang, C. Q., Amster, I. J., *Proc. 49th ASMS Conf Mass Spectrom & Allied Topics*, Chicago, IL (2001)
11. Shaka, A. J., Keeler, J., Frenkiel, T., and Freeman, R. 1983, *J. Magn. Reson*., 52, 335.
12. Glonek, T., Wang, P. J., Van Wazer, J. R., *J. Am. Chem. Soc*. 98:7968 (1976)
13. Ruben, I.B., *Anal. Lett*. 17:1259 (1984)
14. Tsuboi, M., *J. Am. Chem. Soc*. 79: 1351-1354 (1957)
15. Lin-Vien, D., Colthup, N.B., Fateley, W.G., Grasselli, J.G., "*The handbook of infrared and Raman characteristic frequencies of organic molecules*", Academic Press, San Diego, 1991, pp74-75, 90, 92, 139-140
16. Colthup, N.B., Day, L.H., Wiberley, S.E., "*Introduction to infrared and Raman spectroscop*y", Academic Press, Boston, 1990, p247
17. Socrates, G., "*Infrared characteristic group frequencies*", Wiley & Sons, New York, 1994, pp47, 165, 180.
18. Xu, G., Jia, X., Yang, C.Q., Amster, I.J., to be submitted to *Ana. Chem.*
19. McFarlane, W., "Special experimental techniques in phosphorus NMR spectroscopy", in "*Phosphorus-31 NMR spectroscopy in stereochemical analysis*", J.G. Verkade and L.D. Quin Ed., VCH Publishers, Deerfield Beach, FA, 1987

# CHAPTER 5

# CONCLUSION

MALDI-TOF-MS and LC/ESI/MS have been successfully applied to determine the end-groups and molecular weight of poly(maleic acid) prepared by aqueous polymerization of maleic acid in the presence of hypophosphite and free radical initiator. The end-groups of the oligomers were confirmed and the relative amounts of different phosphorus-containing species in the reaction products were quantified by $^{31}$P-NMR. The insight from mass spectroscopy and NMR analysis provided complimentary information for understanding of the mechanism of polymerization.

Maleic acid underwent free radical homopolymerization in the presence of hypophosphite and free radical initiator. Abstraction of a hydrogen atom from hypophosphite produced a hypophosphite radical, which attacked maleic acid monomer and commenced the polymerization. The propagation radicals difficultly attacked more monomers owing to strong electronic repulsion and steric hindrance. They readily extracted a proton from hypophosphite to terminate, produced monoalkyl phosphinate oligomers and another hypophosphite radical, which started another round of oligomerization. The frequent chain transfer led to very low degree of polymerization below 6 even though only catalytic amount of radical initiator was used. The propagation chains might also be terminated by loss of •COOH.

The hypophosphite end-group of the monoalkyl phosphinate oligomers was able to produce another phosphorus radical, and thus the oligomers grew in the other end of chain and produced dialkyl phosphinate oligomers, which was the major species of the polymerization products. As the amount of hypophosphite decreased, the amount of monoalkyl phosphinate oligomers decreased, while the amount of dialkyl phosphinate oligomers increased as result of further reaction of monoalkyl phosphinate. Monoalkyl

phosphonate oligomers was also produced in the polymerization either by oxidation of monoalkyl phosphinate oligomers or by the reaction of phosphite radical with one or more maleic acid monomers.

The new initiation system was also explored for polymerization of itaconic acid, fumaric acid, 3-butene-1, 2, 3-tricarboxylic acid, mesaconic acid, and trans-aconictic acid, the last four of which had never be reported to homopolymerize before. They were all able to homopolymerize in water in the presence of hypophosphate and radical initiator. Fumaric acid and itaconic acid polymerized much faster than other monomers, while mesaconic acid and trans-aconictic acid polymerized slowly due to severe steric hindrance of their tri-substituted ethylene structure. $^{31}$P-NMR spectroscopy indicated that phosphorus was permanently incorporated into oligomers as end-groups or in the middle of oligomer chains, as in the case of maleic acid.

When hypophosphite was used in half molar concentration of monomers, polymerization of the aforementioned monomers except itaconic acid only produced oligomers of very low degree of polymerization (less than 6). Itaconic acid was able to polymerize to a higher degree of polymerization than other monomers. However, the degree of polymerization of poly(itaconic acid) did not change much with the additional amount of hypophosphite possibly due to chain transfer to both hypophosphite and monomer.